Assembly and Localization of the
Intermediate Filament Protein, Nestin

by

Martha Jean Marvin

B.A., University of California, Berkeley, 1984

Submitted to the Department of Biology in partial fulfillment
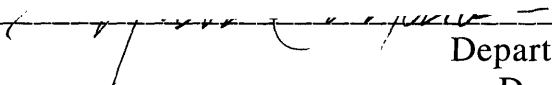of the requirements for the degree of
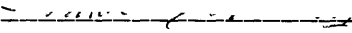
Doctor of Philosophy

at the

Massachusetts Institute of Technology

January, 1995

Signature of Author_____
Department of Biology
December 20, 1994

Certified by_____
Ronald D.G. McKay
Lab Chief, Laboratory of Molecular Biology
National Institute of Neurological Diseases and Stroke
National Institutes of Health

Accepted by_____
Frank Solomon
Professor, Biology
Chair, Department Graduate Committee

Assembly and Localization of the
Intermediate Filament Protein, Nestin

by

Martha Jean Marvin

Submitted to the Department of Biology on December 20, 1994
in partial fulfillment of the requirements for the Degree of
Doctor of Philosophy in Biology

Abstract

Neuroepithelial stem cells can be identified by their expression of the intermediate filament proteins vimentin and nestin.   Vimentin is found in many cell types but nestin shows a more restricted pattern of expression.   To improve the detection of nestin, antisera were raised against a portion of the protein expressed in bacteria and against a synthetic peptide.   The antisera have been widely used to analyse cell types in the developing and adult central nervous systems of mammals.   In cultured cells lacking vimentin protein, nestin was soluble, but when coexpressed with vimentin it was incorporated into intermediate filaments.   The molecular basis of nestin assembly was explored by introducing the nestin gene with specific mutations into cultured cells and into transgenic mice.   As with other intermediate filament proteins, deletions in conserved regions of the α-helical rod domain of nestin perturbed its assembly. Deletion of the amino-terminal portion of the rod rendered the mutant subunits incapable of assembly with vimentin.   A small deletion from the carboxy-terminal end of the rod affected intermediate filament morphology in the cell periphery in vimentin positive, nestin-negative cells.   The same deletion reduced the ability of the mutant protein to incorporate into filaments in nestin positive cells.   In transgenic animals, wild-type nestin incorporated into the endogenous vimentin-nestin filament network, but the small carboxy-terminal rod deletion remained localized near the pial endfoot in spinal cord radial glia.   The two mutant proteins demonstrate that nestin interacts with other interediate filament subunits via the conserved regions of the rod domain.   The results of the carboxyl-terminal rod deletion suggest that nestin may be involved in interactions between intermediate filaments and components of the subcortical cytoskeleton or the plasma membrane.

Table of Contents   Page

Chapter 5:   Transgenic Animals   169

Chapter 6:   Conclusion   190

Dedication

IN MEMORY of Jonas Dahlstrand   1963-1994

Chapter 1: Introduction to the Neuroepithelial Stem Cell

The extraordinary complexity of the adult vertebrate central nervous system (CNS) is reached through the progressive narrowing of the developmental choices presented to the stem cells of the early neuroepithelium. In the first step a region of ectoderm is induced to commit to a neuroepithelial fate by signals from the underlying mesoderm during gastrulation. The presumptive neuroepithelium folds in on itself to generate the neural tube. Through a variety of mechanisms still not well understood, the neural tube develops rostral-caudal and dorsal-ventral axes of polarity, but for a time after the closure of the neural tube, the cells in the columnar epithelium appear as yet undifferentiated. Many lines of evidence demonstrate the existence in the early CNS of a multipotential stem cell capable of giving rise to all the cell types of the brain, but isolating and characterizing a CNS stem cell is a challenging experimental goal.

In the search for developmental intermediates, markers for CNS stem cells and their differentiated progeny were required. Hybridoma technology made possible the development of specific reagents to identify cells by their gene expression. The monoclonal antibody Rat 401 was isolated in a screen for antibodies raised against E15 rat spinal cord (Hockfield and McKay, 1985). At this stage of development, some motor neurons have already terminally differentiated, but many neuronal stem cells are still proliferating. The corresponding antigen was later cloned and demonstrated to be an intermediate filament protein, now called nestin (Lendahl et al., 1990a). This antibody stained radial glia in the E15 spinal cord, but its expression began long before the birthdate of neurons, shortly after neural tube closure. Nestin first appears at E9.5 in the spinal cord and is expressed in 98% of the spinal cord cells by E11. The proportion of expressing cells declines precipitously as neurons are born. Postmitotic neurons do not express nestin, although transient coexpression with neurofilaments is seen (Frederiksen and McKay, 1988; N. Valtz and R. McKay, unpublished data). These data show that nestin is expressed in proliferating CNS stem cells, but not in terminally differentiated neurons. Given the large number of neurons that differentiate on each day in the embryonic spinal cord, the rate of cell proliferation, and the high proportion of nestin positive cells, the embryonic neurons must be derived from nestin positive cells (Frederiksen and McKay, 1988). Astrocytic and oligodendroglial (O2A) precursors also express nestin, but just after

neuronal differentiation, the number of glial precursors is small, accounting for the decline in overall nestin expression (Almazan and McKay, 1992).

In the last decade, substantial progress in the characterization of CNS stem cells and their differentiated products has been made. Cell culture techniques and purified growth factors have made possible long-term in vitro culture of CNS stem cells (Temple, 1989; Cattaneo and McKay, 1990; Vicario et al., 1995; Reynolds et al., 1992). Transplantation experiments have begun to answer questions regarding the role of the environment versus the inheritance of cells in the fate of CNS precursors and the plasticity of that fate (Renfranz et al., 1991; Snyder et al., 1992; Sotelo et al., 1994). Retroviral labeling has made clonal analysis of the progeny of a single cell possible, providing new information about the fate of precursors in vitro and in vivo (Luskin et al., 1988; Price and Thurlow, 1988; Walsh and Cepko, 1988). The selective expression of nestin has played a central role in the study of CNS stem cells (Cattaneo and McKay, 1990; Vicario et al., 1995; Renfranz et al., 1991; Reynolds and Weiss, 1992).

Patterns of nestin expression

Nestin expression was first identified in the CNS, but nestin protein or mRNA has now been found in a wider variety of cells. Nestin is associated with proliferation of some embryonic cells and remodeling in the mature brain.

CNS

Nestin is expressed in the CNS from the closure of the neural tube until the end of gliogenesis. It first appears and remains prominent in the endfeet that contact the basal lamina on the pial surface of the neural tube, but soon nearly all the cells in the CNS are nestin positive, and nestin-positive filaments span the whole cell from ventricle to pia. Although the overall level of nestin drops precipitously as neurons go through their final mitoses, it is expressed in glial precursors as well (Almazan and McKay, 1992). In the rat cerebellum, nestin expression remains high until the proliferating cells of the EGL migrate inward and differentiate into granule neurons in early postnatal life (Hockfield and McKay, 1985). Nestin expression is almost completely silenced in the adult CNS, with

the exception of some cells in the subependymal layer and some midline cells lining the ventricles (Dahlstrand et al., 1994; Dahlstrand et al., 1992b; Hockfield and McKay, 1985; Lendahl et al., 1990b; Zimmerman et al., 1994; Reynolds and Weiss, 1992).

Reactive astrocytes

In spite of its restricted expression in adult animals, nestin mRNA and protein can be induced in the adult brain. In several lesion models, nestin is re-expressed near the site of the lesion. In hamster and rat, ischemic, aspiration and heat lesions all produce nestin-positive reactive astrocytes (R. Lin, O. Brustle, R. McKay, unpublished data). Kainate lesions in the hippocampus induce nestin mRNA (M Dugich, unpublished data). Mechanical lesions in adult cerebellum induce nestin in astrocytes. In addition to reactive astrocytes, host Bergmann glia re-express nestin in a transplantation model. When small pieces of embryonic cerebellum are introduced to the cerebellum of the adult *pcd* mouse mutant (Purkinje cell degeneration), Purkinje cells migrate out of the graft and integrate into the cerebellum. Nestin is induced primarily in areas where Purkinje cells are migrating (Sotelo et al., 1994). Bergmann glia are generated too late to serve as guides for the normal migration of Purkinje cells, the first mature cell type to appear in cerebellum. Bergmann glia serve as guides for the later-born cerebellar granule neurons, however (Rakic, 1971). These experiments show that nestin expression correlates with functional plasticity in the brain.

Other CNS expression

Nestin is expressed in developing retina (D. Hulik and R. McKay, unpublished data). Cell lines from the retina immortalized with temperature sensitive SV40 T antigen show a limited capacity to differentiate in vitro (R. Segal and R. McKay, unpublished data).

Nestin is highly expressed in some classes of CNS tumors, particularly glioblastomas and medulloblastomas (Dahlstrand et al., 1992a; Tohyama et al., 1992; Valtz et al., 1991, and discussed in Chapter 2). Nestin expression may reflect the primitive origin of the cells. Alternatively, the reinduction of nestin may be reinduction correlating to proliferation, as it may be with reactive astrocytes.

PNS

The developing peripheral nervous system shows nestin staining. In
E11 rat, nestin stains the dorsal root ganglion (DRG) and ventral root
(Hockfield and McKay, 1985). Staining persists into adulthood in
Schwann cells surrounding axons from dorsal root and sciatic nerve.
The embryonic nerve root staining is in immature Schwann cells
rather than in the neurons themselves. In adult, staining is highest
in myelinating cells, while non-myelin associated cells stain weakly
(Friedman et al., 1990).

Muscle

Nestin expression in somitic myotome and developing myoblasts is
well established (Kachinsky et al., 1994; Lendahl et al., 1990a;
Sejerson and Lendahl, 1993; Valtz et al., 1991; Zimmerman et al.,
1994). Vimentin is coexpressed with nestin, but nestin is present
later and is co-expressed with desmin in Z bands of early postnatal
myotubes (Sejerson and Lendahl, 1993). Cultured myoblasts and
some myogenic cell lines make nestin protein in the absence of any
of the four myogenic transcription factors, but in other lines nestin is
upregulated by transfection with MyoD or myogenin. The mouse
myoblast line L6 fails to express nestin at all, but forms myotubes in
vitro (Kachinsky et al., 1994). It is therefore apparently dispensable
for fusion of myoblasts into myotubes. Similarly, a normal desmin
filament system in cultured myoblasts is not required for
differentiation of myoblasts in vitro (Schultheiss et al., 1991). In
C2C12 and L6, the nestin distribution is aberrant (Kachinsky et al.,
1994), when compared to staining of the human myogenic line G6 or
the medulloblastoma-like cell line ST15A (Sejerson and Lendahl,
1993; Valtz et al., 1991). The distribution is not filamentous. The
apparently abnormal nestin distribution may be due to the use of the
Rat 401 antibody, which stains mouse nestin with low avidity, or
may indicate that the cells are incapable of normal nestin assembly.
Nestin also stains heart and some adult muscle fibers which are
heavily used, such as the tongue (U. Lendahl, personal
communication).

Endothelial cells

Nestin staining and mRNA hybridization have been observed in
endothelial cells of the brain (Dahlstrand et al., 1992a; Sotelo et al.,
1994; Tohyama et al., 1992; Oliver Brustle, personal communication).

However, nestin staining is infrequent in endothelial cells of normal brain but is stronger and more common in neoplastic tissue (Dahlstrand et al., 1992a). Staining is abundant in an endothelial cell line CBA9(3d)CL2, which will be discussed in Chapter 2.

Other tissues

Nestin mRNA has been observed in human embryonic kidney, although not in the human kidney tumor line 293 (Dahlstrand et al., 1992b). It is detected by antibody staining in the BHK-21 (baby hamster kidney) line both in blots and by immunocytochemistry (this work; see Chapter 2). The level of expression in adult kidney is not known. Nestin is seen in odontoblasts, the cells that generate teeth as well (U. Lendahl, personal communication).

Nestin Promoter

The nestin promoter has been analyzed for tissue specific expression in transgenic mice. Separate elements in the first and second introns control expression in somitic muscle and the CNS, respectively. The upstream region of nestin can be replaced with a different promoter to give basal expression without altering the pattern established by elements within the introns (Zimmerman et al., 1994). These results demonstrate that nestin is specifically and highly expressed in the developing CNS.

Expression of Other IFs During Development and Differentiation

From the above discussion, a picture of nestin expression in select categories of proliferating cells emerges. Nestin is for the most part downregulated in these cells when the differentiation program is completed. Concerted changes in the pattern of intermediate filament expression accompany steps in the development of many tissues. The embryonic ectoderm expresses keratins 8 and 18, which give way to vimentin and nestin following closure of the neural tube (Hockfield and McKay, 1985; Houle and Fedoroff, 1983). CNS neurons in the developing telencephalon switch from vimentin and nestin expression to α-internexin transiently, and then to the neurofilament triplet proteins (Dahlstrand et al., 1994; Fliegner et al., 1994). In astrocyte precursors, nestin and vimentin expression gives way to GFAP expression (Almazan and McKay, 1992). Late in embryonic development, radial glia lose expression of vimentin and a

high molecular weight intermediate filament-associated protein and become GFAP positive (Yang et al., 1992; Yang et al., 1993). In muscle, vimentin, followed by nestin, gives way to desmin. Such abrupt changes are common within the keratin family as well. For instance, basal cells of the dermis express keratins 5 and 14 as the predominant pair, while suprabasal cells express keratins 1 and 10 (Fuchs, 1994a).

Nestin is an Intermediate Filament Protein

Nestin was cloned by screening a rat E15 lgt11 cDNA library with Rat 401. It shares the structural features of the intermediate filament proteins (IF), but differs enough from the five previously identified classes of IFs to have been placed in a new sixth class. Nestin colocalizes with vimentin in filaments at the light microscope level of detection (Lendahl et al., 1990a). The intermediate filaments are a large family of proteins which are under strict temporal and spatial regulation. Antibodies to the various IFs expressed in the developing and mature CNS have provided tools to identify classes of cells by their distinct IF expression.

Intermediate Filament Structure

The intermediate filaments are a diverse set of proteins with a common domain structure. The most conserved is the rod domain, a 310 amino acid sequence (350 for nuclear lamins) which has a heptad repeat motif of hydrophobic residues (often leucine) in the first and fourth positions, interspersed with alternating zones of positive and negative charges. The hydrophobic residues are thought to lie on one side of an alpha helical coiled-coil and to serve as the basis for dimerization and further steps in assembly (Coulombe, 1993; Fuchs, 1994b; Liem, 1993; Oshima, 1992; Steinert, 1993; Stewart, 1993). The general structure of intermediate filament proteins is diagrammed in Figure 1. The rod domain is divided into four helical segments separated by three linker domains. The linkers contain proline and glycine residues which would break the a-helix. The rod segment lengths are conserved through evolution, except for nuclear lamins which have a long insert in coil 1B.

Throughout most of the rod it is the interspersed leucines and charged residues that are conserved, but both ends of the rod are highly homologous between IF classes and throughout evolution.

Numerous experiments have shown that these sites are essential for higher order interactions between subunits in filament formation. A 12 amino acid sequence at the carboxyl terminus of the rod is highly conserved, with the consensus sequence EIATYRKLLEGE. Nestin diverges more than the representatives of the other classes from this sequence. A second site at the amino terminus of the rod in coil 1A is also essential for higher-order filament formation. The 1A consensus sequence more interspersed with unique sites than the coil 2B rod end sequence. The consensus sequence for the coil 1A conserved domain is E K/R X Q M X X L N D R L/F A X Y. These sites are indicated in Figure 2.

Outside the α-helical rod, the sequences of the intermediate filaments diverge rapidly. Structural motifs in both the head and the tail of Type III IFs are involved in the regulation of polymerization, and the presence of part of the head and or tail is required for proper assembly in most of the IFs studied. The non-helical domains may be involved in cell type specific functions, but until recently, few functions have been found in vitro for IF proteins. With the development of transgenic technology, alterations in the structure and content of IF networks have been found to cause disease in vivo.

IF Classes

IF proteins fall into six different classes based their protein and intron structures and subcellular localizations. Type I and II keratins are expressed in epithelial cells. There are about 40 members of the two classes currently known. Class III filaments are comprised of vimentin, desmin, GFAP, and peripherin. Class IV are neuron-specific filaments α-internexin and the neurofilament triplet proteins; Class V are the nuclear lamins (Steinert and Liem, 1990). Nestin is distantly related to neurofilament heavy chain (NFH) with only 24% amino acid identity in the rod domain, and no homology elsewhere. However, it shares two out of three of its intron positions with NFH. On the basis of its sequence, nestin could be placed in its own Class VI (Dahlstrand et al., 1992b; Lendahl et al., 1990a), but could be considered a member of Class IV based on its intron positions (Liem, 1993). The class assignment of the moderately nestin-related Xenopus IF protein, tanabin, will depend on its intron structure (Hemmati-Brivanlou et al., 1992).

Intermediate filaments: Structural and Regulatory Roles in vivo

The most exciting information to emerge from studies on the roles of IFs in vivo is their implication in disease in transgenic animals. Two dominant mutant keratins have been demonstrated to cause skin diseases in transgenic mice (Fuchs et al., 1992; Vassar et al., 1991). These findings inspired researchers to investigate keratins as the cause for a class of human skin diseases. Mutations in both of the predominant keratins expressed in basal cells of the epidermis, K5 and K14, are responsible for epidermolysis bullosa simplex (EBS), a skin disease that causes blistering in the basal epidermis. Similarly, K1 and K10 mutations are found in patients suffering from epidermolysis hyperkeratosis (EH), characterized by superficial skin blistering and hyperproliferation of the basal layer. Keratin 9 mutations cause a similar disorder (Reis et al., 1994). Point mutations in these keratins have been demonstrated in numerous individuals and families afflicted with these and other skin diseases (reviewed in (Fuchs, 1994a). When these mutations were engineered in cloned genes and expressed in cultured cells or assembled in vitro, they caused disruptions in filament assembly. The large deletions and severe phenotypes in the mouse study are rarely seen in humans because only those suffering milder phenotypes survive. The specific point mutations will be discussed below.

Naturally occuring functional knockouts of keratin 14 in patients have also been found to cause EBS (Chan et al., 1994a; Rugg et al., 1994). Oddly, even though patients in both cases completely lacked K14, the severity differed. The milder case was also milder than many of the point mutations, which are generally dominant. In the more severe case, wispy remains of filaments using another type I keratin were found. In the patient with the milder case, no filaments were found at all. This suggests that a malformed keratin filament system may be more destructive than none at all.

Overexpression of either neurofilament light or heavy chains (NFL or NFH) results in neurodegenerative disease in transgenic mice. Both the transgenes result in disease similar to amytrophic lateral sclerosis (ALS). Symptoms include skeletal muscle atrophy, swollen perikarya and axons filled with abnormal accumulations of neurofilaments, and accumulation of phosphorylated NFH. The accumulation of neurofilaments in the cell body and proximal axons may reflect defects in axonal transport. It is not yet clear whether

neurofilament mutations cause some cases of ALS, or whether the abnormal accumulation is a secondary effect of the disease. A mutation in Cu/Zn superoxide dismutase has been linked to the familial form of ALS, but this accounts for only 10% of all cases (Deng et al, 1993). NFH has been shown by electron micrographic studies to be a cross linker between neurofilaments (Gotow et al., 1992; Hirokawa et al., 1984), and the onset of NFH expression slows axonal transport (Cote et al., 1993). The progression of disease differs in the two mouse models. Mice overexpressing NFL recover from the ALS-like symptoms, while NFH mice develop pathology with age. Lower levels of NFH than NFL are required to bring about pathology. It is notable that until two lines expressing NFL were bred together, no axonal pathology was seen (Monteiro et al., 1990). The progression of disease also differs for the two transgenes, but this is likely to be related to the promoter used, rather than intrinsic factors (Cote et al., 1993; Xu et al., 1993).

For some years investigators have accumulated evidence that density of neurofilaments affects axon caliber (Monteiro et al., 1990). However, increasing the number of neurofilaments had no effect on calilber. In support of the caliber hypothesis, the quail mutant quiverer carries a null mutation in the NFL gene, and lacks NFs in axons altogether (Ohara et al., 1993). Axon diameter is reduced, and behavioral and electrophysiological abnormalities result. A transgenic mouse in which part of the tail domain of NFH had been replaced by β-galactosidase had the surprising phenotype of producing axons lacking any IFs. Axon diameters are reduced. The fusion protein disrupts transport of all IF subunits, including α-internexin and peripherin, which aggregate in perikaryal masses. The mice behave normally, even though axonal conduction rates are slowed, as they are in the quail mutant. There is little premature neuronal death or degeneration, and the accumulated protein reaches a steady state in the cell body, so levels do not increase over the life of an animal. There is an increase in the density of microtubules in the axons, which may in part compensate for the lack of IFs (Eyer and Peterson, 1994).

Keratin 8 has been targeted by homologous recombination and both functional alleles have been inactivated. In spite of the early expression of keratin 8 in embryonic and extraembryonic epithelia, in developing yolk sac, gastrointestinal tract, lungs and reproductive organs, the homozygous animals implant normally and do not die

14

until the liver develops blood vessel ruptures at E12-13. K18 and K19, the co-expressed Type 1 partners of K8, are not incorporated into filaments (Baribault et al., 1993). In spite of the lack of compensatory IF systems in the affected tissues, implantation and organ development take place rather normally until midgestation. However, a small fraction (6%) of the animals do survive to adulthood, but have difficulty breeding. The lack of an early phenotype could be due the lack of a requirement for early expression, or to compensation by other cytoskeletal components.

On the other hand, a targeted disruption of the vimentin gene results in mice which are, at least at a gross level, perfectly healthy. Vimentin is the only IF in the lens, but lens structure is normal (Colluci-Guyon et al., 1994). While the NFL-overexpressing transgenic mice develop cataracts at an early age (Monteiro et al., 1990), no pathology is reported here. The animals breed normally, and wound healing is unaffected. Internal organs in which vimentin is usually expressed are healthy as well. Fibroblasts, but not the early CNS, were examined on an ultrastructural level for compensatory IFs, but no 10 nm filaments were seen.. While these mice have yet to be examined in detail, the lack of effect is very surprising, given the conservation of vimentin from chicken to human is on the order of 90%. While the animal colony is free of the insults likely to challenge mice in the wild, the overall function of the animals seems unimpaired. The differing severity of the two human knockout cases may be instructive here. If the cells of the two EBS patients completely lack K14 protein, a factor outside the K14 sequence must be influencing the outcome (Chan et al., 1994a; Rugg et al., 1994).

A few IFs do demonstrate functions in cultured cells. Vimentin negative SW13 tumor cells show altered cholesterol metabolism (Sarria et al., 1992). A role for vimentin was also implied by the inhibition of neurite outgrowth by antibodies and antisense oligos in culture (Shea et al., 1993). In vivo, however, this role could be taken over by α-internexin, which is transiently present in newly born neurons (Fliegner et al., 1994). Glial fibrillary acidic protein antisense RNA inhibits the normal response of an astrocytoma line to the presence of primary neurons. The line exits the cell cycle, but fails to extend processes as usual (Weinstein et al., 1991).

15

In the last eight years, many labs have made intensive efforts to investigate the functions and assembly properties of intermediate filaments using site-directed mutagenesis. The questions regarding assembly have been easier to answer. We now have well supported evidence for the manner of assembly of individual polypeptides into dimers and tetramers, but less confidence about higher order assembly into protofilaments and the interaction of these strands to form IF networks. Although for the most part IF functions have not been demonstrated in culture, several intermediate filaments have been implicated in disease, implying essential roles for them in vivo.

Assembly   of   Intermediate   Filament   Proteins

In vitro studies have clarified the roles of the rod subdomains in intermediate filament assembly steps. Keratins first form head-to-head, in-register dimers. The dimers assemble into larger subunits by forming tetramers that overlap in four different modes. At the tetramer stage, molecules align antiparallel and staggered so that the conserved domains at the each of the rod ends interact with the linkers L12 and L2. Tetramers align end to end forming 2-3 nm protofilaments, so that amino and carboxyl conserved rod ends are brought into direct interaction with each other (Heins et al., 1993). Protofibrils associate laterally to form protofilaments and 10 nm intermediate filaments. Mutations in the coil 1A and 2B conserved domains affect the formation of tetramers and higher order structures, while conserved aliphatic amino acids and alternating charged zones in the rod bring about dimerization by a "leucine zipper" mechanism (Meng et al., 1994; Fuchs, 1994a; Steinert, 1993). The head and tail regions, when required for normal assembly, seem to control or promote lateral interactions among protofibrils.

Self   Assembly

If the ability to self-assemble were a requirement for membership in the IF family, only the nuclear lamins, class III subunits vimentin, peripherin, desmin, GFAP and the class IV α-internexin would be eligible for membership. Cytokeratins require 1:1 stoichiometry between a basic Type I and a neutral to acidic Type II keratin subunit for assembly. They are not restricted to the pairs seen coexpressed in vivo. For instance, K14 can coassemble with K8

16

although they are never expressed in the same cells. A cell type expressing different sets of keratins can assemble them into a single filament network (Albers and Fuchs, 1987; Lu and Lane, 1990). Keratin networks are separate from vimentin-containing networks in cells that express both, although under some circumstances there may be interactions between them (McCormick et al., 1991).

The first identified members of the neuronal Class IV filaments were the neurofilament proteins. The three subunits (NFL, NFM, NFH, at 68, 160 and 200 kD, respectively) are all assembly incompetent individually (Ching and Liem, 1993; Lee et al., 1993). They are able to coassemble with the assembly competent subunits α-internexin or vimentin (Chin et al., 1991; Ching and Liem, 1993; Gill et al., 1990; Wong and Cleveland, 1990). In the absence of other filaments, NFL requires the presence of either NFM or NFH to form normal filaments in cells (Ching and Liem, 1993; Lee et al., 1993). In spite of this, NFL assembles into normal-appearing filaments in vitro, while NFM and NFH assemble into short rodlets (Gotow et al., 1992). In vimentin free cells transfected with NF subunits singly, NFL and NFM incorporate primarily into insoluble material believed to be larger than tetramers. NFH is largely soluble, but some appears in the insoluble fraction (about 20%) (Ching and Liem, 1993). These data invite speculation on the roles of the various filament subunits involved in the differentiation-induced changes in IF composition in the CNS. Do vimentin, α-internexin and nestin play a role in stabilizing the changes in IF expression during development? Does the large tail of nestin play a role in cross-linking filaments as the tails of NFH and NFM are thought to do (Hirokawa et al., 1984)?

The Type III subunits are able to make filaments alone, but as seen above, can assemble with subunits of other classes and with each other. Vimentin and desmin form part of the same system (Schultheiss et al., 1991; Sejerson and Lendahl, 1993), vimentin coassembles with nestin and α-internexin (Chin et al., 1991; Ching and Liem, 1993), and peripherin and the neurofilaments are also coassembled (Parysek et al., 1991). The class V filaments, the nuclear lamins, are capable of some degree of self-assembly in vitro in spite of the usual coexpression of lamins A, B and C in most cells (Moir et al., 1991).

Roles of Filament Subdomains in Assembly

Rod Domain

In all of the intermediate filament subunits investigated, the rod domain has proved to be the most essential structure for filament assembly. Within that structure, the amino and carboxyl termini of the rod are the most intolerant of substitutions or deletions. The overall structure of the rod is also important for normal assembly. The conserved hydrophobic residues in the a and d position of the heptad repeat are thought to be essential for dimerization, but their influence is spread out across the whole rod, so that disruption of a small region does not interfere with assembly (Stewart, 1993). The rod domain has a charge structure superimposed on the heptad repeat, averaging three zones of positive and negative charges every 14 amino acids. Perturbation of the charge structure by alignment of identical charges in opposition along a stretch as short as ~4.75 amino acids results in severe assembly defects and the abolition of tetramer formation (Meng et al., 1994). This charge alternation seems to be more essential that preserving the α-helical structure of the rod, since proline mutations in internal segments of keratins are better tolerated than charge alterations (Letai et al., 1992). Shortening the length of the rod also severely inhibits filament formation at the level of tetramer formation, but only enormous deletions abolish dimer formation (Lu and Lane, 1990).

In a set of domain swapping experiments switching the four rod domains between K14 and vimentin, it was shown that the outer domains 1A and 2B had the strongest effect on filament assembly, and were the least tolerant of substitution. The internal rod domains 1B and 2A were able to substitute to some degree for the normal domain (McCormick et al., 1991). Keratin and vimentin filament systems do not coassemble but are both present in some cells. The long 1B and 2B domains had the strongest influence on which of the two systems the chimeric protein would associate with. The association of some of the chimeric keratin/vimentin constructs with one or the other of the independent filament systems in cells is eloquent testimony to the stability and conservation of the modes of binding between IF subunits of different classes.

Coil 1A conserved sequence

Sites in the conserved rod ends (the coil 1A and 2B consensus sequences) have been extensively investigated in site-directed mutagenesis studies. The same sites are hot spots for mutations in several families which carry the dominant genes for EBS and EHS.

The coil 1A consensus sequence is a domain of approximately 15 amino acids with intermittent homology, but high conservation in those positions between IFs of all classes, including the nuclear lamins. In human patients, the single most common missense mutation is at arginine 10 (respective to the start of the rod domain; marked in boldface in Figure 2) (Cheng et al., 1992; Chipev et al., 1994; Coulombe et al., 1991; Huber et al., 1994; Letai et al., 1993; McLean et al., 1994; Reis et al., 1994; Rothnagel et al., 1992; Syder et al., 1994). This codon contains a CpG dinucleotide. Methylation of cytosine followed by deamination can result in transitions, which account for many of the mutations at this site (Cheng et al., 1992). Mutations in nearby codons in the same domain account for more cases (Chipev et al., 1994; Huber et al., 1994; McLean et al., 1994; Reis et al., 1994; Rothnagel et al., 1994; Syder et al., 1994; Yang et al., 1994). The mild phenotype of larger deletions first used to analyze the 1A sequence did not suggest the dominant character of the amino terminal rod point mutations found in disease. For example deletions into the rod of K14 are recessive, and fail to polymerize in cells (Albers and Fuchs, 1989; Coulombe et al., 1990).

In neurofilaments, the result of amino terminal deletions was similar to that in K14. Deletions of the helix initiation sequences of NFM results in recessive proteins that fail to incorporate, or do so weakly (Chin et al., 1991; Gill et al., 1990). While deletion of some sequences in the head domain of NFL result in dominant, disruptive interactions with vimentin, further deletion into the rod from the amino terminus results in recessive mutations (Wong and Cleveland, 1990).

Coil 2B conserved sequence

Mutations in the conserved EIATYRKLLEGE sequence at the end of rod 2B are also found in skin disease patients (Chipev et al., 1994; Lane et al., 1992; Rothnagel et al., 1992; Syder et al., 1994; Yang et al., 1994). Deletions into the 2B conserved domain result in dominant mutants. Dominant disruptions were marked by the dense aggregation of keratins in the perinuclear zone and the loss of the

keratin filament network in the cytoplasm. Deletion of just the last eight amino acids of the rod of K14 results in less severe keratin filament disruptions in cells and mice than deletion of the entire coil 2B (Albers and Fuchs, 1987; Vassar et al, 1991). Transgenic mice made with this deletion do not blister, although filament clumping is visible by EM. In cells the 8 aa deletion is dominant only in simple epithelia that do not express K14. In cultured keratinocytes, other subunits seem to compensate for its deleterious effects. This lack of severity is interesting with regard to the data with the nestin mutants discussed in this work. In the EBS and EHS cases where point mutations have been localized to coil 2B, the phenotype is more severe than for a small deletion in the domain. Similar results were noted in proline substitutions in the 2B conserved sequence (Letai et al., 1992). The larger the deletion into coil 2B, the worse is the disruption of the keratin network in cultured cells (Albers and Fuchs, 1987).

Among Type IV IFs, large deletions from the carboxy terminus into the rod do not affect the ability of NFL and NFM to bind vimentin and associate, even if huge deletions from the rod are made (Chin et al., 1991; Gill et al., 1990; Wong and Cleveland, 1990). Such mutations always cause disruption of vimentin filaments by bringing about the aggregation and collapse of the IF system in cells.

Linker segments

Mutations in linker domains are tolerated to some extent. Patients suffering from milder forms of EBS have been found to carry mutations in L12 (Chan et al., 1994b). The linkers are less conserved between IF types, but are implicated in inter-dimeric interactions (Geisler et al., 1992). Large substitutions are tolerated in L1 in keratin 19 without affecting incorporation into simple epithelia (Rorke et al., 1992). The linker L12 seems to be less tolerant, and insertions of between 8 and 12 amino acids in NFL result in disruption (Gill et al., 1990). These results are consistent with the most favored IF assembly models, in which L12 interacts with the coil 2B conserved sequence, but L1 is not bound by such constraints (Steinert, 1993).

Non-helical domains

Both the sequences and the functions of the head and tail domains are more variable than those of the rod. Some keratin subunits

require intact head and tail domains, while others remain partially assembly competent without them.

Keratins

Human Keratin 14 is assembly competent with its partner K5 even with all but 8 amino acids of the head deleted (Albers and Fuchs, 1989), both in vitro and in cells. However its partner K5 requires the presence of its own head for normal-appearing assembly *in vitro*. The globular heads contribute to filament diameter in vitro (Coulombe and Fuchs, 1990). K5 also requires its tail for normal in vitro association, and without it, lateral interactions are increased, allowing the filaments to aggregate and to branch. The K14 tail is not essential for in vitro assembly into normal-looking filaments.

The non-helical domains play different roles in the assembly of filaments for different subunits. (Wilson et al., 1992) The authors suggest that the aggregation is caused by the absence of the tail, and speculate that the tail plays a role in covering sites that could otherwise serve as points of lateral interaction between filaments. A mutant K14 lacking both head and tail, while assembly competent, demonstrates greater affinity for K5 than wild type K14 at the level of tetramer formation. When both keratin partners were tailless, aberrant assembly resulted in vitro. Short filaments overlapped abnormally to form longer filaments. Thus, head and tail sequences may be essential for tempering the high affinity between keratin partners, enabling the cell to remodel filament structure.

In two skin disease cases, a mutation was found in the H1 region flanking the amino terminus of the rod domain, 20 amino acids from the conserved arginine in the coil 1A sequence of Type II keratins (Chipev et al., 1992; Yang et al., 1994). A peptide mimicking this region resulted in rapid filament disassembly in vitro. These results linked the disease for the first time to a domain outside the rod (Chipev et al., 1994). The current model for IF assembly puts this domain in close apposition to the rod ends or to the L2 linker, and cross-linking studies on rod fragments confirm these interactions (Steinert and Parry, 1993). This domain is specific to type II keratins, and cannot be generalized to other IFs.

Type III filaments

Sequences in the non-helical domains in Type III IFs are essential for self assembly. A domain in the head of vimentin and desmin has

been investigated through deletions and peptide interference studies (Beuttenmuller et al., 1994; Herrmann et al., 1992; Hoffmann and Herrmann, 1992). Without this 9 aa domain, assembly does not take place in the absence of normal IF s, but in vimentin-containing cells, headless vimentin subunits will incorporate at a low level (Andreoli and Trevor, 1994). The peptide interference experiments result primarily in filament unraveling, suggesting the importance of non-helical sites in regulating interactions between protofibrils (Hoffmann and Herrmann, 1992).

Tailless vimentin is unable to form filaments in vitro and in vivo, instead forming short fibrils. It can be rescued and incorporated into filaments by wild type vimentin in cells or in vitro (Eckelt et al., 1992). A domain in the tail common to vimentin, desmin and peripherin is required for proper assembly. A series of peptide and anti-idiotypic antibody experiments, demonstrated that this sequence on the Type III filament tail prevents aggregation and modulates assembly. The domain to which it binds is in coil 2B, to the amino side of the conserved sequence. Incubation with a peptide carrying the motif results in filament aggregation. The authors propose that this is a kind of intramolecular chaperone that prevents inappropriate filament formation (Kouklis et al., 1993; Kouklis et al., 1991; Kouklis et al., 1992; McCormick et al., 1993).

Neurofilaments

An internal deletion in the head domain of NFL results in dominant disruption of coassembly with vimentin. Larger deletions in the NFL head result in a lack of association with vimentin. Instead, the mutant proteins form aggregates without disruption of the vimentin filaments. More than half the NFL tail is also required for assembly (Gill et al., 1990). This is not the case for NFM. Removal of 90% of the tail has no effect on assembly ability using vimentin as a partner. Similarly, deletion of most of the head of NFM results in normal association with vimentin, but deletions into the rod fail to interact with vimentin at all (Wong and Cleveland, 1990; Ching and Liem, 1993). In vitro studies demonstrate that filaments assembled from headless NFL unravel, while tailless NFL filaments aggregate (Heins et al, 1993). The authors conclude that the head promotes lateral interactions while the tail controls them, although considering the proximity of the non-helical regions to the rod ends, these results could be explained by the destabilization of the rod as well.

Intermediate filament dynamics

A peptide corresponding to the conserved coil 2B sequence has radically altered assumptions about the static quality of cytokeratin filaments. When added to keratin 8 and 18 subunits, it prevents filament formation, instead favoring aggregation. When added to preassembled filaments it reduces them to small, aggregated subunits with astonishing rapidity (Hatzfeld and Weber, 1992). Incubation or microinjection of an antibody (IFA) against the 2B conserved region prevents assembly (Hatzfeld and Weber, 1992) and in vivo disrupts filaments (Klymkowsky, 1981). Thus, in spite of the extremely high affinity of one keratin type for the other (dimers exist in 9M urea) (Coulombe and Fuchs, 1990), the interaction of the oligomers is dynamic. In time-course studies after transfection, it was seen that new flagged subunits were found in filaments within hours, and there was no evidence for addition from any particular organizing center. (Albers and Fuchs, 1987; Albers and Fuchs, 1989). In filaments, the conserved sequence is readily accessible to the peptide and probably to new subunits as well. Both the addition of excess peptide and coassembly with subunits lacking the coil 2B conserved domain disrupt lateral interactions at the level of protofilament association, suggesting that multiple domains along the rod are involved in higher order association as well as dimerization.

Vimentin is also highly dynamic in its assembly. The vimentin network is reorganized at mitosis by phosphorylation by p34^{cdc2} kinase (Chou et al., 1990). The mode of new vimentin incorporation into filaments varies under different conditions. Assembly in fibroblasts began at numerous discrete sites throughout the network if the new subunits were expressed at low levels (Ngai et al., 1990). However, in BHK-21 cells, microinjected vimentin was first incorporated at the nuclear membrane (Vikstrom et al., 1989). The different modes of incorporation into existing filaments could instead be due to conditions in the different cell types used in the studies.

Summary

From this discussion, it is clear there is a hierarchy of interactions in intermediate filament assembly. The amino terminal of the rod domain is required for the earliest stages of interactions, and if it is deleted, the filament subunit is unable to associate with IFs. Point mutations that alter, but do not abolish interactions with wild type IF subunits produce a dominant negative phenotype. Even small

amounts of mutant subunits cause collapse of the whole IF structure of the cell. Deletions or mutations of the carboxyl terminal of coil 2B produce a dominant phenotype which is aggravated by further deletion into coil 2B. The head and tail domains sometimes contain sequences that regulate assembly. Their absence, or excess, in the case of the peptide experiments, leads to aggregation of IF oligomers. Similarly, an excess of the coil 2B conserved domain leads to aggregation.

References

Albers, K. and Fuchs, E. (1987). The expression of mutant epidermal keratin cDNAs transfected in simple epithelial and squamous cell carcinoma lines. J Cell Biol 105, 791-806.

Albers, K. and Fuchs, E. (1989). Expression of mutant keratin cDNAs in epithelial cells reveals posible mechanisms for initiation and assembly of intermediate filaments. J Cell Biol 108, 1477-1493.

Almazan, G. and McKay, R. (1992). An oligodendrocyte precursor cell line from rat optic nerve. Brain Res 579, 234-245.

Andreoli, J. and Trevor, K. (1994). Fate of a headless vimentin protein in stable cell cultures: soluble and cytoskeletal forms. Exp Cell Res 214, 177-188.

Balcarek, J. and Cowan, N. (1985). Structure of the mouse glial fibrillary acidic protein gene: implications for the evolution of the intermediate filament mutigene family. Nucl Acids Res 13, 5527.

Baribault, M., Price, J., Miyai, K. and Oshima, R. (1993). Mid-gestational lethality in mice lacking keratin 8. Genes Devel 7, 1191-1202.

Beuttenmuller, M., Chen, M., Janetzko, A., Kuhn, S. and Traub, P. (1994). Structural elements of the amino-terminal head domain of vimentin essential for intermediate filament formation in vivo and in vitro. Exp Cell Res 213, 128-142.

Cattaneo, E. and McKay, R. (1990). Proliferation and differentiation of neuronal stem cells regulated by nerve growth factor. Nature 347, 762-765.

Chan, Y.-M., I, A.-L., Yu, Q.-C., Jackel, A., Zabel, B., Ernst, J.-P. and Fuchs, E. (1994a). A human keratin 14 "knockout": the absence of K14 leads to severe epidermolysis bullosa simplex and a function for an intermediate filament protein. Genes & Dev 8, 2574-2587.

Chan, Y.-M., Yu, Q.-C., LeBlanc-Straceski, J., Christiano, A., Pulkkinen, L., Kucherlapapti, R., Uitto, J. and Fuchs, E. (1994b). Mutations in the non-helical linker segement L1-2 of keratin 5 in patients with Weber-Cockayne epidermolysis bullosa simplex. J Cell Sci 107, 765-774.

Cheng, J., Snyder, A., Yu, Q.-C., Letai, A., Paller, A. S. and Fuchs, E. (1992). The genetic basis of Epidermolytic Hyperkeratosis: a disorder of differentiation-specific epidermal keratin genes. Cell 70, 811-819.

Chin, S., Macioce, P. and Liem, R. (1991). Effects of truncated neurofilament proteins on the endogenous intermediate filaments in transfected fibroblasts. J Cell Sci 99, 335-350.

Ching, G. and Liem, R. (1993). Assembly of Type IV neuronal intermediate filaments in nonneuronal cells in the absence of preexisting cytoplasmic intermediate filaments. J Cell Biology 122, 1323-1335.

Chipev, C., Korge, B., Markova, N., Bale, S., DiGiovanna, J., Compton, J. and Steinert, P. (1992). A leucine -> proline mutation in the H1 subdomain of keratin 1 causes epidermolytic hyperkeratosis. Cell 70, 821-828.

Chipev, C., Yang, J.-M., DiGiovanna, J., Steinert, P., Marekov, L., Compton, J. and Bale, S. (1994). Preferential sites in Keratin 10 that are mutated in Epidermolytic Hyperkeratosis. Am J of Human Genet 54, 179-190.

Chou, Y.-H., Bischoff, J., Beach, D. and Goldman, R. (1990). Intermediate filament reorganization during mitosis is mediated by p34^{cdc2} phosphorylation of vimentin. Cell 62, 1063-1071.

Colluci-Guyon, E., M.-M. Portier, et al. (1994). Mice lacking vimentin develop and reproduce without an obvious phenotype. Cell 79, 679-694.

Cote, F., Collard, J.-F. and Julien, J.-P. (1993). Progressive Neuronopathy in transgenic mice expressing the human neurofilament heavy gene: a mouse model of amyotrophic lateral sclerosis. Cell 73, 35-46.

Coulombe, P. (1993). The cellular and molecular biology of keratins: Beginning a new era. Curr Opin Cell Biol 5, 17-29.

Coulombe, P., Chan, Y.-M., Albers, K. and Fuchs, E. (1990). Deletions in epidermal keratins leading to alteration in filament organization in vivo and in intermediate filament assembly in vitro. J Cell Biol 111, 3049-3064.

Coulombe, P. and Fuchs, E. (1990). Elucidating the early stages of keratin filament assembly. J Cell Biol 111, 153-169.

Coulombe, P. A., Hutton, M. E., Letai, A., Hebert, A., Paller, A. P. and Fuchs, E. (1991). Point mutations in human Keratin 14 genes of Epidermolysis Bullosa Simplex patients: genetic and functional analysis. Cell 66, 1301-1311.

Dahlstrand, J., Collins, V. and Lendahl, U. (1992a). Expression of the Class VI intermediate filament nestin in human central nervous system tumors. Cancer Res 52, 5334-5341.

Dahlstrand, J., Lardelli, M. and Lendahl, U. (1994). Nestin mRNA expression correlates with the CNS progenitor cell state in many, but not all, regions of the CNS. Dev Brain Res in press.

Dahlstrand, J., Zimmerman, L., McKay, R. and Lendahl, U. (1992b). Characterization of the human nestin gene reveals a close evolutionary relationship to neurofilaments. J Cell Sci 103, 589-597.

Deng, H.-X., Hentati, A., Tainer, J., Iqbal, Z., Cayabyab, A., Hung, W.-Y., Getzoff, E., Hu, P., Herzfeldt, B., Roos, R., Warner, C., Deng, G., Soriano, E., Smyth, C., Parge, H., Ahmed, A., Roses, A., Hallewell, R., Pericak-Vance, M. and Siddique, T. (1993). Amyotrophic lateral sclerosis and structural defects in CuZn superoxide dismutase. Science 261, 1047-1051.

Eckelt, A., Herrmann, H. and Franke, W. (1992). Assembly of a tail-less mutnt of the intermediate filament protein, vimentin, in vitro and in vivo. Eur. J Cell Biol 58, 319-330.

Eyer, J. and Peterson, A. (1994). Neurofilament-deficient axons and perikaryal aggregates in viable transgenic mice expressing a neurofilament-b-galactosidase fusion protein. Neuron 12, 389-405.

Fliegner, K., Kaplan, M., Wood, T., Pintar, J. and Liem, R. (1994). Expression of the gene for the neuronal intermediate filament protein a-internexin conicides with the onset of neuronal differentiation in the developing rat nervous system. J Comp Neurol 342, 161-173.

Frederiksen, K. and McKay, R. (1988). Proliferation and differentiation of rat neuroepithelial precursor cells *in vivo*. J Neurosci 8, 1144-1151.

Friedman, B., Zaremba, S. and Hockfield, S. (1990). Monoclonal antibody Rat 401 recognizes Schwann cells in mature and developing peripheral nerve. J Comp Neurol 295, 43-51.

Fuchs, E. (1994). Intermediate filaments and disease: mutations that cripple cell strength. J Cell Biol 125, 511-516.

Fuchs, E., Esteves, R. and Coulombe, P. (1992). Transgenic mice expressing a mutant keratin 10 gene reveal the likely genetic basis for epidermolytic hyperkeratosis. PNAS (USA) 89, 6906-6910.

Geisler, N., Schuenemann, J. and Weber, K. (1992). Chemical cross-linking indicates a staggered and anti-parallel protofilament of desmin intermediate filaments and characterizes on higher-level complex between protofilaments. Eur J Biochem 206, 841-852.

Gill, S., Wong, P., Monteiro, M. and Cleveland, D. (1990). Assembly properties of dominant and recessive mutations in the small mouse nuerofilament (NF-L) subunit. J Cell Biol 111, 2005-2019.

Gotow, T., Takeda, M., Tanaka, T. and Hashimoto, P. (1992). Macromolecular structure of reassembled neurofilaments as revealed by the quick-freeze deep-etch mica method: difference between NF-M and NF-H subunits in their ability to form cross bridges. Eur J Cell Biol 58, 331-345.

Hatzfeld, M. and Weber, K. (1992). A synthetic peptide representing the consensus sequence motif at the carboxy-terminal end of the rod domain inhibits intermediat filament assembly and disassembles preformed filaments. J Cell Biol 116, 157-166.

Heins, S., P. Wong, et al. (1993). The rod domain of NF-L determines neurofilament architecture, whereas the end domains specify filament assembly and network formation. J Cell Biol 123, 1517-1533.

Hemmati-Brivanlou, A., Mann, R. and Harland, R. (1992). A protein expressed in the growth cones of embryonic vertebrate neurons defines a new class of intermediate filament protein. Neuron 9, 417-428.

Herrmann, H., Hoffmann, I. and Franke, W. (1992). Identification of a nonapeptide motif in the vimentin head domain involved in intermediate filament assembly. J Mol Biol 223, 637-650.

Hirokawa, N., Glicksman, M. and Willard, M. (1984). Organization of mammalian neurofilament polypeptides within the neuronal cytoskeleton. J Cell Biol 98, 1523-1536.

Hockfield, S. and McKay, R. (1985). Identification of major cell classes in the developing mammalian nervous system. J Neurosci 5, 3310-3328.

Hoffmann, I. and Herrmann, H. (1992). Interference in vimentin assembly in vitro by synthetic peptides derived from the vimentin head. J Cell Sci 101, 687-700.

Houle, J. and Fedoroff, S. (1983). Temporal relationship between the appearance of vimentin and neural tube development. Dev Brain Res 9, 189-195.

Huber, M., Scaletta, C., Benathan, M., Frenk, E., Greenhalgh, D., Rothnagel, J., Roop, D. and Hohl, D. (1994). Abnormal keratin 1 and 10 cytoskeleton in cultured keratinocytes from Epidermolytic Hyperkeratosos caused be keratin 10 mutations. J Invest Dermatol 102, 691-694.

Julien, J.-P., Cote, F., Beaudet, L., Sidky, M., Flavell, D., Grosveld, F. and Mushynski, W. (1988). Sequence and structure of the mouse gene coding for the largest neurofilament subunit. Gene 68, 307-314.

Kachinsky, A., Dominov, J. and Miller, J. (1994). Myogenesis and the intermediate filament protein, nestin. Dev Biol165, 216-228.

Klymkowsky, M. (1981). Intermediate filaments in 3T3 cells collapse after the intracellular injection of a monoclonal anti-intermediate filament antibody. Nature 291, 249-251.

Knapp, B., Rentrop, M., Schwiezer, J. and Winter, H. (1986). Non-epidermal members of the keratin multigene family: cDNA sequences and in situ localizations of the mRNAs. Nucl Acids Res 14, 751-763.

Kouklis, P., Hatzfeld, M., Brunkener, M., Weber, K. and Georgatos, S. (1993). In vitro assembly properties of vimentin mutagenized at the b-site tail motif. J Cell Sci 106, 919-928.

Kouklis, P., Papamarcaki, T., Merdes, A. and Georgatos, S. (1991). A potential role for the COOH-terminal domain in the lateral packing of Type III intermediate filaments. J Cell Biol 114, 773-786.

Kouklis, P., Traub, P. and Georgatos, S. (1992). Involvement of the consensus sequence motif at coil 2b in the assembly and stability of vimentin filaments. J Cell Sci 102, 31-41.

Lane, E., Rugg, E., Navsaria, H., Leigh, I., Heagerty, A., Ishida-Yamamoto, A. and Eady, R. (1992). A Mutation in the Conserved Helix Termination Peptide of Keratin 5 in Hereditary Skin Blistering. Nature 356, 244-246.

Lee, M., Xu, Z., Wong, P. and Cleveland, D. (1993). Neurofilaments are obligate heteropolymers in vivo. Journal of Cell Biology 122, 1337-1350.

Lendahl, U., Zimmerman, L. and McKay, R. (1990a). CNS stem cells express a new class of intermediate filament protein. Cell 60, 585-595.

Letai, A., Coulombe, P. and Fuchs, E. (1992). Do the ends justify the mean? Proline mutations at the ends of the keratin coiled-coil rod segment are more disruptive than internal mutations. J Cell Biol 116, 1181-1195.

Letai, A., Coulombe, P., McCormick, M., Yu, Q.-C., Hutton, E. and Fuchs, E. (1993). Disease severity corrlelates with position of keratin point mutations in patients with epidermolysis bullosa simplex. PNAS 90, 3197-3201.

Liem, R. (1993). Molecular biology of neuronal intermediate filaments. Curr Opin Cell Biol 5, 12-16.

Lu, X. and Lane, E. (1990). Retrovirus-mediated transgenic keratin expression in cultured fibroblasts: specific domain functions in keratin stabilization and filament formation. Cell 62, 681-696.

Luskin, M., Pearlman, A. and Sanes, J. (1988). Cell lineage in the cerebral cortex of the mouse studied in vitro and in vivo. Neuron 1, 635-647.

McCormick, M., Coulombe, P. and Fuchs, E. (1991). Sorting out IF networks: Consequences of domain swapping on IF recognition and assembly. J Cell Biol 113, 1111-1124.

McCormick, M., Kouklis, P., Snyder, A. and Fuchs, E. (1993). The roles of the rod end and the tail in vimentin IF assembly and IF network formation. Journal of Cell Biology 122, 395-407.

McKeon, F., Kirschner, M. and Caput, D. (1986). Homologies in both primary and secondary structure between nuclear envelope and intermediate filament proteins. Nature 319, 463-468.

McLean, W., Eady, R., Dopping-Hepenstal, P., McMillan, J., Leigh, I., Navsaria, H., Higgins, C., Harper, J., Paige, D., Morley, S. and Lane, E. (1994). Mutations in the Rod 1A domain of keratins 1 and 10 in Bullous Congenital Ichthyosiform Erythroderma (BCIE). J Invest Dermatol102, 24-30.

Meng, J.-J., Khan, S. and Ip, W. (1994). Charge interactions in the rod domain drive formation of tetramers during intermediate filament assembly. J Biol Chem 269, 18679-18685.

Mitanyi, S., Winkles, J., Sargent, T. and Dawid, I. (1986). Stage-specific keratins in *Xenopus Laevis* embryos and tadpoles: the XK81 gene family. J Cell Biol 103, 1957-1965.

Moir, R., Donaldson, A. and Stewart, M. (1991). Expression in Escherichia coli of human lamins A and C: influence of head and tail domains on assembly properties and paracrystal formation. J Cell Sci 99, 363-372.

Monteiro, M., Hoffman, P., Gearhart, J. and Cleveland, D. (1990). Expression of NF-L in both neuronal and nonneuronal cells of transgenic mice: Increased Neurofialment density in axons without affecting caliber. J Cell Biol 111, 1543-1557.

Ngai, J., Coleman, T. and Lazarides, E. (1990). Localization of newly synthesized vimentin subunits reveals a novel mechanism of intermediate filament assembly. Cell 60, 415-427.

Ohara, O., Gahara, Y., Miyake, T., Teraoke, H. and Kitamura, T. (1993). Neurofilament deficiency in quail caused by nonsense mutation in neurofilament-L gene. J Cell Biol 121, 387-395.

Oshima, R. (1992). Intermediate filament molecular biology. Curr Opin Cell Biol 4, 110-116.

Parysek, L., McReynolds, M., Goldman, R. and Ley, C. (1991). Some neural intermediate filaments contain both peripherin and the neurofilament proteins. J Neurosci Res 30, 80-91.

Price, J. and Thurlow, L. (1988). Cell lineage in the rat cerebral cortex: a study using retroviral mediated gene transfer. Development 104, 473-482.

Rakic, P. (1971). Neuron-glia relationship during granule cell migration in developing cerebellar cortex. J Comp Neurol 141, 283-312.

Reis, A., Hennies, H.-C., Langbein, L., Digweed, M., Mischke, D., Drechsler, M., Schrock, E., Royer-Pokora, B., Franke, W., Sperling, K. and Kuster, W. (1994). Keratin 9 gene mutations in epidermolytic palmoplantar keratoderma (EPPK). Nature Genetics 6, 174-179.

Renfranz, P., Cunningham, M. and McKay, R. (1991). Region-specific differentiation of the hippocampal stem cell line HiB5 upon implantation into the developing mammalian brain. Cell 66, 713-729.

Reynolds, B., W. Tetzlaff, et al. (1992). A multipotent EGF-responsive striatal embryonic progenitor cell produces neurons and astrocytes. J Neurosci 12, 4565-74.

Reynolds, B. and S. Weiss (1992). Generation of neurons and astrocytes from isolated cells of the adult mammalian central nervous system. Science 255, 1707-1710.

Rorke, E., Crish, J. and Eckert, R. (1992). Central rod domain insertion and carboxy-terminal fusion mutants of human cytokeratin K19 are incorporated into endogenous keratin filaments. J Invest Dermatol 98, 17-23.

Rothnagel, J., Dominey, A., Dempsey, L., Longley, M., Greenhalgh, D., Gagne, T., Huber, M., Frenk, E., Hohl, D. and Roop, D. (1992). Mutations in the Rod Domains of Keratins 1 and 10 in Epidermolytic Hyperkeratosis. Science 257, 1128-1130.

Rothnagel, J., Longley, M., Holder, R., Kuster, W. and Roop, D. (1994). Prenatal diagnosis of Epidermolytic hyperkeratosis by direct gene sequencing. J Invest Dermatol102, 13-16.

Rugg, E., McLean, W., Lane, E., Pitera, R., McMillan, J., Dopping-Hepenstal, P., Navsaria, H., Leigh, I. and Eady, R. (1994). A functional "knockout" of human keratin 14. Genes & Dev 8, 2563-2573.

Sarria, A., Panini, A. and Evans, R. (1992). A functional role for vimentin intermediate filaments in the metabolism of lipoprotein-derived cholesterol in human SW13 cells. J Biolo Chem 267, 19455-19463.

Schultheiss, T., Lin, Z., Ishikawa, H., Zamir, I., Stoeckert, C. and Holtzer, H. (1991). Desmin/Vimentin intermediate filaments are dispensible for many aspects of myogenesis. JCB 114, 953-966.

Sejerson, T. and Lendahl, U. (1993). Transient expression of the intermediate filament nestin during skeletal muscle differentiation. J Cell Sci 106, 1291-1300.

Shea, T., Beermann, M. and Fischer, I. (1993). Transient requirement for vimentin in neuritogenesis: intracellular delivery of anti-vimentin antibodies and antisense oligonucleotieds inhibit neurite initiation but not elongation of existing neurites in neuroblastoma. J Neurosci Res 36, 66-76.

Snyder, E., Diechter, D., Walsh, C., Arnold-Aldea, S., Hartweig, E. and Cepko, C. (1992). Multipotent neural cell lines can engraft and participate in development of mouse cerebellum. Cell 68, 33-51.

Sotelo, C., Alvarado-Mallart, R.-M., Frain, M. and Vernet, M. (1994). Molecular plasticity of adult Bergmann fibers is associated with radial migration of grafted Purkinje cells. J Neurosci 14, 124-133.

Steinert, P. (1993). Structure, function and dynamics of keratin intermediate filaments. J Invest Dermatol 100, 729-734.

Steinert, P. and Liem, R. (1990). Intermediate filament dynamics. Cell 60, 521-523.

Steinert, P. and Parry, D. (1993). The conserved H1 domain of the Type II keratin 1 chain plays an essential role in the alignment of nearest neighbor molecules in mouse and human keratin 1/keratin 10 intermediate filaments

at the two- and four-molecule level of structure. J Biol Chem 268, 2878-2887.

Steinert, P. and Roop, D. (1988). Molecular and cellular biology of intermediate filaments. Annu Rev Biochem 57, 593-625.

Stewart, M. (1993). Intermediate filament structure and assembly. Curr Opin Cell Biol 5, 3-11.

Syder, A., Yu, Q.-C., Paller, A., Giudice, G., Pearson, R. and Fuchs, E. (1994). Genetic mutations in the K1 and K10 genes of patients with Epidermolytic Hyperkeratosis. J Clin Invest 93, 1533-1542.

Temple, S. (1989). Division and differentiation of isolated CNS blast cells in microculture. Nature 340, 471-473.

Tohyama, T., Lee, V. M.-Y., Rorke, L., Marvin, M., McKay, R. and Trojanowski, J. (1992). Nestin expression in embryonic human neuroepithelium and in human neuroepithlial tumor cells. Lab Invest 66, 303-313.

Valtz, N., Hayes, T., Norregard, T., Liu, S. and McKay, R. (1991). An embryonic origin for medulloblastoma. New Biologist 3, 364-371.

Vassar, R., Coulombe, P. A., Degenstein, L., Albers, K. and Fuchs, E. (1991). Mutant keratin expression in transgenic mice causes marked abnomalities resembling a human genetic skin disease. 64, 365-380.

Vicario, C., Johe, K., Hazel, T., Collazo, D. and McKay, R. (1995). Proliferation and differentiation of hippocampal cells in resonse to basic-fibroblast growth factor and neurotrophins. Submitted

Vikstrom, K., Borisy, G. and Goldman, R. (1989). Dynamic aspects of intermediate filament networks in BHK-21 cells. PNAS 86, 549-553. Walsh, C. and Cepko, C. (1988). Widespread dispersion of neuronal clones across functional regions of the cerebral cortex. Science 241, 1342-1345.

Weinstein, D., Shelanski, M. and Liem, R. (1991). Suppression by antisense mRNA demonstrates a requirement for the glial fibrillary acidic protein in the formation fo stable astrocytic processes in response to neurons. J Cell Biol 112, 1205-1213.

Wilson, A., Coulombe, P. and Fuchs, E. (1992). The roles of K5 and K14 head, tail, and R/KLLEGE domains in keratin filament assembly in vitro. J Cell Biol 119, 404-414.

Wong, P. C. and Cleveland, D. W. (1990). Characterization of dominant and recessive assembly-defective mutation in mouse neurofilament NF-M. J Cell Biol 111, 1987-2003.

Xu, Z., Cork, L., Griffin, J. and Cleveland, D. (1993). Increased expression of neurofilament subunit NF-L produces morphological alterations that resemble the pathology of human motor neuron disease. Cell 73, 23-33.

Yang, H.-Y., Lieska, N., Goldman, R., Johnson-Seaton, D. and Pappas, G. (1992). Distinct developmental subtypes of cultured non-stellate rat astrocytes distinguished by a new glial intermediate filament-associated protein. Brain Res. 573, 161-168.

Yang, H.-Y., Lieska, N., Shao, D., Kriho, V. and Pappas, G. (1993). Immunotyping of radial glia and their glial derivatives during development of the rat spinal cord. J Neurocytol 22, 558-571.

Yang, J.-M., Chipev, C., DiGiovanna, J., Bale, S., Marekov, L., Steinert, P. and Compton, J. (1994). Mutations in the H1 and 1A domains in the Keratin 1 gene in Epidermolytic Hyperkeratosis. J Invest Dermatol 102, 17-23.

Zimmerman, L., Lendahl, U., Cunningham, M., McKay, R., Parr, B., Gavin, B., Mann, J., Vassileva, G. and McMahon, A. (1994). Independent regulatory elements in the nestin gene directs transgene expression to neural stem cells or muscle precursors. Neuron 12, 11-24.

Figure 1. (Upper) Schematic diagram of organization of each class of intermediate filaments and nestin. Gray boxes represent the central α-helical domain and the open boxes the N- and C-terminal parts of the proteins. The percentage of identical amino acids between nestin and the other intermediate filaments in the α-helical domain is presented (amino acid identity). Vertical bars indicate splice sites (Julien et al., 1988). The core region is expanded (redrawn from (Steinert and Roop, 1988)) to show heptad containing coil regions (1A, 1B, 2A, 2B) separated by non-heptad linkers (L1, L12, L2). The conserved stutter in coil 2B, represented by an offset, corresponds to a phase shift in the heptad structure. Lamin A contains an extra six heptads in coil 1B; its intron/exon structure is not known. (Lower) Predicted amino acid residues 7-314 of nestin (the core domain) are aligned with the corresponding regions of the other intermediate filaments; the usually hydrophobic heptad residues a and d are indicated. K1 is a Xenopus type I keratin (Class I) (Mitanyi et al., 1986); K2 is a mouse type II keratin (Class II) (Knapp et al., 1986); GFA is mouse astrocytic glial fibrillary acidic protein (Class III) (Balcarek and Cowan, 1985), NFH is mouse neurofilament heavy chain (class IV) (Julien et al., 1988); LAM is human lamin A (Class V) (McKeon et al., 1986). Reprinted from (Lendahl et al., 1990) with permission.

IF   aa identity
K1   (21%)
K2   (20%)
LAM (16%)
GFA (29%)
NFH (24%)
NES

```
N          L1          L12  L2            C
    1A          1B        2A       2B
```

```
i            coil 1A                      linker L1    51       coil 1B                              100
         a   d   a   d   a   d   a   d   a   d                 d   a   d   a   d   a   d   a   d   a   d
K1   EKHAMQNLNDRLASYLEKVRALEATNSDLEGKIRNW-YDKQSDAGIGAGSKDYSK-YFEIIAELRNKIRAATIDNATVTLQIDNARLAADDFRL------
K2   EREQIKTLNNKFASFIDKVRFLEQQNKVLETKWNLL-QQQTTTTSPKSLDPF----FETYINALRKNLDTLSNDKGRLQSELKMMQDSVEDFKT------
LAM  LQELNDRLAVYIDRVRSLETENAGLRLRITESEEVV-SREVSGIKAA---------YEAELGDARKTLDSVAKERARLQLELSKVREEFKELKARNTKKE
GFA  ERAEMMELNDRFASYIEKVRFLEQQNKALAAELNQL-RAKEPTKLADV--------YQAELRELRLRLDQLTANSARLEVERDNFAQDLGTLRQ-----
NFH  EKEQLQALNDRFAGYIDKVRQLEAHNRSLEGEAAAL-RQQKGRAAMGEL-------YEREVREMRGAVLRLGAARGQLRLEQEHLLEDIAHVRQ------
NES  ESFQMWELNRRLEAYLTRVKTLEEQNQLLSAELGGL-RAQSGDTSWRAR-------ADDELASLRILVDQRWREKLEAEVQRDNLAEELESVAG------

     101                          151                                          200
         a   d   a   d   a   d   a   d   a   d   a   d   a   d   a   d   a   d   a   d   a   d   a   d   a linker L12
K1   ----------------------------------QFENELALRQSVEGDSNGLRRVLDELILARGDFELQIESLTEELAYLKKNEEEMSHA-KSQSA
K2   ----------------------------------KYEEEINKRTAAENDFVVLKKDVDAAYMIKVELEAKMESLKDEINFTRVLYEAELAQM-QTHVS
LAM  GDLIAAQARLKDLEALLNSKEAALSTALSEKRTLEGELHDLRGQVAKLEAALGEAKKQLQDEMLRRVDAENRLQTMKEELDFQKNIYSEELRET-KRRHE
GFA  ----------------------------------KLQDETNLRLEAENNLAAYRQEAHEATLARVDLERKVESLEEEIQFLRKIYEEEVRDL-REQLA
NFH  ----------------------------------RLDEEARQREEAEAAARALAFAQEAE-AARVELQKKAQALQEECGYLRRHQEEVGEL-LGQIQ
NES  ----------------------------------RCQQVRLARERTVQEAACSRRALEAEKNARGWLSTQAAELERELEALRAAHEEERAHL-NAQAA

     201                  coil 2A               linker L2   251      coil 2B                           300
             d   a   d   a   d                 a   d   a   d   a   d   a   d   a   d   a   d   a   d
K1   GKVSVEMDAALGVOLT------SILNNMRADYEILAEKNRR-DAELWFNQ-KSGELKKEISVGVEQVQAHKSEITELKRSLQSLEIELQSQLAMKQSVEG
K2   DTSVVLSMDNNRNLDLD------GIIAEVRAQYEDIARKSKA-EVESWYQI-KVQQLQMSADQHGDSLKTTKNEISELNRMIQRLRAEIENIKKQSQTPQA
LAM  TRLVEIDNGKQREFESRLA----DALQELRAQHEDQVEQYKK-ELEKTYSA-KLDNARQSAERNSNLVGAAHEELQQSRIRIDSLSAQLSQLQKQLAAKEA
GFA  QQQVHVEMDVAKPDLT------AALREIRTQYEAVATSNMQ-ETEEWYRS-KFADLTDAASRNAELLRQAKHEANDYRRQLQALTCDLESLRGTNESLER
NFH  GCGAAQAQAQAEARDALKCDVT-SALREIRAQLEGHAVQSSL-QSEEWFRV-RLDRLSEAAKVNTDAMRSAQEEITEYRRQLQARTTELEALKSTKESLER
NES  CAPRRPPAPPHGSPVRAP-----EVEDLARRLGEVWRGAVRD------YQE-RVAHMESSLGQARERLSQAVRGARECRLEVQQLQADRDSLQERREALEQ

     301      "stutter"                       351            370
         a   d   a   a   d   a   d   a   d   a   d   a   d   a   d   a   d   a
K1   NLNELQGFYSSQLQQIQNTIGSLEEQLLQIRSDMEHQNTEYKLLLDIKTRLEMEIQTYRRLLEGELGQV
K2   SVADAEQRGELALKDAYSKRAELETALQKAKEDLARLLRDYQALMNVKLALDVEIATYRKLLEGEECRM
LAM  KLRDLEDSLARERDTSRRLLAEKEREMAEMRARMQQQLDEYQELLDIKLALDMEIHAYRKLLEGEEERL
GFA  QMREQEERHARESASYQEALARLEEEGQSLKEEMARHLQEYQDLLNVKLALDIEIATYRKLLEGEENRI
NFH  QRSELEDRHQADIASYQDAIQQLDSELRNTKWEMAAQLREYQDLLNVKMALDIEIAAYRKLLEGEECRI
NES  RLEGRWQDRLQATDKFQLAVEALEQEKQGLQSQIAQILEGGQQLAHLKMSLSLEVATYRTLLEAENSRL
```

36

Figure 2. Diagram of the consensus sites at the rod ends in intermediate filament proteins. The schematic diagram does not represent any individual intermediate filament protein. *Coil 1A consensus:* 15 amino acid consensus sequence found in all intermediate filaments at the amino terminus of coil 1A. The amino acid residue in italics is conserved in the head domain. The boldface arginine **R** represents a hot spot for mutations in human keratins 1, 10, 14, 5 and 9 which causes a set of skin diseases. *Coil 2B consensus:* 12 amino acid consensus sequence found at the C terminus of coil 2B.

Coil 1A consensus
E(X/R)XQMXXLND**R**(L/F)AXY

Coil 2B consensus
EIATYRKLLEGE

N ⸺ [1A] [1B] ⸺ [2A] [2B] ⸺ C

L1   L12   L2
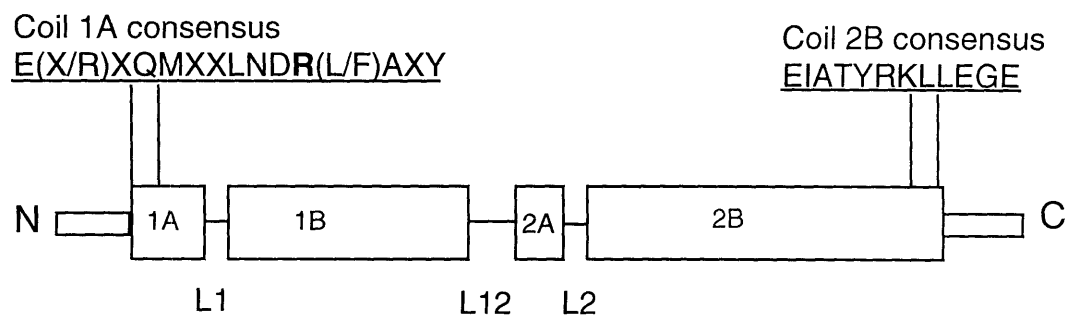
Multipotential stem cells in the vertebrate CNS

Martha Marvin and Ron McKay

The functional differences between the many mature neuronal types make the origins of cellular diversity in the nervous system one of the most intriguing problems in biology. This paper discusses recent experiments which explore the mechanisms generating cell diversity in the vertebrate central nervous system, focusing particulary on the immediate precursor to neurons and on neuronal differentiation. Transplantation experiments have been used to explore regional and temporal differences in the cells of the neuroepithelium. The effects of specific genes on neuronal development have been examined by mutational analysis in transgenic mice and in established neuronal stem cell lines. The combination of methods now available allow increasingly powerful dissection of the molecular and cellular mechanisms that generate the large number of different neurons in the vertebrate brain.

Key words: stem cells / lineage / brain development / transplants

AN OVERVIEW OF CNS development demonstrates there are many points at which cells make decisions that influence their fate. The classic Spemann-Mangold experiments in *Xenopus* showed that transplanting the dorsal lip of the blastopore to a second embryo induces host tissue to form a duplicate nervous system.[1] This result demonstrates that the formation of the vertebrate nervous system is initiated by an inductive signal which passes from mesoderm to the presumptive neuroectoderm during gastrulation. The sheet of cells that will give rise to the nervous system then folds to form the neural tube. Changes in morphology and gene expression reflect the division of the neuroepithelium into regions which correspond to the major subdivisions of the adult CNS. These observations show that events important to differentiation occur during gastrulation and neurulation, before neurons are generated. Recent studies with mutant mice have now identified some of the genes that play a part in these early steps of CNS differentiation.

Neurons and glia differentiate during embryonic development on a precise, region-specific schedule, with neurons born first, followed by the different types of glia. Quiescent glial precursors are found in the adult brain, but in mammals, neuronal precursors are found only in the developing brain. Thus, unlike their counterparts in the hemopoietic system, neuronal stem cells generally have a limited lifespan *in vivo*. Many recent experiments have fate mapped embryonic CNS precursors. Among their major conclusions is the description of a multi-potential neuronal stem cell.

The identification of a multipotential precursor that becomes committed to specific fates suggests either a stochastic mechanism or the presence of extracellular signals that regulate differentiation. *In vivo* transplant experiments define the timing of fate restriction and support a model in which extracellular signals drive the precursor cell to different fates. *In vitro* studies of cultured precursors are valuable tools to determine the extracellular signals that influence the fate of the precursor cells. Although this problem is just begining to be studied, techniques have been developed that allow the identification of growth factors acting on neuronal precursor cells.

This overview shows that a series of sequential differentiation events specify cell type in the adult brain.[2,3] Clearly, many different mechanisms must regulate these differentiation events. This review is focused on the immediate precursor to neurons, the lineage of this cell, when it becomes committed, how it is identified, how it behaves *in vitro*, the fact that it can be immortalized, and the role of specific genes in its differentiation.

Committment to a neuronal fate

When does a young neuron commit itself to a particular fate? Thymidine labelling studies show that the cerebral cortex develops from the inside out.[4,5] Stem cells divide in the ventricular zone, then their post-mitotic progeny migrate outward. Neurons of the inner layers are born first, and later neuronal cell bodies move past them along radial glia toward the pial surface. Each layer

is made up of functionally and molecularly distinct neuronal types.

In the reeler mouse mutant, migrating neurons are unable to pass the neurons born earlier. This results in a cortex in which the layers are inverted and disorganized.[6] Despite their altered environment, the cells do make long range functional connections appropriate for their birthdates.[7-9] These and other studies suggest that the proper ordering of neurons in cortical layers is not necessary to the development of the identity of neurons (reviewed in ref 10).

Embryonic cortical cells taken from the mitotic ventricular zone and transplanted to the neonatal ferret cortex will migrate to the position they would have taken in the donor, but only if they remain in the donor for several hours after their final S-phase. If their final S-phase takes place nearer the time of the transplant, the cells that differentiate go to the same cortical layer as the host cells which are currently differentiating.[11] These experiments show that neuronal precursor cells make a committment to a laminar fate within 4 h after their final S-phase.[12] Embryonic cells are competent to respond to signals in the older brain if they are not already committed. This suggests that there is little difference between neuronal precursors at early and late stages of cortical development. Taken with the reeler results, it says that, in response to extracellular signals, a multipotent neuronal stem cell becomes committed to a particular laminar fate while still in the proliferative ventricular zone of the neuroepithelium.

Lineage studies

In lineage experiments, stem cells are marked at an early stage of development and the distribution of their progeny is observed later in development. Analysis of clones of cells in the developing embryo traces their descent from a common precursor. Knowledge of the lineage relationships between cells is important in determining when and how fate restrictions are applied to cells, and whether closely related cells may contribute to the establishment of the functional architecture of the brain.

The two primary techniques for marking clones are microinjection of a molecule that cannot diffuse out of the cells, such as fluorescently tagged dextran, and marking with a genetic tag. Retroviruses carrying the *lac Z* gene encoding β-galactosidase

infect dividing cells and make them visible upon reaction with a chromogenic substrate.[13,14] Each technique has its limitations. Dextran can be diluted by cell division, while infected cells can stop expressing *lac Z*. Provided the number of clones marked is small and clone members are not too widely dispersed, the lineage of marked cells can be traced to a single precursor. Several different brain regions have been analyzed with lineage tracing methods.

Retina

Because it is the most accessible, the retina was the vertebrate CNS region first studied with lineage tracing methods. The retina is derived from an outfolding of the neural tube. The postnatal neural retina develops four types of neurons and the non-neuronal Müller glial cell, arranged in distinct layers. Location and morphology are good indicators of cell type. Independent studies using fluorescent tracing or genetic marking showed that in the rat and frog retina, the precursors can contribute cells of any type. There is no evidence for committed progenitors.[15-18] These results show unequivocally that both different types of neurons and non-neuronal cells can be derived from a common precursor cell, even at the terminal mitosis.

In non-mammalian vertebrates, the presence of extracellular signals regulating stem cell differentiation is suggested by two different manipulations of the retina. In amphibians, the peripheral ciliary margin remains mitotic after the central retina matures. The peripheral cells are multipotential precursors for cells of both the neural retina and pigmented epithelium.[19] These cells receive feedback from the differentiated retina that enables them to preferentially replace experimentally ablated cell types.[20,21] Cells in the pigment epithelium can resume proliferation and give rise to retinal cells if the entire retina is removed.[22,23] These observations emphasize that the differentiation of some cells is not terminal and that cell fate is regulated by extracellular signals.

Optic tectum

Retinal ganglion cells project axons through the optic nerve to the thalamus. The optic tectum is a major part of the visual thalamus in chickens. In the chick

optic tectum, clones containing astrocytes, radial glia, and several types of neurons have been observed.[24,25] Neurons migrate from the proliferative zone along radial glia, a transient cell type found in the developing brain (reviewed in ref 26).[5] Immunohistochemical studies of neuronal precursor cell development suggested that radial glial cells might have a close lineage relationship to neurons.[27,28] The presence of radial glial cells in clones containing neurons supports this relationship.

If the marking is done early, there are several columns of cells in a clone, while later infection results in single columns. This suggests that daughter cells migrate in the plane of the neuroepithelium after early divisions but cells produced later migrate radically, perpendicular to the plane of the epithelium.[29] In many regions of the brain, clustered columns of neurons process information of the same type.[30] It has been proposed that radial migration of lineage-related cells contributes to the establishment of functional columns.[5] The arrangement of radially arrayed groups of neurons does resemble the functional units of neurons seen in optic tectum but there is no evidence that lineage relations are an obligatory step in establishing functional columns.

Spinal cord

The motor neurons of the ventral spinal cord are among the first neurons to become postmitotic in the central nervous system. Two quite distinct techniques show that motor neurons are derived from uncommitted precursors. First, fate mapping experiments in the spinal cord show that motor neurons are related both to other neurons, and to astrocytes and oligodendrocytes scattered throughout the ventral half of the spinal cord.[31] Second, transplants of a supernumerary notochord to a dorso-lateral position induce a second floorplate in the section of spinal cord nearest the graft.[32] The newly specified floorplate then induces motor neurons to differentiate on either side of it, as demonstrated by transplants and explant cultures from surgically altered embryos.[33,34] These transplant experiments suggest that cells normally destined to generate interneurons can switch their fate to motor neurons in the presence of an inducing signal from either notochord or floorplate. In addition, these results provide direct evidence for soluble factors from notochord affecting the fate of multipotential neuronal precursor cells.

Cortex

Lineage studies are difficult in cortex because some cells migrate over long distances, so that clone members become widely dispersed and mixed with cells from other clones.[35,36] If animals are infected very early in development, just after the first cortical neurons are born, the majority of clones are entirely composed of neurons.[37] This indicates that many cortical precursors give rise to neurons alone, and if a common precursor for neurons and glia exists, it must be as a very small population. Other groups found evidence for the existence of a small population of common precursors for neurons and oligodendrocytes (N-O cell), which accounts for less than 5% of the clones.[35,38,39] Therefore, most neurons arise from a precursor that will not also give rise to glia. In this respect, differentiation mechanisms in spinal cord and cortex are distinct.

The distribution of clone members has been controversial, because some groups found that clones formed loose columns,[37] while others found that clones were more widely distributed.[40,41] A recent study used a mixture of 100 different retroviruses with individual DNA markers that can be detected by PCR to determine whether cells which happen to be near each other are clonally related.[35] The results show that there are both clustered and dispersed clones in the cortex. Some clones can be dispersed across the entire width of the cortex, observing no boundaries between functional areas.

In all the cortical studies, cells in individual clones were found to be distributed across several layers, indicating that related neurons adopt distinct neuronal fates. In this sense, the neuronal precursors are multipotential because their progeny become different types of neurons characteristic of the cortical layers to which they migrate. The radial distribution is obscured by horizontal migrations so that clones are generally interspersed with many unrelated cells. Therefore, the formation of functional columns is unlikely to depend substantially on the inter-relatedness of the cells in the cortex.

In vitro studies of differentiation

Lineage studies have shown that the ancestry of a CNS cell does not strictly determine its fate. The direct implication is that information from the surroundings regulates the differentiation of multipotential precursors. In order to determine the nature

of external influences which affect a cell, a system in which the cell's environment can be manipulated is necessary. Culture experiments have several advantages over lineage marking because the progeny cells cannot escape by migration and differentiation occurs independently of interactions which may occur *in vivo*. This strategy has been used on cells from the peripheral nervous system (PNS) to yield considerable information about fate potentials of primary cells and fate switching.[42-44]

Monoclonal antibodies have been invaluable for identifying cell types both *in vitro* and *in vivo*. They are critical to *in vitro* studies because the morphology and location which may be used to identify a cell *in vivo* are lost. Antibodies which recognize antigens specific to differentiated cell types such as galactocerebroside in oligodendrocytes, glial fibrilary acidic proteins in glia, and neurofilaments in neurons are widely used. Stem cells also have specific antigens. The monoclonal antibody A2B5 is specific for a multipotent precursor in the optic nerve.[45] The monoclonal antibody Rat 401 binds to an epitope on an intermediate filament, nestin, that is specifically expressed in neuro-epithelial stem cells, but not in adult neurons or glia.[27,28,46]

Primary cultures of cells from optic nerve have been central to the identification of factors that influence the differentiation of the 02A cell, which is a common precursor to oligodendrocytes and type 2 astrocytes (see Noble *et al*, pp 413-422, this issue). *In vitro*, it will differentiate into astrocytes in the presence of 10% serum, but in serum free medium it will produce primarily oligodendrocytes. The rate of differentiation to oligodendrocytes is affected by the presence of type 1 astrocytes, a cell type already present in the optic nerve. The activity of type 1 astrocytes can be substituted by PDGF alone.[47,48] Ciliary neurotrophic factor (CNTF) promotes differentiation to astrocytes, but is less effective than fetal calf serum.[49]

In vitro culture of primary cells in serum-free medium has been used to define the conditions required for the continued proliferation of neuronal precursors. Clones of nestin positive cells from the embryonic rat CNS will expand in the presence of mitogens and then differentiate into nestin negative, neurofilament positive neurons when growth factors are withdrawn.[50] Neuronal precursors from retina also proliferate and differentiate in culture.[23] Another strategy is to grow single neuroepithelial cells in isolation. Individual septal forebrain cells cultured small wells in the presence of feeder cells will divide and differentiate. The development of individual clones has been followed by microscopy and immuno-

histochemistry.[51] Individual cells produced neurons and glia alone as well as mixed clones of neuronal and non-neuronal cells. With *in vitro* methods it is now feasible to explore further how changes in the extracellular environment affect the potential of individual precursors and explore the capacity of precursor cells for self-renewal.

A major difficulty with dissociated cell culture is that neurons normally differentiate in a complex three-dimensional environment that is absent in dissociated cell culture. A culture system is available that allows neuronal differentiation while retaining the cell contacts found *in vivo*. In organotypic culture, slices of embryonic tissue can be kept under conditions in which differentiation occurs and mature neurons are stable for many days. This culture system has recently been simplified and used under serum free conditions to show that neurotrophins act on neuronal precursor cells. In the neonatal rat cerebellum, the neurotrophin BDNF induces c-Fos in the precursor cells of the external granular layer, while more mature cells respond to the related factor NT-3. In dissociated culture, BDNF, but not NT-3, is a survival factor for cerebellar granule cells.[51a] In the embryonic hippocampus, BDNF and NT-3 induce the *c-fos* message. In neonatal organotypic culture, NT-3 induces c-Fos in the dentate gyrus, pyramidal layer and CA1 and CA3 tracts. NT-3 has a strong neurotrophic effect on cells positive for calbindin, a protein found in most granule neurons, and some pyramidal and interneurons.[51b] c-Fos immunohistochemistry was used to identify cells that respond to neurotrophins. The neurotrophin BDNF induces c-Fos in the precursor cells of the cerebellar external granular layer. This result points out the advantage of the slice culture system as it maintains the normal anatomy of the developing embryo.

Cell lines differentiate into neurons and glia

The *in vitro* experiments described above use primary cells to define growth factors with potentially important actions on neuronal precursors. Cell lines have several advantages over primary cultures, because they are clonal and available in large numbers. Stem cell lines allow study of the molecular biology of differentiation in a pure culture. They can also be genetically manipulated *in vitro*, and transplanted back into animals. Recently, cell lines have been deliberately established by the immortalization of primary cells from the developing nervous system using an oncogene carried in a

retroviral vector (for review see ref 58).[52-58] Some oncogenes, introduced singly, can immortalize cells without rendering them tumorigenic, since oncogenic transformation is a multi-step process.[59,60] An alternative strategy used cells from a human patient suffering from a disease in which it is believed CNS stem cells proliferate inordinately.[61] Cell lines have many potential uses but here we consider the single property of differentiation from precursor to neuron.

These cell lines show a variety of phenotypes *in vitro*. Lines which differentiate in response to growth factors reveal signals which promote differentiation or fate switching.[53,56,57] Other lines differentiate in response to culture conditions or spontaneously.[52,55,62,63] *In vitro* differentiation of cell lines has begun to yield results in studies of genes involved in the differentiation process. A sympathetic nervous system stem cell line has been shown to express a pair of genes (*MASH-1* and *MASH-2*) related to the *Drosophila achaete-scute* genes, which may be involved in neuroblast differentiation.[64] A cerebellar cell line has been used to demonstrate that *cdc2* homologs are downregulated during differentiation.[65]

The extent of differentiation for a cell line *in vitro* does not strongly reflect its developmental potential *in vivo*. We will concentrate our discussion on the differentiation of cell lines transplanted to a normal embryonic environment.

The rat cell line ST15A was immortalized from primary cultures of proliferating cells from the postnatal day 2 cerebellum, using the temperature sensitive tsA58 allele of SV40 T antigen. Active oncogenes can in some cases block cellular differentiation, and the temperature sensitive allele was selected to avoid this difficulty.[58] The protein is stable at 33°C, but rapidly degraded at 39°C, the body temperature of the rat. ST15A cells express nestin at 33°C, suggesting that they have neuronal precursor properties. This clonal cell shows some changes in gene expression when moved to the non-permissive temperature for the immortalizing oncogene.[52,62] However neuronal differentiation is inefficient *in vitro*, even when ST15A is co-cultured with primary cerebellar cells. When transplanted to the cerebellum, ST15A integrates into the host tissue, does not form tumors and expresses morphological features characteristic of differentiated cerebellar cell types. For example, transplanted ST15A cells labeled with ³H-thymidine and DiI, a lipid soluble fluorescent dye, have morphology indistinguishable from granule neurons and Bergmann glia.[66]

Similar results were seen in transplants of the cerebellar cell lines C27-3 and C17-2, which were established with avian *myc*. Subpopulations of these lines express a variety of differentiated markers *in vitro* and spontaneously alternate between neuronal and glial phenotypes. In transplants to the cerebellum, cells which co-stain for β-galactosidase and with a marker for cerebellar neurons or glial fibrillary acidic protein were found in appropriate layers. Transplanted cells which resemble oligodendrocytes and basket cells were also seen, but Bergmann glia were not reported.[63]

HiB5, a ts T antigen immortalized cell line, derived from embryonic day 16 (E16) hippocampus, does not differentiate *in vitro*. When grown at the permissive temperature for the oncogene, the cell lines are stable in morphology and do not express differentiated markers, but are nestin positive. HiB5 cells transplanted to the neonatal hippocampus populate the granule layer of the dentate gyrus and persist in large numbers in the adult animal. Labeling of the cells with the lipid-soluble dye DiI reveals cells which have morphologies expected of hippocampal granule neurons. Retrograde tracing with a fluorescent marker shows that the transplanted cells have sent projections to the CA3 subregion of the hippocampus.[67] This is the normal projection pattern for hippocampal granule neurons. These results show that HiB5 cells become stably integrated into the brain and the basic rules of cell interaction between neurons suggest that this would only be possible if the immortal cells were functionally active.

HiB5 cells integrate into the developing cerebellum as well. Cerebellar granule neurons have characteristic axons running parallel to the pial surface and transplanted HiB5 cells have neuronal morphologies appropriate for cerebellar granule neurons. HiB5 cells expressing Bergmann glial morphologies were also found.[67]

In both cerebellum and hippocampus HiB5 cells differentiate into cell types that are being generated in the newborn host at these sites. The cerebellum develops from the mitotic ventricular zone early in development when the Purkinje layer is born, but cells born later migrate inward from a mitotic zone near the pial surface. In spite of this difference in organization, HiB5 can populate both hippocampus and cerebellum with the appropriate cell types. The immortalization process does not eliminate the ability of these cells to heed signals present in the developing brain. The remarkable plasticity of the cell lines may be due either to equal plasticity of the primary stem cells from which they were derived, or from a loss of 'memory' of their origins due to culture and immortalization (see article by Smith, pp 385-399,

this issue). If the cells were once regionally specified, that specification may not be stable, but recent data using the tsA58 SV40 T-antigen to immortalize muscle cell precursors suggests that immortalized cells can retain regional positional information.[67a] Whether or not the HiB5 cells 'remember' their hippocampal origin is an important question that speaks to the stability of regional identity in the embryonic brain. What is clear from these recent studies is that cell lines are powerful tools in mammalian embryology.

Clinical applications for neuronal stem cell lines

The successful differentiation of transplanted immortal cells suggests that such lines may be of clinical utility. Fibroblasts genetically engineered to secrete NGF[68] were found to rescue cholinergic neurons in fimbria-fornix lesioned rats, a model for human Alzheimer's disease. Similarly, cells transfected with tyrosine hydroxylase to produce L-dopa reduced spinning behavior in lesioned animals, whose symptoms resemble those of Parkinson's patients.[69] Cell lines derived from developing tissue may have advantages over fibroblasts as they may integrate into the tissue more easily and survive indefinitely (reviewed in ref 70).

In CNS lesions which involve the loss of a particular cell type, grafts of fetal tissue have been shown to replace lost or non-functioning cells and in some cases to alleviate symptoms of the lesion. For instance, fetal cells have been used to rescue deficits in lesioned monkeys and rats,[71,72] and the results of fetal transplants in the treatment of Parkinson's disease have been moderately encouraging.[73] The mouse mutant *pcd* (Purkinje cell degeneration) may be a model for human hereditary ataxia. Fetal CNS cells can repopulate the Purkinje layer of the cerebellum in these mice, though they do not establish normal connections.[74] In these cases, the use of cell lines may help avoid the ethical issues surrounding the use of fetal tissue. There are potential disadvantages that would have to be addressed before cell lines were to be used clinically, such as the possibility of increased tumorigenesis due to long periods in culture or of immune rejection. However, the recent results from transplants suggests that immortal cells will be powerful tools in animal models. In particular they offer a new genetic approach to the differentiation of the CNS that could be applied in mammals, such as cats, monkeys and man, that are not suited to standard transgenic strategies.

Regional identity

Cells from such different regions as cerebellum and hippocampus are capable of responding appropriately to local signals. This section discusses experiments that ask how different regions of the brain are established.

In a set of reciprocal transplants to and from limbic and sensorimotor cortex in rats, the ability of the donor cells to appropriately express a limbic system marker depended on the age at which the donor cells are transplanted.[75] The LAMP (limbic associated membrane protein) antigen is normally expressed in migratory and post-migratory neurons on and after E15. Cells of limbic origin will not express LAMP if they are transplanted on E12, prior to the differentiation of neurons. Donor cells from E14 embryos do express the LAMP antigen after transplantation to other cortical sites. The reciprocal transplant shows that sensorimotor tissue is competent to express LAMP if it is derived from E12, but not E14 donors. The loss of developmental plasticity coincides with the beginning of neurogenesis on E13 as well as the first opportunity for the cells to interact with afferents. The timing of the developmental restriction is similar to that in the ferret heterochronic transplants discussed above.[11,12]

Some positional identities are established earlier, before neurons differentiate. The presumptive avian cerebellum and optic tectum form from the mes/metencephalon border. The region expresses chick-*en*, the chick homolog of the *Drosophila* homeobox containing gene *engrailed*, in a gradient increasing caudally. Chick-*en* is a sensitive marker of cell fate. If a block of tissue from this region is transplanted from quail to chick in a rostrocaudally inverted orientation, the expression of chick-*en* in the transplant adjusts to its new position and the brain develops normally.[76] If the same piece of tissue is transplanted to the prosencephalon, the gradient does not regulate, but instead induces the host cells to express *en*. The transplanted tissue then gives rise to an ectopic cerebellum, while the induced tissue forms a supernumerary tectum.[77] The mes/metencephalic tissue may be source of an inductive signal that recruits prosencephalon to a tectal fate. The prosencephalon is competent to respond to this signal, although it normally is distant from it at this stage of development. When the tissue is inverted, the surrounding cells are dominant and impose the local level of chick-*en* expression. These results suggest that some cells in some regions of the neuroepithelium can exert long range effects on the fate of surrounding precursor cells.

The experiments described above suggest that brain regions are distinct early in development, before axon ingrowth. Other experiments point to a role for interactions with afferents in organizing the cyto-architecture of the brain. For instance, experimental lesions in the newborn ferret can reroute visual input to the auditory cortex. The observed conversion of an area which normally processes information on a one-dimensional map into a two-dimensional map of visual space, without altering the redundant inputs from the medial geniculate nucleus, implies some rewiring in the cortex itself.[78-80] Discrete functional units of the somatosensory cortex, the barrel fields, can be reproduced in visual cortex transplanted to the area.[81] In both these cases, the organization is imposed from outside the area.

Genetics of neuronal differentiation

Recent advances in mammalian genetics allow the generation of mutations in targeted genes. The distinct regions of the CNS appear early after gastrulation and a number of genes which may be important in specifying CNS regions are now being studied using transgenic techniques.

The normal cerebellum is a chimeric structure, with the anterior, medial portion primarily derived from mesencephalon and the rest from metecephalon.[84] Three genes have been implicated in the specification of the cerebellum by expression and analysis of mutants. During early embryonic development, *En-1* and *En-2* are expressed in a ring at the mes/metencephalon border. *Wnt-1* is expressed in a partially overlapping domain, and in other parts of the CNS.[83-85] In *Drosophila*, genetic evidence suggests that the fly homolog of *Wnt-1*, *wingless*, is required for *engrailed* expression.[86] *Wnt-1* is thought to be a secreted protein, while *En* is a homeobox-containing nuclear gene. Homozygous mutations in *Wnt-1*, either the spontaneous mutant *swaying*, or mutations generated by gene targeting, show major defects in cerebellar development.[87-89] The phenotypes range from the absence of the anterior, medial portion of the cerebellum to the absence of the entire cerebellum and all midbrain structures. The missing structure does not die, but fails to develop. Mice mutant in *En-2* have also been made by gene targeting.[90] Homozygotes have smaller cerebella with an altered pattern of folia. There may be functional redundancy between *En-1* and *En-2*, resulting in a milder phenotype than for *Wnt-1* mutants. Although *Wnt-1* is expressed in spinal cord,
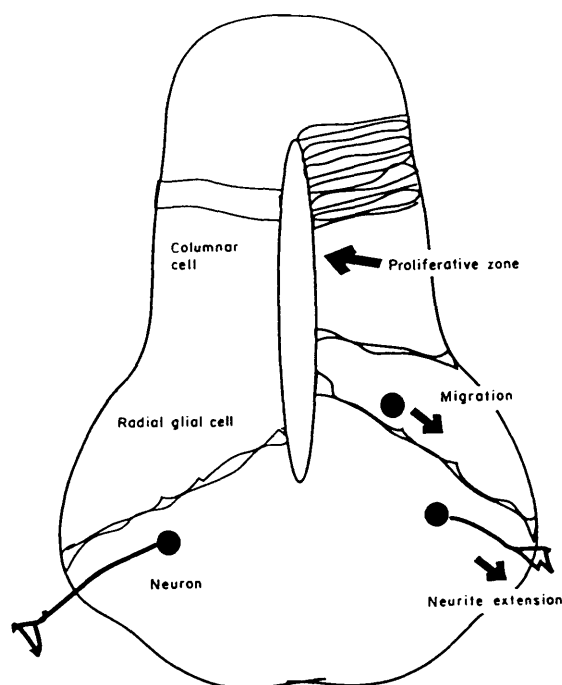
Figure 1. Cell types and developmental processes in the E13 spinal cord. The first neurons differentiate on embryonic day 12 in the spinal cord of the rat. This figure illustrates the major morphologically distinct cell types found in the neurogenic neuroepithelium (on the left). The right hand side of the figure shows how the major differentiation processes, proliferation, migration and neurite extension occur in distinct regions of the neuroepithelium. These processes occur in a temporal sequence that initiates in the ventral (lower) region of the spinal cord.

it is necessary only for cerebellar development. *Wnt-1* is a member of a large gene family, and other members may complement it elsewhere. Its members have restricted distributions in the developing nervous system. A member of this family may have an important role in setting up the body axis in *Xenopus*.[91,92]

A second group of genes that influence regional specification are the *Pax* family. Named for two motifs in their sequences, they contain homeobox and paired boxes. In *Drosophila*, a member of this family, *paired (prd)* is implicated in the establishment of segment polarity. In mammals, there are several *Pax* genes which are expressed in restricted regions of the neural tube. The mouse mutation small eye (*Sey*) is a mutation in *Pax-6*.[93] Homozygotes lack eyes and nasal cavities, while heterozygous mice suffer from a variety of visual abnormalities. *Pax-6* is homologous to the human aniridia gene, in which mutations result in abnormalities similar to those in the heterozygous mice.[94] The gene is normally expressed in the brain,

spinal cord and eye, as is the zebrafish homolog, pax(zf-a), but only the eye is affected.[95] The lens placode fails to form, depriving the optic cup of an interaction it needs to develop.[93] Another paired-box gene, *Pax-3*, is the location of the splotch (Sp[2H]) mutation which results in spina bifida and anencephaly in homozygotes. The protein is normally expressed in the dorsal part of the neuroepithelium just before neural tube closure, and may be critical for proper joining of the roof of the neural tube.[96] Like *Wnt*, the *Pax* genes appear to be necessary for the development of specific regions of the embryonic CNS.

In *Drosophila*, homeobox genes are involved in specifying segment identities, and mutations in homeobox genes result in a transformation of one segment to another. The single array of *Drosophila* homeobox genes has been multiplied to four complexes in vertebrates, but the order of individual genes has been conserved. Vertebrate homeobox (*Hox*) genes are expressed in a pattern such that the genes at the 3' end of·the complex have the most anterior border of expression and genes 5' to them are expressed with successively more posterior boundaries of expression.[97] The known *Hox* genes are not expressed anterior to the hindbrain, which is the only brain structure that does appear segmented. The hindbrain contains compartments of clonally related cells (rhombomeres) which do not mix across the segment boundaries.[98] Individual members of the homeobox gene family *Hox-2* are expressed in some, but not all of the rhombomeres, so that each segment has a different homeobox code.[99,100]

In mesoderm, if the pattern of *Hox* expression is disturbed with retinoic acid, vertebrae take on the appearance normally found in their anterior neighbors. The transformation can be predicted by the pattern of homeobox gene expression in the tissue that gives rise to each vertebra.[101] Null mutations in *Hox-1.5* and *Hox-1.6* generated by gene targeting in mice resulted in recessive lethal phenotypes. *Hox-1.5* affects tissues derived from pharyngeal arches and neural crest.[102] The *Hox-1.6* mutation slows neural tube closure and results in defects in structures derived from mesoderm, neural crest derivatives and nerve nuclei in the hindbrain.[103] Both of these phenotypes are consistent with a role in the specification of positional information, across multiple embryonic tissues including the neural tube.

Conclusion

Lineage experiments show that the nervous system is derived from multipotential precursors. Transplants of primary tissue and cell lines show that although individual brain regions have characteristic gene expression patterns before neurons are born, they can be respecified by external signals until neuronal differentiation takes place. *In vitro* primary cultures and immortalised cell lines show that precursor cells from many parts of the brain are competent to differentiate into different cell types. Mutant mice implicate the *Wnt*, *Pax*, and *Hox* gene families in specifying regional differences in the developing brain. It appears as if the neuroepithelium is divided into distinct regions through the actions of these genes. There is overwhelming evidence that the neuroepithelium is composed of multipotential stem cells. Therefore there must be mechanisms that lead from the expression of region specific genes to the subsequent fate choices made by neuronal stem cells. Although our current understanding is incomplete, the new experimental methods available point to a new phase in our understanding of the development of the vertebrate central nervous system.

Acknowledgements

References

1. Spemann H (1938) Embryonic Development and Induction. Yale University Press, New Haven
2. Purves D, Lichtman JW (1985) Principles of Neural Development. pp 3-103. Sinauer Associates, Sunderland, MA
3. McKay RDG (1989) The origins of cellular diversity in the mammalian central nervous system. Cell 58:815-821
4. Angevine JB, Sidman RL (1961) Autoradiographic study of cell migration during histogenesis of cerebral cortex in the mouse. Nature 192:766-768
5. Rakic P (1988) Specification of cerebral cortical areas. Science 241:170-176
6. Caviness VS, Sidman RL (1973) Time of origin of corresponding cell classes in the cerebral cortex of normal and reeler mutant mice: an autoradiographic analysis. J Comp Neurol 148:141-152
7. Caviness VS (1976) Patterns of cell and fiber distribution in the neocortex of the reeler mutant mouse. J Comp Neurol 170:435-448
8. Drager U (1981) Observations on the organization of the visual cortex in the reeler mouse. J Comp Neurol 201:555-570

9. Lemmon V, Pearlman AL (1981) Does laminar position determine the receptive field properties of cortical neurons? A study of corticotectal cells in area 17 of the normal mouse and the reeler mutant. J Neurosci 1:83-93
10. McConnell SK (1991) The generation of neuronal diversity in the central nervous system. Annu Rev Neurosci 14:269-300
11. McConnell (1988) Fates of visual cortical neurons in the ferret after isochronic and heterochronic transplantation. J Neurosci 8:945-974
12. McConnell S, Kaznowski C (1991) Cell cycle dependence of laminar determination in developing neocortex. Science 254:282-285
13. Sanes JR, Rubenstein JLR, Nicolas J-F (1986) Use of a recombinant retrovirus to study post-implantation cell lineage in mouse embryos. EMBO J 5:3133-3142
14. Price J, Turner D, Cepko C (1987) Lineage analysis in the vertebrate nervous system by retrovirus mediated gene transfer. Proc Natl Acad Sci USA 84:156-160
15. Wetts R, Fraser S (1988) Multipotent precursors can give rise to all major cell types of the frog retina. Science 239:1142-1145
16. Turner D, Cepko C (1987) A common precursor for neurons and glia persists in rat retina late in development. Nature 328:131-136
17. Holt CE, Bertsch TW, Ellis HM, Harris WA (1988) Cellular determination in the *Xenopus* retina is independent of lineage and birthdate. Neuron 1:15-26
18. Turner DL, Snyder EY, Cepko CL (1990) Lineage independent determination of cell type in embryonic mouse retina. Neuron 4:833-845
19. Wetts R, Serbedzija GN, Fraser SE (1989) Cell lineage analysis reveals multipotent precursors in the ciliary margin of the frog retina. Dev Biol 136:254-263
20. Reh TA, Tully T (1986) Regulation of tyrosine hydroxylase-containing amacrine cell number in larval frog retina. Dev Biol 114:463-469
21. Reh TA (1987) Cell-specific regulation of neuronal production in the larval frog retina. J Neurosci 7:3317-3324
22. Park CM, Hollenberg MJ (1989) Basic fibroblast growth factor induces retinal regeneration *in vivo*. Dev Biol 134:201-205
23. Reh TA, Nagy T, Gretton H (1987) Retinal pigmented epithelial cell induced to transdifferentiate to neurons by laminin. Nature 330:68-71
24. Galileo DS, Gray GE, Owens G, Majors J, Sanes JR (1990) Neurons and glia arise from a common progenitor in chicken optic tectum : demonstration with two retroviruses and cell type specific antibodies. Proc Natl Acad Sci USA 87:458-462
25. Gray GE, Sanes JR (1991) Origins and fate of radial glia in chick optic tectum. Soc Neurosci (Abstr) 1:923
26. Hatten ME (1990) Riding the glial monorail: a common mechanism for glial-guided neuronal migration in different regions of the developing mammalian brain. Trends Neurosci 13:179-184
27. Frederiksen K, McKay RDG (1988) Proliferation and differentiation of rat neuroepithelial precursor cells *in vivo*. J Neurosci 8:1144-1151
28. Hockfield S, McKay RDG (1985) Identification of major cell classes in the developing mammalian nervous system. J Neurosci 5:3310-3328
29. Gray G, Glover J, Majors J, Sanes J (1988) Radial arrangement of clonally related cells in the chicken optic tectum: lineage analysis with a recombinant retrovirus. Proc Natl Acad Sci USA 85:7356-7360
30. Mountcastle VB (1957) Modality and topographic properties of cat's somatic-sensory cortex. J Physiol 20:408-434
31. Leber SM, Breedlove SM, Sanes JR (1990) Lineage, arrangement and death of clonally related motoneurons in chick spinal cord. J Neurosci 10:2451-2462
32. van Straaten HWM, Hekking JWM, Wiertz-Hoessels EJLM, Thors F, Drukker J (1988) Effect of the notochord on the differentiation of a floor plate area in the neural tube of the chick embryo. Anat Embryol 177:317-324
33. Placzek M, Tessier-Lavigne A, Yamada T, Jessel T, Dodd J (1990) Mesodermal control of neural cell identity: floor plate induction by the notochord. Science 250:985-988
34. Yamada T, Placzek M, Tanaka H, Dodd J, Jessell TM (1991) Control of cell pattern in the developing nervous system: polarizing activity of the floor plate and notochord. Cell 64:635-647
35. Walsh C, Cepko C (1992) Widespread dispersion of neuronal clones across functional regions of the cerebral cortex. Science 255:434-440
36. Austin CP, Cepko CL (1990) Cellular migration patterns in the developing mouse cerebral cortex. Development 110:713-732
37. Luskin MB, Pearlman AL, Sanes JR (1988) Cell lineage in the cerebral cortex of the mouse studied *in vivo* and *in vitro* with a recombinant retrovirus. Neuron 1:635-647
38. Williams BP, Read J, Price J (1991) The generation of neurons and oligodendrocytes from a common precursor cell. Neuron 7:685-693
39. Price J, Williams B, Grove E (1992) The generation of cellular diversity in the cerebral cortex. 2:23-29
40. Walsh C, Cepko C (1988) Clonally related cortical cells show several migration patterns. Science 241:1342-1345
41. Price J, Thurlow L (1988) Cell lineage in the rat cerebral cortex: a study using retroviral mediated gene transfer. Development 104:473-482
42. Yamamori T, Fukada K, Aebersold R, Korsching S, Fann M-J, Patterson P (1989) The cholinergic neuronal differentiation factor from heart cells is identical to leukemia inhibitory factor. Science 246:1412-1416
43. Anderson DJ (1989) The neural crest cell lineage problem: neuropoiesis? Neuron 3:1-12
44. Barrofio A, Dupin E, LeDouarin NM (1988) Clone-forming ability and differentiation potential of migratory neural crest cells. Proc Natl Acad Sci USA 85:5325-5329
45. Raff MC, Miller RH, Noble M (1983) A glial progenitor cells that develops *in vitro* into an astrocyte or an oligodendrocyte depending on culture medium. Nature 303:390-396
46. Lendahl U, Zimmerman L, McKay RDG (1990) CNS stem cells express a new class of intermediate filament protein. Cell 60:585-595
47. Raff M, Abney E, Fok-Seang J (1985) Reconstitution of a developmental clock *in vitro*: a critical role for astrocytes in the timing of oligodendrocyte differentiation. Cell 42:61-69
48. Raff MC, Lillien LE, Richardson W, Burne J, Noble MD (1988) Platelet-derived growth factor from astrocytes drives the clock that times oligodendrocyte development in culture. Nature 333:562-565
49. Raff MC (1989) Glial cell diversification in the rat optic nerve. Science 243:1450-1455
50. Cattaneo E, McKay R (1990) Proliferation and differentiation of neuronal stem cells regulated by nerve growth factor. Nature 347:762-765
51. Temple S (1989) Division and differentiation of isolated CNS blast cells in microculture. Nature 340:471-473
51a. Segal RA, Takahashi H, McKay RDG (1993) Changes in neurotrophic responsiveness during development of cerebellar granule neurons. Neuron, in press
51b. Collazo D, Takahashi H, McKay RDG (1992) Cellular targets and trophic functions of Neurotrophin-3 in the developing rat hippocampus. Neuron 9:643-656

52. Frederiksen K, Jat PS, Valtz N, Levy D, McKay R (1988) Immortalization of precursor cells from the mammalian CNS. Neuron 1:439-448

53. Bartlet PF, Reid HH, Bailey KA, Bernard O (1988) Immortalization of mouse neural precursor cells by the *c-myc* oncogene. Proc Natl Acad Sci USA 85:3255-3259

54. Ryder EF, Snyder EY, Cepko CL (1990) Establishment and characterization of multipotent neural cell lines using retrovirus vector-mediated oncogene transfer. J Neurobiol 21:356-375

55. Evrard C, Borde I, Marin P, Galiana E, Premont J, Gros F, Rouget P (1990) Immortalization of bipotential and plastic glio-neuronal precursor cells. Proc Natl Acad Sci USA 87:3062-3066

56. Birren SJ, Anderson DJ (1990) A *v-myc*-immortalized sympathoadrenal progenitor cell line in which neuronal differentiation is initiated by FGF but not NGF. Neuron 4:189-201

57. Almazan G, McKay R (1992) An oligodendrocyte precursor line from rat optic nerve. Brain Res 579:234-245

58. Lendahl U, McKay RDG (1990) The use of cell lines in neurobiology. Trends Neurosci 13:132-137

59. Ruley HE (1983) Adenovirus early region 1A enables viral and cellular transforming genes to transform primary fibroblasts. Nature 304:602-606

60. Land H, Parada LF, Weinberg RA (1983) Tumorigenic conversion of primary fibroblasts requires at least two cooperating oncogenes. Nature 304:596-602

61. Ronnett G, Hester L, Nye J, Connors K, Snyder S (1990) Human cortical neuronal cell line: establishment from a patient with unilateral megencephalopathy. Science 248:603-605

62. Valtz NLM, Hayes TE, Norregard T, Liu S, McKay RDG (1991) An embryonic origin for medulloblastoma. New Biol 3:364-371

63. Snyder E, Dietcher DL, Walsh C, Arnold-Aldea S, Hartwieg E, Cepko C (1992) Multipotent neural cell lines can engraft and participate in development of mouse cerebellum. Cell 68:33-51

64. Johnson JE, Birren SJ, Anderson DJ (1990) Two rat homologues of *Drosophila* achaete-scute specifically expressed in neuronal precursors. Nature 346:858-861

65. Hayes TE, Valtz NLM, McKay RDG (1991) Down-regulation of CDC2 upon terminal differentiation of neurons. New Biol 3:259-269

66. McKay R, Valtz N, Cunningham M, Hayes T (1990) Mechanisms regulating cell number and type in the mammalian central nervous system. Cold Spring Harb Symp Quant Biol LV:291-301

67. Renfranz PR, Cunningham MG, McKay RDG (1991) Region-specific differentiation of the hippocampal stem cell line HiB5 upon implantation into the developing mammalian brain. Cell 66:713-729

67a. Donoghue MJ, Morris-Valero R, Johnson YR, Merlie JP, Sanes JR (1992) Mammalian muscle cells bear a cell autonomous, heritable memory of their rostrocaudal position. Cell 69:67-77

68. Rosenberg M, Friedmann T, Robertson R, Tuszynki M, Wolff J, Breakefield X, Gage F (1988) Grafting genetically modified cells to the damaged brain: restorative effects of NGF expression. Science 242:1575-1578

69. Wolff JA, Fisher LJ, Xu L, Jinnah HA, Langlais PJ, Iuvone PM, O'Malley KL, Rosenberg MB, Shimohama S, Friedmann T, Gage FH (1989) Grafting fibroblasts genetically modified to produce L-dopa in a rat model of Parkinson disease. Proc Natl Acad Sci USA 86:9011-9014

70. Gage FH, Fisher LJ (1991) Intracerebral grafting: a tool for the neurobiologist. Neuron 6:1-12

71. Dunnett S (1991) Cholinergic grafts, memory and ageing. Trends Neurosci 14:371-376

72. Ridley RM, Baker HF (1991) Can fetal neural transplants restore function in monkeys with lesion-induced behavioural deficits? Trends Neurosci 14:366-370

73. Lindvall O (1991) Prospects of transplantation in human neurodegenerative diseases. Trends Neurosci 14:376-384

74. Sotelo C, Alvarado-Mallart RM (1991) The reconstruction of cerebellar circuits. Trends Neurosci 14:350-355

75. Barbe MF, Levitt P (1991) The early commitment of fetal neurons to the limbic cortex. J Neurosci 11:519-533

76. Martinez S, Alvarado-Mallart R-M (1990) Expression of the homeobox chick-*en* gene in Chick/Quail chimeras with inverted mes-metecephalic grafts. Dev Biol 139:432-436

77. Martinez S, Wassef M, Alvarado-Mallart R-M (1991) Induction of mesencephalic phenotype in the 2-day-old chick prosencephalon is preceded by the early expression of the homeobox gene en. Neuron 6:971-981

78. Pallas SL, Roe AW, Sur M (1990) Visual projections induced into the auditory pathway of ferrets. I. Novel inputs to primary auditory cortex (AI) from the LP/Pulvinar complex and the topography of the MGN-AI projection. J Comp Neurol 298:50-68

79. Roe AW, Pallas SL, Hahm J-O, Sur M (1990) A map of visual space induced in primary auditory cortex. Science 250:818-820

80. Sur M, Pallas SL, Roe AW (1990) Cross-modal plasticity in cortical development: differentiation and specification of sensory neocortex. Trends Neurosci 13:227-233

81. Schlaggar BL, O'Leary DDM (1991) Potential of visual cortex to develop an array of functional units unique to somatosensory cortex. Science 252:1556-1560

82. Hallonet M, Teillet M-A, Le Douarin N (1990) A new approach to the development of the cerebellum provided by the quail-chick marker system. Development 108:19-31

83. Davis CA, Joyner AL (1988) Expression patterns of the homeo box-containing genes *En-1* and *En-2* and the proto-oncogenes *int-1* diverge during development. Genes Dev 2:1736-1744

84. Davis CA, Noble-Topham SE, Rossant J, Joyner AL (1988) Expression of the homeo box-containing gene *En-2* delineates a specific region of the developing mouse brain. Genes Dev 2:361-371

85. Wilkinson DG, Bailes JA, McMahon AP (1987) Expression of the proto-oncogene *int-1* is restricted to specific neural cells in the developing mouse embryo. Cell 50:79-88

86. DiNardo S, Sher E, Heemskerk-Jongens J, Kassis JA, O'Farrell PH (1988) Two-tiered regulation of spatially patterned *engrailed* gene expression during Drosophila embryogenesis. Nature 332:604-609

87. Thomas KR, Capecchi MR (1990) Targeted disruption of the murine *int-1* proto-oncogene resulting in severe abnormalities in midbrain and cerebellar development. Nature 346:847-850

88. Thomas KR, Musci TS, Neumann PE, Capecchi MR (1991) Swaying is a mutant allele of the proto-oncogene *wnt-1*. Cell 67:969-976

89. McMahon AP, Bradley A (1990) The *wnt1* (*int1*) proto-oncogene is required for development of a large region of the mouse brain. Cell 62:1073-1085

90. Joyner AL, Herrup K, Auerbach BA, Davis CA, Rossant J (1991) Subtle cerebellar phenotype in mice homozygous for a targeted deletion of the en-2 homeobox. Science 251:1239-1243

91. Smith WC, Harland RM (1991) Injected Xwnt-8 RNA acts early in *Xenopus* embryos to promote formation of a vegetal dorsalizing center. Cell 67:753-765

92. Sokol S, Christian JL, Moon RT, Melton DA (1991) Injected Wnt RNA induces a complete body axis in *Xenopus* embryos. Cell 67:741-752

93. Hill RE, Favor J, Hogan BLM, Ton CCT, Saunders GF, Hanson IM, Prosser J, Jordan T, Hastie ND, van Heyningen V (1991) Mouse small eye results from mutations in a paired-like homeobox-containing gene. Nature 354:522-525

94. Ton CCT, Hirvonen H, Miwa H, Well MM, Monaghan P, Jordan T, van Heyningen V, Hastie ND, Meijers-Heijboer H, Dreschler M, Royer-Pokora B, Collins F, Swaroop A, Strong LC, Saunders G (1991) Positional cloning and characterization of a paired box- and homeobox-containing gene from the aniridia region. Cell 67:1059-1074

95. Krauss S, Johansen T, Korzh V, Fjose A (1991) Expression pattern of zebrafish *pax* genes suggests a role in early brain regionalization. Nature 353:267-270

96. Epstein DJ, Vekemans M, Gros P (1991) splotch (Sp^{2H}), a mutation affecting development of the mouse neural tube, shows a deletion within the Paired homeodomain of Pax-3. Cell 67:767-774

97. McGinnis W, Krumlauf R (1992) Homeoboxes and axial patterning. Cell 68:283-302

98. Fraser SE, Keynes R, Lumsden A (1990) Segmentation in the chick embryo hindbrain is defined by cell lineage restrictions. Nature 344:431-435

99. Keynes R, Lumsden A (1990) Segmentation and the origin of regional diversity in the vertebrate central nervous system. Neuron 4:1-9

100. Lumsden A, Keynes R (1989) Segmental patterns of neuronal development in the chick hindbrain. Nature 337:424-428

101. Kessel M, Gruss P (1991) Homeotic transformations of murine vertebrae and concomitant alteration of Hox codes induced by retinoic acid. Cell 67:89-104

102. Chisaka O, Capecchi MR (1991) Regionally restricted developmental defects resulting from targeted disruption of the mouse homeobox gene hox-1.5. Nature 350:473-479

103. Lufkin T, Dierich A, LeMeur M, Mark M, Chambon P (1991) Disruption of the Hox-1.6 homeobox gene results in defects in a region corresponding to its rostral domain of expression. Cell 66:1105-1119

Chapter 2: Antibodies to Nestin

Introduction

The expression of nestin in the early CNS is a marker for stem cells. The identification and manipulation of stem cells and differentiating intermediates in the hematopoietic system has yielded both understanding of the immune system and practical medical benefits. If CNS stem cells could be isolated in vitro and their differentiation programs controlled, it would bring similar understanding of CNS development, enhance the classification of tumors, and improve transplantation therapies for neurodegenerative diseases.

Many types of CNS tumors have properties similar to embryonic CNS stem cells. The use of nestin as a diagnostic tool for tumor typing could lead to to better diagnosis of these cancers. In the treatment of neurodegenerative disease, many labs have been exploring the possibility of transplanting embryonic cells to the brain (for review, see insert at end of Chapter 1: Marvin and McKay, 1992). These experiments have been controversial and are limited by the availability of embyronic tissue. If the identification and expansion of stem cells were possible in vitro, some of these difficulties would be alleviated.

Limitations on nestin identification

However, practical limitations exist on the use of the Rat 401 monoclonal antibody in the identification of nestin. It recognizes mouse nestin poorly and human nestin not at all. In the laboratory, expanding the species in which nestin antibodies could be identified was also essential for in vitro proliferation and differentiation studies and for lesioning studies. To overcome the limits imposed by Rat 401, new antisera to nestin were generated using two different antigens. Recognition by Rat 401 of a fusion protein generated from the nestin gene and the staining patterns of antibodies raised against the fusion protein would unequivocally identify the cloned nestin gene as that of the Rat 401 epitope.

Materials and methods

Peptide synthesis and conjugation

A peptide corresponding to the 19 amino acids at the C-terminus of nestin was synthesised. The sequence of the peptide was CPLKFTLSGVDGDSWSSGED. The cysteine residue was added to facilitate conjugation to carrier protein. Peptides, conjugation to KLH, immunizations of rabbits and bleeds were done by Immuno-dynamics, Inc; San Diego, CA. Test bleeds were made at 5, 7 and 9 weeks after injection and terminal bleeds were made at 11 weeks.

DNA Constructs

The large EcoR1 fragments from λgt10.401.16 and λgt10.401.8 (Lendahl et al., 1990) representing the C terminal 1197 and 984 amino acids, respectively, of the nestin protein were cloned in frame into the EcoR1 site in the pATH1 vector (Tohyama et al., 1992; Tzalagoff et al., 1986). The resulting constructs were called pATH1:401:16 and pATH:401:8, respectively. The upstream EcoR1 sites in λgt10.401.16 and λgt10.401.8 were introduced in making the library and do not exist naturally in nestin. DNA was introduced to E. coli strain HB101 by $CaCl_2$ transformation (Sambrook et al., 1989).

Induction of fusion protein and immunization

Induction of fusion proteinns in 5μg indoleacrylic acid for 1 hour as recommended (Tzalagoff et al., 1986) was inadequate to express either nestin fusion protein or TrpE alone, so the more stringent approach of Tapscott et al. (1988) was used. At the same time, bacteria containing only the parent vector pATH1 were induced to express TrpE. Cells were lysed in 6 M urea, 1% SDS and 50 mM Tris, pH 6.8. Lysates of the two strains were compared by SDS PAGE on a 6% polyacrylamide gel. The nestin fusion protein appeared as a ladder of material extending from the top of the gel. Since the largest endogenous bacterial protein was less than 120 kD, nestin fusion protein was simply cut out of the top of the gel. Approximately 500μg of crude bacterial lysate mixed 1:1 with SDS-PAGE loading buffer (125mM Tris pH 6.8, 4% SDS, 20% glycerol, 5% β-mercaptoethanol) were loaded into a 12 cm well on a gel with 1 mm spacers. The top three bands, running from 170 to 200 kD, were excised from the gel. The gel was broken up by mixing with

incomplete Freund's adjuvant and passing the suspension back and forth between two syringes until a smooth mixture was formed. Female NZW rabbits were injected subcutaneously with (0.2 ml) of the mix in two places on the back. One boost was done two weeks later using the same protocol (Harlow and Lane, 1988). Bleeds were taken at intervals of 3 weeks for six months.

Mammalian Cells

The endothelial cell line CBA9(3d)CL2 was obtained from Dr Jane Welsh. Endothelial cells and ST15A (Frederiksen et al., 1988) were grown in 10% FCS/DMEM. P19 teratocarcinoma cells were grown as described in Chapter 3.

Cells were lysed in 0.1M Tris pH 6.8, 15% glycerol, 5mM EDTA, 2% SDS with 1mM freshly added PMSF, 10 μg/ml aprotinin, 2 μg/ml leupeptin and 1 μg/ml pepstatin added to inhibit proteolysis. Samples were boiled for three minutes, dispensed into 100 μl aliquots and stored at -80°. Before running SDS PAGE gels, samples were diluted 1:1 in SDS loading buffer (recipe here). 6% gels were as described above, but with 0.8 mm spacers and 3-5 mm wells. After running in 25 mM Tris, 192 mM glycine, 0.1% SDS buffer, gels were transferred overnight at 200mA or 5 hours at 400 mA to nitrocellulose for chemiluminescence or to Immobilon (Millipore) for chromogenic detection. Towbin buffer without methanol (25 mM Tris, 192 mM glycine) was the transfer buffer (Harlow and Lane, 1988). After blocking in 1% BSA in Tris buffered saline (TBS) (Harlow and Lane, 1988), primary antibodies were incubated on the blots for 1 hour at room temperature in TBS. Horseradish peroxidase conjugated anti-rabbit or -mouse secondary antibodies were from BioRad (1:3000) or Amersham (1:10000). Chemiluminescent detection was accomplished using DuPont Renaissance reagents. 4-chloronaphthol was used as the substrate for chromogenic detection.

Blocking experiments

Competition of nestin antibody binding to Western blots with bacterial lysate expressing nestin fusion protein was allowed to proceed in TBS for one hour at room temperature. Bacterial lysate in urea lysis buffer was limited to 0.2 ml of lysate for 10 ml of buffer, so the urea concentration did not exceed 0.12M. In control experiments, this urea concentration had no effect on staining with the nestin antisera.

52

Results

In order to generate new antibodies to nestin, two different antigens were generated representing regions of the unique carboxyl tail of nestin. The rod domain conserved in intermediate filaments was avoided. A synthetic peptide representing the 20 amino acids at the extreme carboxyl terminal was generated, conjugated to KLH, and injected into two rabbits. The antipeptide antibodies were named AS 79 and AS 80. The second antigen was a fusion protein of the carboxyl terminal 1197 amino acids of nestin joined to the amino terminus of the TrpE protein in the pATH1 vector (Tohyama et al., 1992; Tzalagoff et al., 1986). The fusion protein was induced in bacteria (Tapscott et al., 1988), gel purified and injected in to three rabbits. These sera were identified as AS 128, AS 129, and AS 130. The relative positions of these epitopes are diagrammed in Figure 3.

Fusion protein from pATH:401:16 was recognized by the Rat 401 antibody, confirming that the cloned nestin gene did indeed encode the Rat 401 antigen (Figure 4). Furthermore, fusion protein from pATH:401:8 (a clone that began 213 amino acids downstream) was not recognized by Rat 401, suggesting that its epitope lies between the amino termini of the two fusion proteins (Figure 4). These results indicate that the putative nestin gene cloned from an E15 rat brain library (Lendahl et al., 1990) does indeed encode the Rat 401 antigen.

Sera from all five animals showed specific reactions with and high avidity for a band which had the same mobility as nestin as that identified by Rat 401 staining on Western blots (Figure 5, lanes 1,2 and 3). While Rat 401 often recognizes a ladder of smaller polypeptides in addition to the 240 kD band, the antipeptide antibodies 79 and 80 never recognized any smaller bands. Unlike Rat 401, AS 79 and 80 identified a band of the same molecular weight in differentiating P19 mouse cells. Preimmune sera showed no reaction to any component of the cell extracts. By immunocytochemistry, AS 79 and AS80 staining overlapped with that of Rat 401 in ST15A, a rat cell line derived from postnatal cerebellum that stains with Rat 401 (Frederiksen et al., 1988).

The three rabbits immunized with the fusion protein produced AS 128, 129 and 130, which were nearly indistinguishable in their properties. All recognized a long ladder of proteins in Western blots

Figure 5, lane 3). The ladder began at the same position as the band recognized by Rat 401. The antisera were able to stain nestin in 30 μg of cell lysate on Westerns without diminution of the signal at dilutions greater than $1:10^4$. The antisera recognized proteins from rat, mouse (Figure 5, lane 4) and human tissue (Tohyama et al., 1992; Tohyama et al., 1993). Staining of the lower proteins in the ladder was more robust for the rabbit antisera than for Rat 401, however, so further investigation of the specificity of the proteins was undertaken.

Since so many reactive bands were seen, and such a large fragment of nestin was used as the antigen, it was essential to determine whether all the bands were related to the antigen. If the antiserum were specific for nestin, binding to all the bands should be reduced or eliminated by competition with free nestin protein in the antibody incubation buffer. Although purification of intact, soluble nestin was not undertaken, competition of antiserum with bacterial lysate containing nestin fusion proteins compared with lysate from bacteria making TrpE from the vector without insert would answer the same question. Figure 5 (lanes 3-8) shows the result of co-incubation of the antiserum 129 with lysates of bacteria expressing nestin fusion protein, TrpE or with buffer alone. Binding to all the steps in the ladder was inhibited by nestin fusion protein (lanes 7-8), but not by the other conditions. Staining of the top step, which is the same size as the band recognized by Rat 401, was reduced. Lysate inhibited binding to the reactive antigen in ST15A, and in P19 teratocarcinoma cells treated with retinoic acid (Chapter 3).
In variation on the blocking experiment, AS 130 binding was competed with a urea lysate from the vimentin and nestin negative human cell line SW13 which had been transfected with nestin and expressed it at high levels (Chapter 4). Untransfected SW13 was used as a control. Only the parent line inhibited staining in the bands from endothelial cells and adult mouse brain, indicating that this staining comes from a protein highly related to the cloned gene. It also inhibited binding to proteins from a mouse endothelial cell line CBA(3d)CL2 and from the weakly reactive hippocampus of the adult mouse (Figure 6).

Discussion

Antibodies raised against nestin fusion protein and the C terminal peptide had both high specificity and high avidity for nestin. The fusion protein extended the species range of nestin antisera, making

possible identification of stem cells from mouse and human brain tissue. The fusion proteins proved that the cloned nestin gene contained the Rat 401 epitope and localized the epitope to within 200 amino acids in the part of the tail domain proximal to the rod.

The appearance of multiple bands in Western blots for nestin could have several explanations. Rat 401 also recognizes a faint ladder of smaller material in gels, but its staining is much weaker, so the ladder is not as obvious for it as it is for AS 129. The antipeptide antisera never see any but the top band, no matter how long the exposure. Addition of six protease inhibitors: PMSF, aprotinin, leupeptin, pepstatin, diisochlorocoumarin and bestatin were insufficient to prevent proteolysis in the SDS-glycerol-based extraction buffer. Some other investigators have reported the lability of nestin (Friedman et al., 1990; Tohyama et al., 1992; Tohyama et al., 1993) although others have no evidence of it (Almazan et al., 1993; Sejerson and Lendahl, 1993). Production of the ladder may be cell type specific.

Alternatively, the band pattern might be due in part to posttranslational modification. NFH is highly phosphorylated in repeats in the tail which regulate binding to tubulin (Hisanaga et al., 1991). Vimentin is differentially phosphorylated during the cell cycle (Chou et al., 1990). Nestin is highly phosphorylated after treatment of cells with a phosphatase inhibitor (Almazan et al, 1993). Multiple phosphorylations on the tail could account for at least part of the complexity of nestin's gel migration pattern. Work on the nucleotide level has never detected a second nestin gene or message in any species or cell type (Dahlstrand et al., 1992b; Lendahl et al., 1990; Sejerson and Lendahl, 1993). However, experiments discussed in Chapter 5 suggest that the bands are due to proteolysis.

Nestin in tumors and in stem cell identity

The antisera generated from the fusion protein, AS 128, 129 and 130 have been used extensively to detect nestin in human tumors (Dahlstrand et al., 1992a; Tohyama et al., 1992; Valtz et al., 1991) Nestin expression is found extensively in childhood medulloblastomas, and ependymomas (Tohyama et al., 1992; Valtz et al., 1991), as well as most glioblastomas, and a muscle-derived rhabdomyosarcoma (Dahlstrand et al., 1992a) examined. Cerebellar medulloblastomas are often found to contain three cell types: neurons, glia and muscle. Due to the variety of cell types found, the

existence of a stem cell which could give rise to all of these cell types was postulated. The ts SV40 T antigen-immortalized rat cerebellar cell line ST15A isolated in this lab shows such a tri-potent phenotype and expresses nestin strongly. Its relation to the medulloblast has been proposed based on these findings (Frederiksen and McKay, 1988; Valtz et al., 1991). The strong expression in ependymomas is consistent with previous findings, since weak nestin expression in ependyme and tanicytes in adults has been reported (Reynolds et al., 1992; Reynolds and Weiss, 1992; and Dr. O. Brustle, personal communication). In primitive neurectodermal tumors, nestin expression is more common in those that express glial markers than in those that are of neuronal types. Nestin is also expressed strongly in all of the gliomas studied. This is consistent with the persistence of nestin expression in radial glia which differentiate into astrocytes at late stages in development (Edwards et al., 1990; Yang et al., 1992) but its extinction in differentiating neurons. Nestin is reexpressed in reactive gliosis, but this is thought to be secondary to the initial insult of the tumor (Lin et al., 1995; Dahlstrand et al., 1992a).

The antisera raised against the fusion protein have also been used to detect neuronal precursors in the adult brain, which can be induced to proliferate by aggregation in the presence of FGF and TGF-α (Reynolds et al., 1992; Reynolds and Weiss, 1992). Proliferated cells can then be induced to differentiate to neurons in vitro. This protocol and others derived from it could have significant impact on cell transplant-based therapies for neurodegenerative diseases in the adult.

References

Almazan, G., Afar, D. and Bell, J. (1993). Phosphorylation and disruption of intermediate filament proteins in oligodendrocyte precursor cultures treated with Calyculin A. J Neurosci Res 36, 163-172.

Chou, Y.-H., Bischoff, J., Beach, D. and Goldman, R. (1990). Intermediate filament reorganization during mitosis is mediated by p34^{cdc2} phosphorylation of vimentin. Cell 62, 1063-1071.

Dahlstrand, J., Collins, V. and Lendahl, U. (1992a). Expression of the Class VI intermediate filament Nestin in human central nervous system tumors. Cancer Res 52, 5334-5341.

Dahlstrand, J., Zimmerman, L., McKay, R. and Lendahl, U. (1992b). Characterization of the human nestin gene reveals a close evolutionary relationship to neurofilaments. J Cell Sci 103, 589-597.

Edwards, M., Yamamoto, M. and Caviness, V. (1990). Organization of radial glia and related cells in the developing murine CNS. An analysis based upon a new monclonal antibody marker. Neurosci 36, 121-144.

Frederiksen, K., Jat, J., Valtz, N., Levy, D. and McKay, R. (1988). Immortalization of precursor cells from the mammalian CNS. Neuron 1, 439-448.

Frederiksen, K. and McKay, R. (1988). Proliferation and differentiation of rat neuroepithelial precursor cells *in vivo*. J Neurosci 8, 1144-1151.

Friedman, B., Zaremba, S. and Hockfield, S. (1990). Monoclonal antibody Rat 401 recognizes Schwann cells in mature and developing peripheral nerve. J Comp Neurology 295, 43-51.

Harlow, E. and Lane, D. (1988). Antibodies: A Laboratory Manual (Cold Spring Harbor: Cold Spring Harbor Press)

Hisanaga, S., Kusubata, M., Okumura, E. and Kishimoto, T. (1991). Phosphorylation of neurofilament H subunit at the tail domain by CDC2 Kinase dissociates the association to microtubules. J Biol Chem 266, 21798-21803.

Lendahl, U., Zimmerman, L. and McKay, R. (1990). CNS stem cells express a new class of intermediate filament protein. Cell 60, 585-595.

Lin, R., Brustle, O. and McKay, R. (1995). in preparation.

Marvin, M. and McKay, R. (1992). Multipotential stem cells in the vertebrate CNS. Seminars in Cell Biol 3, 401-411.

Reynolds, B., Tetzlaff, W. and Weiss, S. (1992). A multipotent EGF-responsive striatal embryonic progenitor cell produces neurons and astrocytes. J Neurosci 12, 4565-74.

Reynolds, B. and Weiss, S. (1992). Generation of neurons and astrocytes from isolated cells of the adult mammalian central nervous system. Science 255, 1707-1710.

Sambrook, J., Fritsch, E. and Maniatis, T. (1989). Molecular Cloning: A Laboratory Manual (Cold Spring Harbor: Cold Spring Harbor Press)

Sejerson, T. and Lendahl, U. (1993). Transient expression of the intermediate filament nestin during skeletal muscle differentiation. J Cell Sci 106, 1291-1300.

Tapscott, S., Davis, R., Thayer, M., Cheng, P.-F., Weintraub, H. and Lassar, A. (1988). MyoD1: A nuclear phosphoprotein requiring a myc homology region to convert fibroblasts to myoblasts. Science 242, 405-411.

Tohyama, T., Lee, V. M.-Y., Rorke, L., Marvin, M., McKay, R. and Trojanowski, J. (1992). Nestin expression in embryonic human neuroepithelium and in human neuroepithlial tumor cells. Lab Invest 66, 303-313.

Tohyama, T., Lee, V. M.-Y., Rorke, L., Marvin, M., McKay, R. and Trojanowski, J. (1993). Monoclonal antibodies to a rat nestin fusion protein recognize a 220 kD polypeptide in subsets of fetal and adult human CNS neurons and primitive neuroectodermal tumors. Am J Path 143, 258-268.

Tzalagoff, A., Wu, M. and Crivellone, M. (1986). Assembly of the mitochondrial membrane suystem. Characterization of CORI, the structural gene for the 44-kilodalton core protein of yeast coenzyme QH_2-cytochrome c reductase. J Biol Chem 261, 17163-17169.

Valtz, N., Hayes, T., Norregard, T., Liu, S. and McKay, R. (1991). An embryonic origin for medulloblastoma. New Bioologist 3, 364-371.

Yang, H.-Y., Lieska, N., Goldman, R., Johnson-Seaton, D. and Pappas, G. (1992). Distinct developmental subtypes of cultured non-stellate rat astrocytes distinguished by a new glial intermediate filament-associated protein. Brain Res. 573, 161-168.

Figure 3. Map of the positions of the Rat 401 epitope and the antigens used to generate new antisera against nestin. The AS 130 antigen overlapped the Rat 401 epitope. AS 79/AS 80 antigen corresponded to 19 amino acids at the carboxyl terminus of nestin.

N 1A 1B 2A 2B C

L1 L12 L2

AS 79/AS 80 antigen

AS 130 antigen

Rat 401 epitope

60
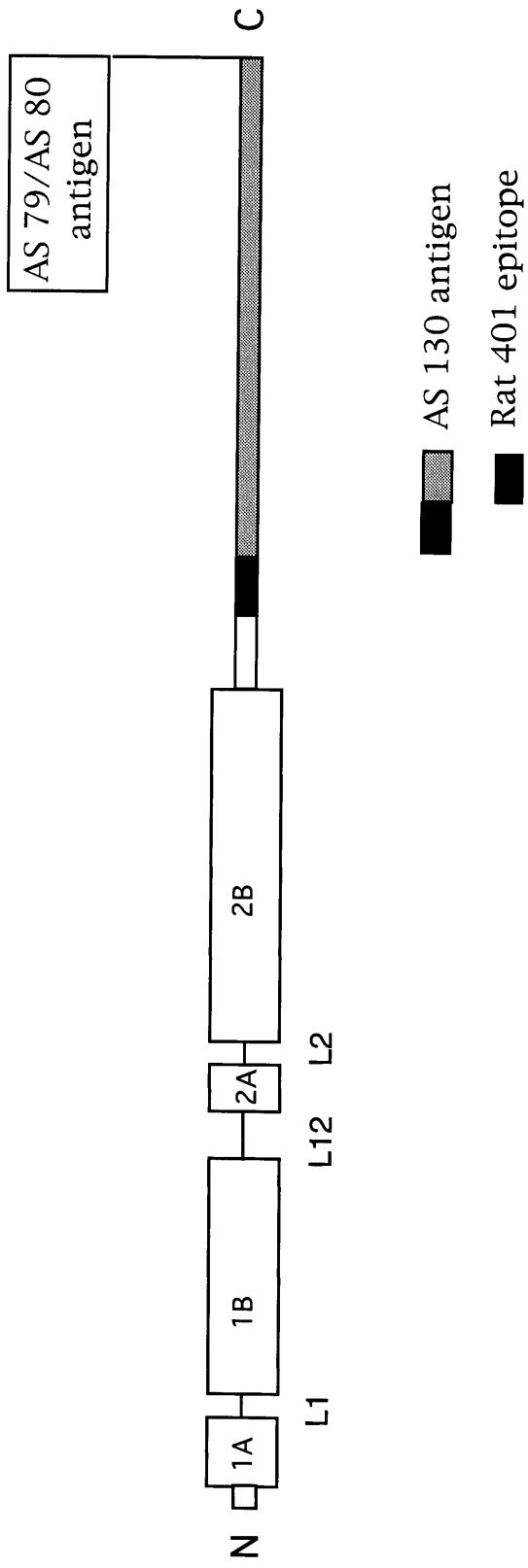
Figure 4. Lanes 1-3, Coomassie Blue stained polyacrylamide gel. Lanes 4 and 5, Western blot of nestin fusion proteins probed with Rat 401. Lane 1, total protein from cerebellar cell line ST15A. Lane 2, HB101 E. coli extract in cells expressing TrpE fusion protein alone. Fusion protein is at the migration front and cannot be seen as a discrete band here. Lane 3, HB101 extract from bacteria expressing the TrpE/401:16 fusion protein. Lane 4, Western blot of bacterial lysate expressing fusion protein TrpE/401:8 and probed with Rat 401. In Coomassie stained gels, the fusion protein is expressed and migrates faster than TrpE/401:16, but slower than any HB101 native proteins. Lane 5, Western blot of bacterial lysate expressing TrpE/401:16. Rat 401 recognizes a set of degradation products of the fusion protein running in nearly contiguous bands on the gel.

1 2 3   4   5

— 2 2 0

— 1 0 0

— 6 8
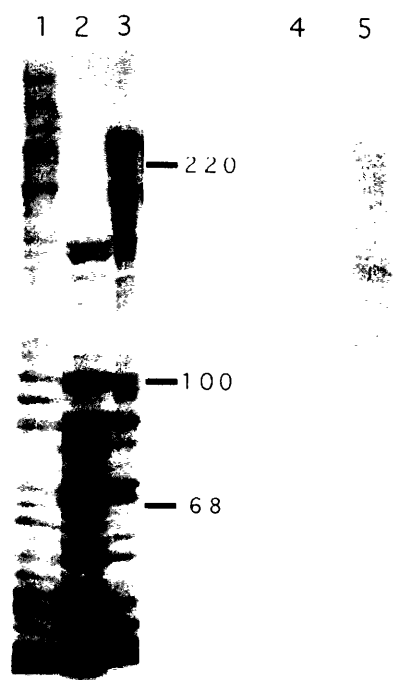
Figure 5. Western blots showing reaction of nestin with Rat 401, AS129 and AS 80 antibodies. Lane 1, ST15A cerebellar cell line is stained with Rat 401. Lane 2, ST15A stained with AS 80. Lanes 3 and 4 incubated with AS129 with bacterial lysis buffer. Lane 3, ST15A. Lane 4, P19 mouse teratocarcinoma, differentiated for 5 days in retinoic acid. Lane 5 and 6 incubated with AS 129 in the presence of bacterial lysate from bacteria transformed with pATH1 vector. Lane 5, ST15A. Lane 6, P19. Lane 7 and 8 incubated with AS 129 and lysate from bacteria expressing TrpE/401:16 fusion protein. Lane 7, ST15A. Lane 8, P19. Only lysate expressing nestin fusion protein blocks binding of AS 129.

195 kD-

105 kD-

1　2　3　4　5　6　7　8

64

Figure 6. Lysates of nestin-expressing mammalian cells. SW13 blocks binding of AS 130 to endothelial and hippocampal extracts. Lane 1 and 3, lysate of CBA(3d)CL2 cells. Lanes 2 and 4, extract of adult mouse hippocampus. Lanes 1 and 2 are incubated with a urea extract of untransfected SW13 cells in the presence of AS130. Lanes 3 and 4 have the same volume of urea extract from SW13 cells expressing a full length genomic clone of nestin (Chapter 5).

Nestin Expression in Embryonic Human Neuroepithelium and in Human Neuroepithelial Tumor Cells

TAKASHI TOHYAMA, VIRGINIA M.-Y. LEE, LUCY B. RORKE, MARTHA MARVIN, RON D. G. MCKAY, AND JOHN Q. TROJANOWSKI

Department of Pathology and Laboratory Medicine, University of Pennsylvania School of Medicine, Philadelphia, Pennsylvania; the Department of Pathology, Children's Hospital of Philadelphia, Philadelphia, Pennsylvania; and the Department of Brain and Cognitive Science, Department of Biology, Massachusetts Institute of Technology, Cambridge, Massachusetts

Nestin is a recently described member of the intermediate filament (IF) protein family that is especially abundant in neuroepithelial stem cells of the rat. The studies described here examine this class VI IF protein in the normal human developing central nervous system (CNS), human brain tumor-derived cell lines, and tissue samples of human CNS tumors. Human nestin exhibited biochemical and immunochemical properties similar to those of rat nestin. Further, as in the rat, nestin was detected immunohistochemically in several different types of immature human CNS cells, i.e. germinal matrix cells, neuroepithelial cells lining the central canal, radial glia and vascular cells. Nestin appeared in these cells at the earliest gestational age (i.e., 6 weeks) examined here and then it declined in all but the vascular cells at later embryonic stages. Nestin also was detected by immunocytochemistry in 6 of 7 primitive neuroectodermal tumor cell lines and in both of 2 malignant glioma cell lines examined. In these cell lines, nestin co-localized incompletely with bundles of IFs containing other IF proteins (i.e., vimentin, glial filament, neurofilament). Nestin was ubiquitous in a wide variety of brain tumors, but was most prominent in gliomas. The transient expression of nestin in primitive neuroepithelial cells at early stages of human embryogenesis and its abundance in neuroepithlelial tumors suggest a role for nestin IFs in cellular events that precede the exit of embryonic CNS stem cells from the cell cycle and the commitment of the progeny of these stem cells to a specific lineage. The subsequent induction of different members of the IF protein family in phenotypically distinct CNS cells (i.e. neurons, glia) and the elimination of nestin from almost all differentiated CNS cells, imply that different classes of IFs subserve functions that are closely linked to the maturational state, as well as the lineage, of CNS cells.

Additional key words: Primitive neuroectodermal tumor, Glioma, Neurofilament protein, Glial fibrillary acidic protein.

Nestin is a newly identified intermediate filament (IF) protein that is distinct from all other classes of IF proteins because it is abundantly expressed in neuroepithelial stem cells early in embryogenesis and then is extinguished from nearly all mature central nervous system (CNS) cells. Nestin was originally described as the antigen recognized by a mouse monoclonal antibody (MAb) known as Rat-401. Notably, this MAb was generated by immunizing mice with fixed spinal cord extracts from embryonic day 15 (E15) rats (20). Initial studies with Rat-401 showed that it recognized transient radial glial cells and dividing neuroepithelial stem cells in the embryonic rat CNS. The developmentally regulated induction and subsequent elimination of nestin in rat CNS tissue using Rat-401 has been described extensively using immunohistochemistry (14, 20) and flow cytometric analyses of dissociated Rat-401 labeled neural tube stem cells (9). In sharp contrast to other IF proteins expressed in the CNS, nestin appears for an extremely short period of time in the developing CNS, i.e., it is detectable at E11 in rat CNS stem cells and then is completely eliminated by postnatal day 6 (P6) in spinal cord and by P21 in cerebellum (20). Unlike CNS nestin, nestin in the peripheral nervous system continues to be expressed in Schwann cells of the adult rat (10). Recently, the cDNA of rat nestin was cloned and the predicted amino acid sequence of the nestin gene indicated that it belonged to the IF family of proteins (26). However, because its sequence does not obviously fit into any of the known IF proteins (i.e., class I-V IF subunits), nestin was designated a class VI IF protein. Nestin is the largest IF subunit with an apparent molecular weight of 210–240

kilodaltons (kd) and a predicted molecular weight of 200 kd.

The present study was designed to characterize human nestin and determine the timing of its induction in the normal human developing CNS. We also probed the expression of nestin in 9 human brain tumor-derived cell lines and in 34 samples of different primary human brain tumors. These studies document the existence of a human counterpart of rat nestin. Further, our data suggest that this class VI IF protein may play a role in primordial CNS stem cells distinct from that played by other IF proteins which supplant nestin in the progeny of these stem cells.

EXPERIMENTAL DESIGN

To characterize human nestin, a new antiserum, designated anti-nestin 129, was raised to recombinant rat nestin expressed in *E. coli*, since the Rat-401 MAb failed to recognize human nestin in immunohistochemical and immunochemical assays. First, this antiserum was compared with the Rat-401 MAb in immunochemical and immunohistochemical studies of postnatal day 6 (P6) rat cerebellum. Then, anti-nestin 129 was used to probe human CNS tissues, tumors and tumor derived cell lines. To determine if nestin co-localized with other IF proteins, double and triple immunofluorescence experiments also were performed using anti-nestin 129 and antibodies to vimentin, glial fibrillary acidic protein (GFAP) and neurofilament (NF) triplet proteins. Finally, Western blots were performed on cytoskeletal extracts of some of the tumor derived cell lines to identify human nestin and to compare it with rat nestin as well as with the class III and IV IF proteins expressed by CNS cells.

RESULTS AND DISCUSSION

SPECIFICITY OF ANTI-NESTIN 129 IN THE RAT

The new rabbit anti-nestin antiserum, *i.e.*, anti-nestin 129 yielded results identical with those produced by the Rat-401 MAb when both were used to probe P6 and adult rat CNS tissues by immunoblots and immunohistochemistry. On immunoblots of cytoskeletal extracts from P6 rat cerebellum separated by sodium dodecyl sulfate (SDS) polyacrylamide gel electrophoresis, anti-nestin 129 identified a band with an apparent molecular weight of 240 kd (Fig. 1, *lane 2*). This band was identical to the band labeled by Rat-401 (Fig. 1, *lane 4*). Further, both antibodies labeled similar bands in lysates of the induced bacteria producing the TrpE-nestin fusion protein (Fig. 1, *lanes 1* and *3*).

In immunohistochemical studies of the P6 rat cerebellum, anti-nestin 129 labeled radial glial cells very intensively. The processes of these cells radiated from the internal granular layer to the external granular layer (Fig. 2A). These radial glia also were labeled with Rat-401 and the anti-vimentin MAb (Fig. 2B and C, respectively). Neither of the anti-nestin antibodies stained immature Purkinje cells or other neurons. In contrast to the P6 rat cerebellum, the anti-nestin 129 and Rat-401 antibodies only stained vascular cells in the adult rat cerebellum (Fig. 2D and E), while the anti-vimentin MAb
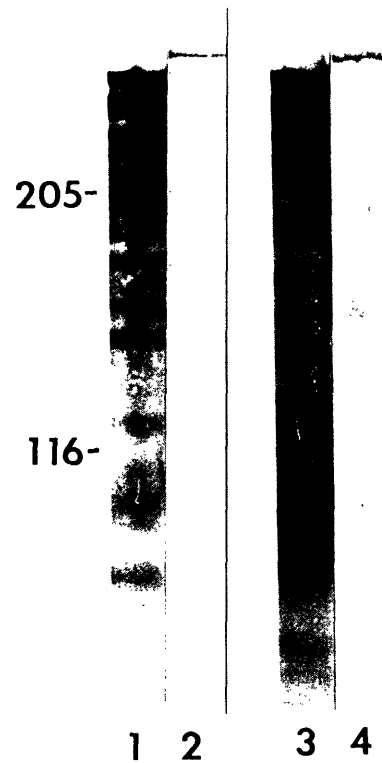

FIG. 1. This figure shows representative Western blot data from the *E. coli* nestin fusion protein (*lanes 1* and *3*) and cytoskeletal extracts (100 μg/lane) from P6 rat cerebellum (*lanes 2* and *4*). The nestin immunobands were produced with anti-nestin 129 (*lanes 1* and 2) and the Rat-401 MAb (*lanes 3* and *4*). Molecular weight markers are indicated (in kD) to the *left* of *lane 1*. The cascade of immunoreactive break down products (*lanes 1* and *3*) was typical of the *E. coli* nestin fusion protein.

(V9) labeled vascular cells, white matter astrocytes and radial glial fibers (Fig. 2F). Furthermore, nestin immunoreactivity was demonstrated by both anti-nestin antibodies in immature skeletal muscle of the P6 rat as well as in Schwann cells of adult rats (data not shown). This is consistent with earlier studies using Rat-401 (10, 20). Thus, the specificity of anti-nestin 129 was equivalent to that of the Rat-401 MAb in these studies. However, like most antisera raised in rabbits, anti-nestin 129 cross reacted at low dilutions with keratins that commonly contaminate SDS-polyacrylamide gel electrophoresis reagents (data not shown).

IMMUNOHISTOCHEMICAL DISTRIBUTION OF NESTIN IN THE HUMAN DEVELOPING CNS

Cervical levels of six developing human spinal cords with gestational ages (GAs) of 6 to 40 weeks were immunohistochemically stained with anti-nestin 129. The spinal cord of the 6-week GA human fetus was composed of three distinct layers, *i.e.*, a layer of primitive neuroepithelial cells lining the central canal, a mantle layer and an outer marginal layer. Anti-nestin 129 stained most cells in the primitive neuroepithelial layers, *i.e.*, the presumptive multipotential stem cells that give rise to CNS neurons and glia. In addition, thin elongated radial glial fibers extending from the primitive neuroepithelial
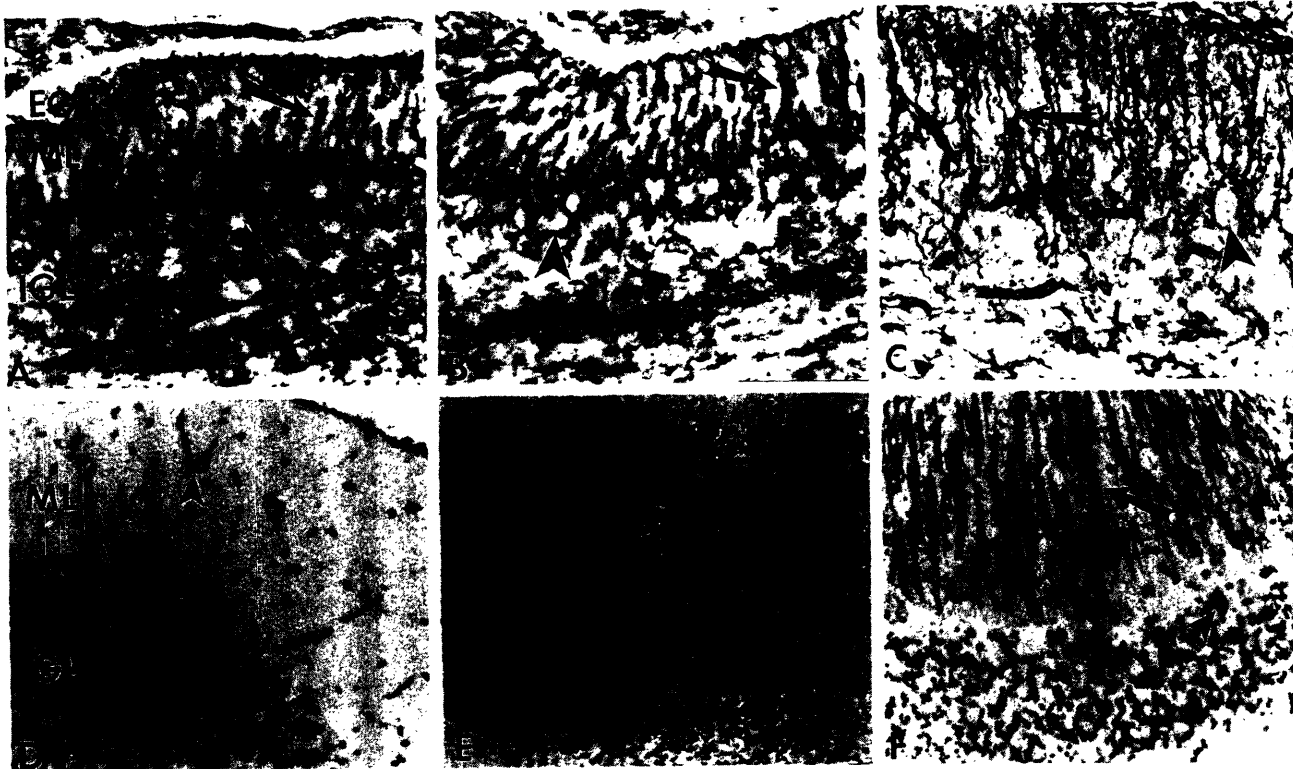
FIG. 2. Representative immunoperoxidase results from the P6 (A, B, and C) and adult (D, E, and F) rat cerebellum are shown here. Radial glial fibers in P6 rat cerebellum (arrows) are positively stained with anti-nestin 129 (A), Rat-401 (B) and the anti-vimentin MAb V9 (C). Immature Purkinje cells (large arrowheads) or other neurons are not stained by these antibodies. On the other hand, radial glial fibers in the adult rat cerebellum are not stained with anti-nestin 129 (D) or Rat-401 (E), but they are strongly positive for vimentin (arrow in F). Vascular cells (small arrowheads) in P6 and adult rats are positively stained with each of these three antibodies. The sections in these and the subsequent histologic photographs are counterstained with hematoxylin. EGL, external granular layer; GL, granular layer; IGL, internal granular layer; ML, molecular layer. Figure 2A, B, and C, ×250; D, E, and F, ×125.

layer to the subpial region were stained by this antiserum (Fig. 3A). These neuroepithelial stem cells and radial glial fibers also expressed vimentin but not GFAP, as described earlier (39). Neuroblasts in the mantle layer (identified by their morphology and NF protein positivity) did not express nestin.

At 11 weeks GA, cells in the ependymal layer were positively stained with anti-nestin 129 as were radial glial fibers (Fig. 3B). These radial glial fibers were also stained with the anti-GFAP MAb, especially at the subpial region, and with the anti-vimentin MAb (data not shown). Nestin immunoreactivity decreased at 17 weeks GA (Fig. 3C), and disappeared at 20 weeks GA. At this gestational age to maturity, GFAP positive glial cells and NF positive neurons were seen in the spinal cord (39), but no elements other than vascular cells were nestin positive.

The telencephalic germinal matrix of two cases with GAs of 17 and 20 weeks were examined with anti-nestin 129. At both time points, many presumptive neuroepithelial stem cells in the germinal matrix were nestin positive (Fig. 3D). These neuroepithelial precursor cells also were labeled by the anti-vimentin MAb, but no germinal matrix cells were stained by the MAbs to GFAP or NF proteins (data not shown). At 40 weeks GA, a well defined germinal matrix was not evident, but clusters of morphologically immature cells (presumably residual,

multipotential precursor cells) were seen in the subependymal region. Nestin immunoreactivity was recognized in only a few of these cells (data not shown).

To determine if neuroepithelial precursors in the cerebellum also expressed nestin, four developing human cerebelli at GAs of 17 to 40 weeks were studied. Late in development, the cerebellar cortex has four distinct layers, i.e., the internal and external granular layers, the Purkinje cell layer, and the molecular layer. However, these layers were not yet evident at 17 weeks GA, and Purkinje cells were not recognizable by morphologic criteria. Nevertheless, immature NF positive cells were observed at 17 weeks GA in the superficial internal granular layer, and these cells probably correspond to nascent Purkinje cells (Fig. 4C). Nestin immunoreactivity was detected at this time in radial glial cells in the internal granular layer and in radial glial processes that extended to the external granular layer (Fig. 4A). These radial glial cells, that mature into the Bergmann glia of the adult cerebellum (13), were also stained by the anti-vimentin MAb (data not shown), but not by the anti-GFAP MAb (Fig. 4B). However, the anti-GFAP MAb did stain ependymal cells lining the fourth ventricle. At 20 weeks GA, nestin immunoreactivity in radial glia was markedly diminished and by 40 weeks GA, it was weakly present in only a few radial glia fibers, whereas vascular cells at 40 weeks GA were clearly nestin-positive (Fig.
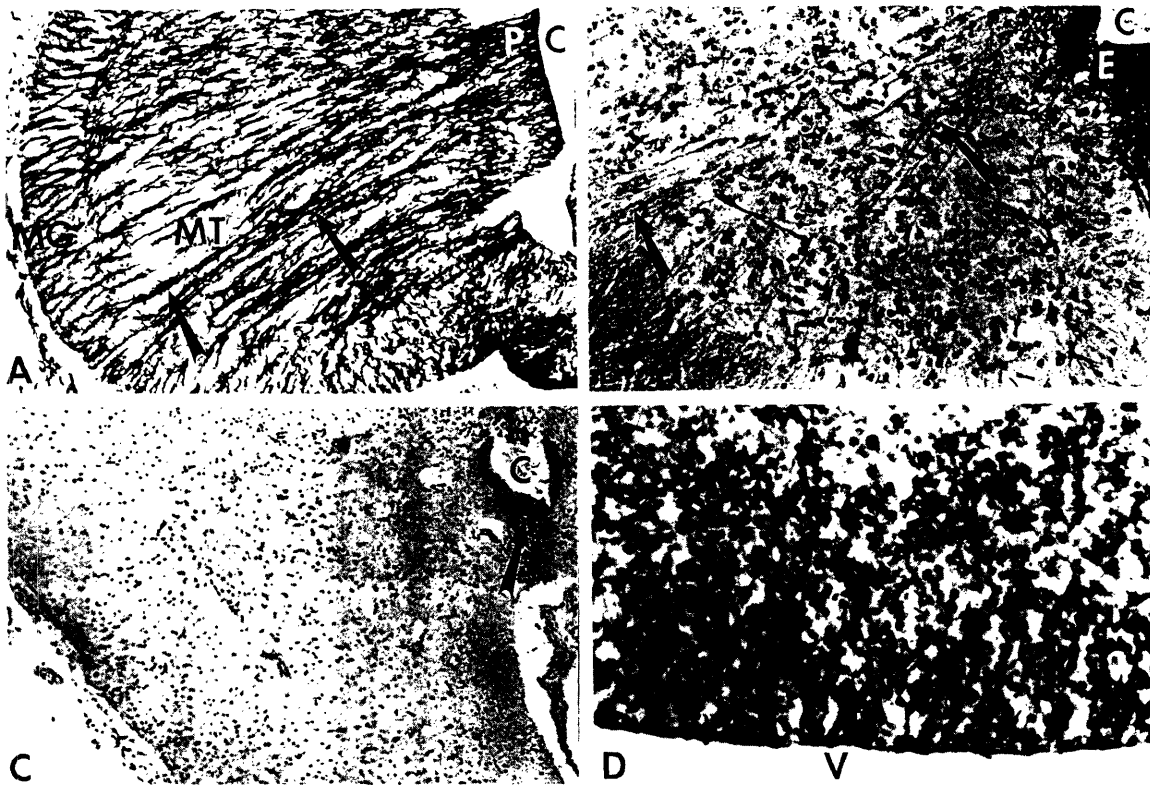
FIG. 3. *A*, *B*, and *C*, show immunohistochemical staining by the anti-nestin 129 antibody in human developing spinal cord. At a GA of 6 weeks (*A*), nearly all of the presumptive stem cells in the primitive neuroepithelial layer (*P*) lining the central canal (*C*) are positively stained. Note the strongly stained radial glial fibers (*arrows*) that radiate through the mantle (*MT*) and marginal layers (*MG*) to the surface of the spinal cord. At 11 weeks GA (*B*), nestin staining is dramatically reduced in radial glial fibers (*arrows*) and in the ependymal layer (*E*). At 17 weeks GA (*C*), very few nestin positive profiles remain around the central canal (*arrow*). In contrast with the spinal cord, nestin positive stem cells were still abundant in the germinal matrix of the lateral ventricle (*V*) at a GA of 17 weeks (*D*). Figure 3*A* and *B*, ×125; *C*, ×60; *D*, ×250.

NESTN   **GFAP**   **NF**
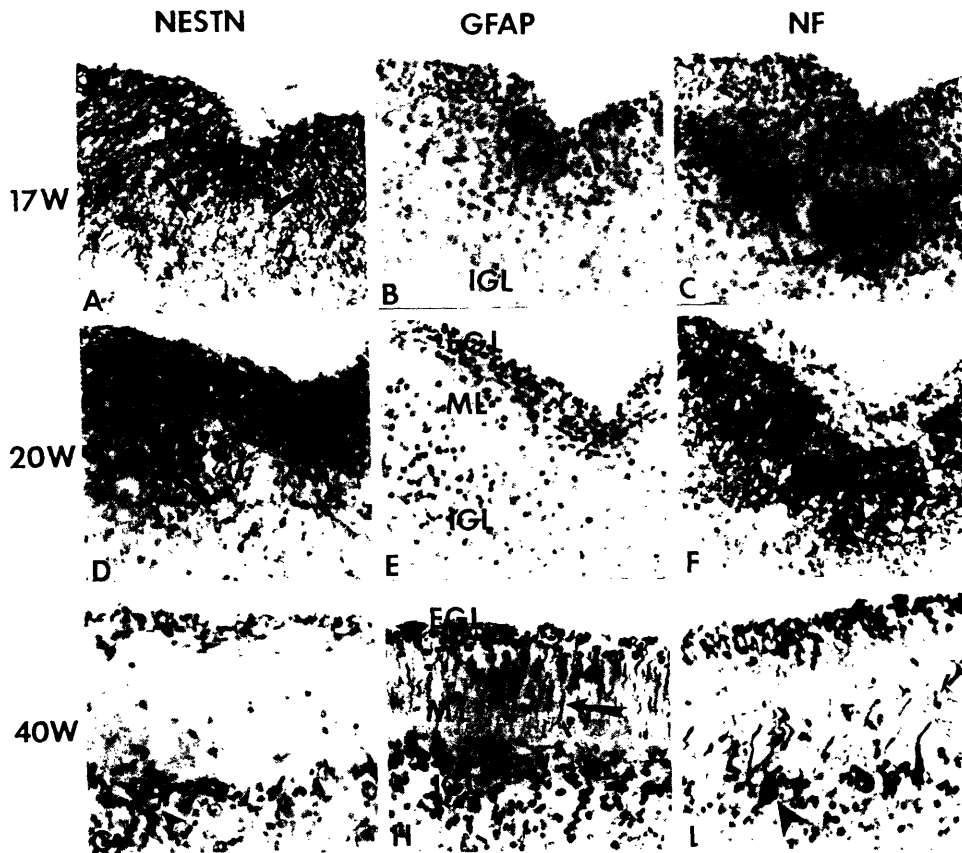
FIG. 4. This figure illustrates sections of the developing human cerebellum with GAs of 17 (*A*, *B*, and *C*), 20 (*D*, *E*, and *F*) and 40 weeks (*G*, *H*, and *I*). The sections were stained with anti-nestin 129 (*A*, *D*, and *G*), a MAb (2.2B10) to GFAP (*B*, *E*, and *H*) or a MAb (RMdO20) that recognizes a non-phosphorylated epitope in NF-M (*C*, *F*, and *I*). At 17 weeks GA, radial glial fibers (*arrows*) are positively stained with anti-nestin 129 (*A*), but nestin immunoreactivity decreases at 20 weeks GA (*D*) and is completely gone by 40 weeks GA (*G*). Note that vascular cells (*small arrowhead* in *G*) are stained. GFAP immunoreactivity in cerebellar radial glial fibers (*arrow*) is shown in the 40 week GA cerebellum (*H*). Purkinje cells (*large arrowheads* in *C*, *F*, and *I*) are stained at all of these GAs with anti-NF MAb (RMdO20) even though Purkinje cells cannot be identified by morphologic criteria at the two earliest time points. *EGL*, external granular layer; *IGL*, internal granular layer; *ML*, molecular layer. ×250.

4G). In contrast, radial glial fibers expressed both GFAP (Fig. 4H) and vimentin (data not shown) at these time points.

The foregoing studies demonstrated that this new anti-nestin antiserum yielded immunohistochemical results in the human developing spinal cord, cerebrum and cerebellum that were nearly identical with those produced by Rat-401 and the anti-nestin antiserum in the rat (20). The expression of nestin in vascular cells had not been described earlier (10, 20), and this may reflect the use of ethanol fixation here.

The highly orchestrated and sequential replacement of 1 or more IF proteins by other members of this family of structural proteins during the progressive differentiation and maturation of developing CNS cells is a remarkable but poorly understood aspect of the biology of IFs (3, 27, 38, 39). Like other IF proteins, the expression of nestin was developmentally regulated in the CNS. For example, radial glial cells expressed nestin and vimentin at the earliest developmental stages of the spinal cord and cerebellum that we examined here. However, nestin immunoreactivity disappeared by about 20 weeks GA in the spinal cord and by 40 weeks GA in the cerebellum. At later developmental stages, GFAP was coexpressed with vimentin in nestin positive radial glia of the spinal cord (11 weeks GA) and cerebellum (27 weeks GA). The extreme brevity of the transient induction of the nestin gene in CNS stem cells is unique among IF proteins, and the biologic significance of this phenomenon as well as the co-expression of three different IF proteins (nestin, vimentin, GFAP) in the same cells (radial glia) remains enigmatic.

NESTIN EXPRESSION IN BRAIN TUMOR-DERIVED CELL LINES

Indirect immunofluorescence studies of 9 well characterized human brain tumor derived cell lines showed variable nestin immunoreactivity in 6 of 7 primitive neuroectodermal tumor (PNET) cell lines, and very intense nestin staining in 2 glioma cell lines. Table 1

TABLE 1. IMMUNOFLUORESCENCE ASSAY OF BRAIN TUMOR-DERIVED CELL LINES

	Nestin	Vimentin	GFAP	NF-L	NF-M	NF-H
PNET cell lines						
Daoy	−	+	−	−	−	−
D283 Med	+	+	−	+	+	+
D341 Med	+	+	−	−	+	+
D384 Med	+	+	−	+	+	+
D425 Med	+	+	−	+	+	+
D458 Med	+	+	−	+	+	+
CHP707 m	+	+	−	+	−	−
Glioma cell lines						
U251 MG	+	+	+	−	−	−
U373 MG	+	+	+	−	−	−

Summary of the data obtained from the indirect immunofluorescence studies of each cell line. The patterns of staining are described as −, no staining; +, positive staining. NF-L, NF-M and NF-H are the low, middle and high molecular weight neurofilament subunits, respectively. The following antibodies were used to obtain these data; nestin (rabbit anti-nestin antiserum 129), vimentin (V9), GFAP (2.2B10), NF-L (NR-4, RMS12), NF-M (RMdO20, RMO254, HO14), NF-H (DP1, TA51, RMO24).

summarizes the data on the expression of nestin and other IF proteins in these cell lines. Except for CHP707m, which was derived from a cerebral neuroblastoma (1), the other 6 PNET cell lines were obtained from cerebellar medulloblastomas (see ref. 19, 21 and 44 as well as citations therein). Daoy does not exhibit any evidence of glial or neuronal differentiation and it was nestin-negative, whereas the other 6 PNET cell lines expressed nestin, and the molecular phenotype of these cell lines resembled that of embryonic neuroblasts (18, 19). Double immunofluorescent staining of D283 Med, which is the most differentiated PNET cell line (21, 40, 41, 44), showed incomplete co-localization of nestin and NF proteins (Fig. 5A and B) in bundles of IFs in the same cells. Similar observations were made using nestin and vimentin antibodies. CHP707m expressed extensive nestin immunoreactivity and double immunofluorescence of nestin and vimentin in this cell line co-localized both proteins in the same cells (Fig. 5C and 5D), but the nestin positive filament bundles were located mainly in the perinuclear area, whereas vimentin-positive filament bundles were present throughout these cells. The Daoy line expresses vimentin, but not NF proteins, GFAP, or other molecular markers of neurons or glia (18, 22). Hence, Daoy is the least differentiated PNET cell line (44), and it did not express nestin (compare Fig. 5E and F). The foregoing co-localization studies also indicated that the anti-nestin 129 did not cross-react with vimentin or NF proteins.

Since nestin is expressed primarily in CNS stem cells and is eliminated during the progressive differentiation and maturation of the progeny of these stem cells, the Daoy cell line may resemble a CNS precursor that subsequently develops into a vimentin and nestin positive CNS stem cell like those observed here in the human spinal cord at a GA of 6 weeks. Alternatively, tumor cell lines contain genetic mutations and their phenotype may not fully replicate that of normal cells. However, the 2 glioma cell lines (U251 MG and U373 MG) resembled immature spinal cord radial glia (i.e. at 11 weeks GA) since these cells co-expressed nestin, GFAP, and vimentin in the triple fluorescence studies (Fig. 5G and H).

Finally, Western blot studies were performed that showed that anti-nestin 129 labeled a single band in cytoskeletal extracts of U251 MG cells, and this immunoband had a molecular weight similar to that of the bacterial TrpE-nestin fusion protein and lower than that of rat nestin expressed in P6 rat cerebellum (compare lane 2 in Fig. 6 and Fig. 1). A similar molecular weight for human nestin was observed in the human teratocarcinoma cell line (NTera 2) as described elsewhere (31). The significance of the difference in the molecular weight of rat and human nestin is unclear and will require further studies. Since these extracts contained vimentin, GFAP and other cytoskeletal proteins, these data further demonstrate the specificity of the anti-nestin antiserum for human nestin.

NESTIN EXPRESSION IN BRAIN TUMOR SAMPLES

Immunohistochemical data on the expression of nestin, other IF proteins and synaptophysin (SYP) by a diverse group of 34 CNS tumors are summarized in Table
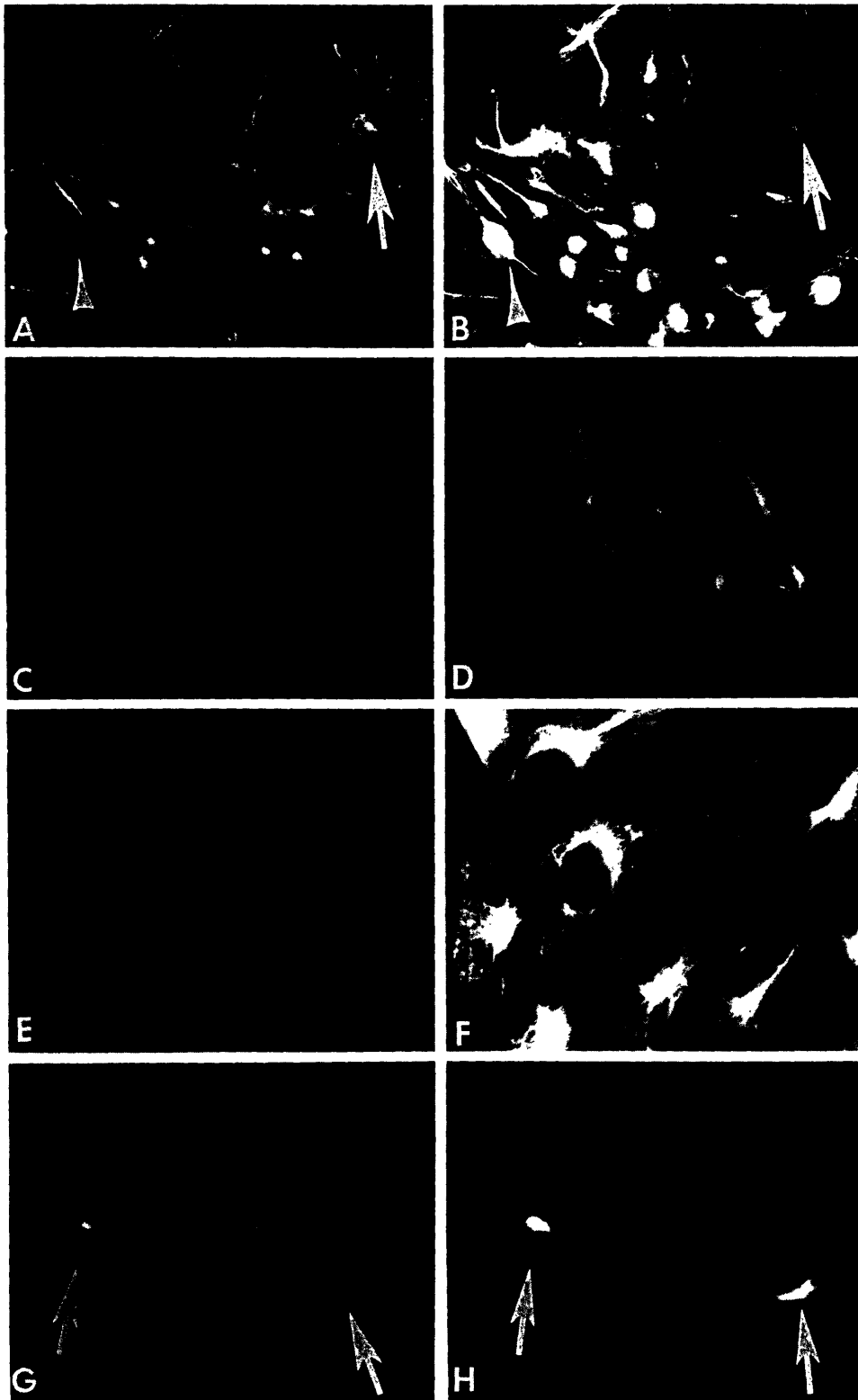
FIG. 5. Double immunofluorescence studies of brain tumor-derived cell lines are shown here. D283 Med (*A* and *B*) was stained for nestin (*A*) and with a MAb (RMO254) to NF-M (*B*). Note that the cell indicated by an *arrow* expresses more nestin immunoreactivity than NF-M, but the cell indicated by an *arrowhead* shows less nestin immunoreactivity than NH-M; CHP707m (*C* and *D*) was stained for nestin (*C*) and with the anti-vimentin (V9) MAb (*D*); Daoy (*E* and *F*) also was stained for nestin (*E*) and vimentin (*F*). Only vimentin was expressed in the Daoy line; *G* and *H* are pictures from the triple immunofluorescence study of U251 MG stained for nestin (*G*), GFAP (*H*) and vimentin (data not shown). Note the co-localization of nestin with GFAP in the cells indicated by *arrows*. These cells were also positive for vimentin. ×375.

2. The results from frozen and ethanol-fixed paraffin-embedded samples from the same biopsy are combined in the 10 cases from which these paired samples were available. Notably, the immunohistochemical results obtained from each of these paired samples were identical, although the primary antibodies were used at slightly higher dilutions on the frozen material compared with the paraffin material.

PNETs. The anti-nestin antiserum stained tumor cells in 12 of the 15 PNETs examined here. Nestin immunoreactivity was found in the cytoplasm of individual neoplastic cells (Fig. 7*A*). Reactivity was also observed in the coarse processes of large stellate cells (Fig. 7*B*), as well as in vascular cells. These stellate cells have generally been regarded as reactive astrocytes, but it has been suggested that some may be neoplastic (6, 17, 28, 32) In

205-

116-

1 2
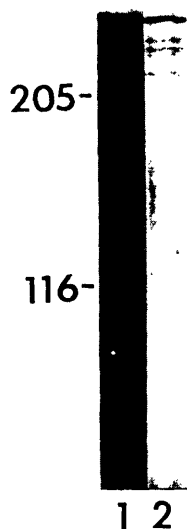
FIG. 6. Immunoblots of human glioma cell line (U251 MG) cytoskeletal extracts and *E. coli* nestin fusion protein probed with antinestin 129 are shown here. *Lane 1* shows the E. coli nestin fusion protein immunoband detected by this antiserum and *lane 2* illustrates a similar band labeled by the anti-nestin 129 in extracts of the U251 MG cells (30 µg/lane). Molecular weight markers (in kD) are indicated to the left lane.

the PNETs with an insular architecture, nestin reactive cells were found both within and outside the islands. Since PNETs express SYP and other neuroendocrine markers as well as all classes of IF proteins (16), we probed the PNETs for SYP. These studies demonstrated SYP in 14 of 15 PNETs. This is concordant with previous reports showing that SYP is expressed in nearly all PNETs (36, 48), peripheral neuroendocrine tumors (49), and central neurocytomas (7). Vimentin was detected in all the PNETs. Ten of the 15 PNETs expressed GFAP and 10 expressed 1 or more NF proteins. Double immunofluorescence studies of nestin and NF proteins (Fig. 7C and D), as well as nestin and GFAP (Fig. 7E and F) on frozen sections showed their co-localization in the same cells. The immunohistochemical data on GFAP and NF proteins suggested that 15 PNETs could be classified into 4 subtypes, i.e., 3 cases of PNET-NOS (not otherwise specified), 2 cases of PNET+G (PNET with glial differentiation), 2 cases of PNET+N (PNET with neuronal differentiation) and 8 cases of PNET+G,N (PNET with glial and neuronal differentiation). All 8 cases of PNET+G,N showed nestin immunoreactivity and 2 cases of PNET+G expressed nestin. On the other hand, 2 cases of PNET+N were negative for nestin. These results may indicate that PNETs with neuronal differentiation tend to lack nestin expression in contrast to PNETs with glial differentiation. This phenomenon paralleled normal differentiation in that postmitotic neuroblasts did not express nestin whereas radial glial cells did, even at relatively late developmental stages. Two of 3 cases of PNET-NOS showed nestin positive tumor cells. This immunohistochemical phenotype might represent primitive neuroepithelial cells or immature radial glial cells in the developing CNS. The other PNET-NOS

case was negative for nestin and it might correspond to extremely immature CNS precursor cells just like the most undifferentiated PNET cell line (*i.e.*, Daoy).

Astrocytic Tumors. Five of 7 astrocytic tumors displayed positively for nestin in the perinuclear cytoplasm of the tumor cells as well as in the cytoplasmic processes of these cells. Additionally blood vessel walls were nestin-positive. Two of 4 benign astrocytomas were negative for nestin. One anaplastic astrocytoma and 2 glioblastomas showed strong nestin positivity. In the glioblastomas, multinuclear giant cells were stained strongly (Fig. 7G).

Ependymomas. Six tumors were histologically diagnosed as ependymomas and all showed nestin positivity. Immunoreactivity for nestin was found in the tumor cells that formed perivascular pseudo-rosettes (Fig. 7H). One ependymoma (with marked nuclear pleomorphism, necrosis and a few mitoses) was diagnosed as an anaplastic ependymoma and it demonstrated the strongest nestin immunoreactivity among the 6 ependymomas.

Other Tumors. No immunoreactivity for nestin was seen in 2 choroid plexus papillomas. In 2 gangliogliomas, nestin was detected only in the glial component. Two meningiomas also showed nestin immunoreactivity.

CONCLUDING REMARKS

This study describes the distribution of nestin in the developing human CNS and tumors derived therefrom. The developmentally regulated and anatomically restricted expression of nestin described here indicates that nestin is a major IF protein of early CNS precursor cells. However, nestin is rapidly extinguished in neurons, glia and other CNS cell types derived from these precursors. The mechanisms responsible for these rapid changes in IF protein expression are unknown, but nerve growth factor has been shown to induce the differentiation of nestin positive precursor cells into NF positive neuronal cells *in vitro* (5). A recent study shows that a nestin positive cell line derived from rat cerebellum can differentiate into multiple fates similar to those seen in medulloblastomas (46). The regulated expression of nestin in primary and immortalized stem cells (5, 9) may allow further studies of nestin during stem cell differentiation and maturation using these culture systems. In contrast to the restricted expression of nestin in normal developing CNS cells, this IF protein was ubiquitously present in a wide variety of CNS neoplasms. Nestin was expressed in a subset of PNETs, but was more abundant in gliomas. The presence of nestin in diverse types of neuroepithelial tumors is similar to vimentin, but distinct from the distribution of GFAP and NF proteins in CNS tumors. Notably, nestin appeared to be more abundant in the phenotypically least mature gliomas that exhibit the most malignant behavior. These findings may be interpreted to suggest that the patterns of IF protein expression in CNS tumors partially recapitulate those seen in the developing CNS.

METHODS

PRODUCTION OF A NEW ANTI-NESTIN ANTISERUM

The insert from the clone λgt10 401:16 (26) was isolated and ligated into the pATH1 vector (45), producing a clone in which

TABLE 2. IMMUNOPEROXIDASE STAINING OF BRAIN TUMORS

No.	Age (yr)	Sex	Material	Location	Nestin	Vim	GFAP	NF	SYP
PNETs									
PNET+N,G									
1	1	M	F	posterior fossa	+	+++	+	+	−
2	1	M	F	posterior fossa	+	+++	+	+++	+++
3	5	F	F	posterior fossa	++	+	+	+	++
4	1	M	F	posterior fossa	++	++	+	+	+++
5	1 month	F	F	posterior fossa	++	++	+	+++	+
6	5	M	F	posterior fossa	++	++++	++	+	+
7	8 months	F	F	posterior fossa	+++	+++	++	+	+
8	1	F	F+P	posterior fossa[a]	++	++	+	+	+++
PNET+N									
9	13	F	F	posterior fossa[b]	−	++++	−	++	++
10	6	M	F	posterior fossa	−	+	E	++	++
PNET+G									
11	11	M	F	posterior fossa	+	+++	++	P	+
12	4	F	F	posterior fossa	+++	++++	++	P	+++
PNET,NOS									
13	2	M	F	pineal	++	++	−	−	++
14	11	M	F	posterior fossa[b]	−	+	−	−	++
15	14	M	F	posterior fossa[b]	+	+++	−	−	+
Astrocytic tumors									
16	2	F	F	posterior fossa[c]	++	++++	++++	−	−
17	6	F	F+P	posterior fossa[c]	−	++++	+++	−	
18	6 months	M	F	hypothalamus[c]	++	+++	+++	−	−
19	17	M	F+P	posterior fossa[d]	−	+++	+++	−	−
20	3	M	F	frontal[e]	+++	NA	+	−	NA
21	6	M	F+P	occipital[f]	+++	+++	+++	−	−
22	13	M	F	posterior fossa[f]	+++	+++	+++	−	−
Ependymomas									
23	3	F	F	parietal	++	++++	+	−	−
24	2	M	F	posterior fossa	+	−	+	−	−
25	3	M	F+P	posterior fossa	++	++++	+++	−	−
26	5	M	F+P	posterior fossa	++	++++	++	−	−
27	15	F	F+P	cerebral hemisphere[g]	++	++++	+	−	−
28	8	F	F+P	parietal[h]	+++	+++	++	−	−
Choroid plexus papillomas									
29	1	M	F	posterior fossa	−	+++	+	−	−
30	2	M	F	lateral ventricle[i]	−	+++	−	−	−
Gangliogliomas									
31	2	F	F	temporal	++	+++	+++	+	+
32	1	F	F	occipital	++	++	+++	+	NA
Meningiomas									
33	8	M	F	posterior fossa	++	++	−	−	−
34	27	M	F+P	anterior fossa	+	+++	−	−	−

Summary of the data obtained from the immunoperoxidase studies of each or the brain tumor samples. Results from frozen (F) and paraffin (P) material are combined in the cases in which both kinds of material were studied. The patterns of staining are described as −, no staining; +, positive in less than 5% of tumor cells, ++, positive in 5 to 50% of tumor cells; +++, positive in 50 to 95% of tumor cells; ++++, positive in more than 95% of tumor cells; E, positive cells equivocal, *i.e.*, reactive astrocytes or tumor cells; P, interstitial filamentous staining in the neuropil. The following antibodies were used to obtain these data; nestin (rabbit anti-nestin antiserum 129), vimentin (V9), GFAP (2.2B10), NF (RMS12, RMdO20, RMO254, HO14, DP1, TA51, RMO24), SYP (SY38). NA, Not available due to limited material; PNET+N,G, PNET with neuronal and glial differentiation; PNET+N, PNET with neuronal differentiation; PNET+G, PNET with glial differentiation; PNET-NOS, PNET, not otherwise specified.

[a] Recurrent tumor of case 7.

[b] Autopsy case.

[c] Benign astrocytoma.

[d] Benign strocytoma + angioma.

[e] Anaplastic astrocytoma.

[f] Glioblastoma multiforme.

[g] Mixed ependymo-astrocytoma.

[h] Anaplastic ependymoma.

[i] Choroid plexus carcinoma.

the bacterial TrpE protein (37.2 kd) was fused at its C-terminus with the last 1197 amino acids of nestin. The fusion protein was induced in *E. coli* strain HB101 with 20 μg/ml indoleacrylic acid (Sigma I1625) for 4 hours as described in (37). The TrpE-nestin fusion protein migrates at greater than 200 kD in 6% SDS-polyacrylamide gel electrophoresis gels, making it the largest protein in the bacterial lysate. The fusion protein was purified by cutting the top band from the gel. Anti-nestin
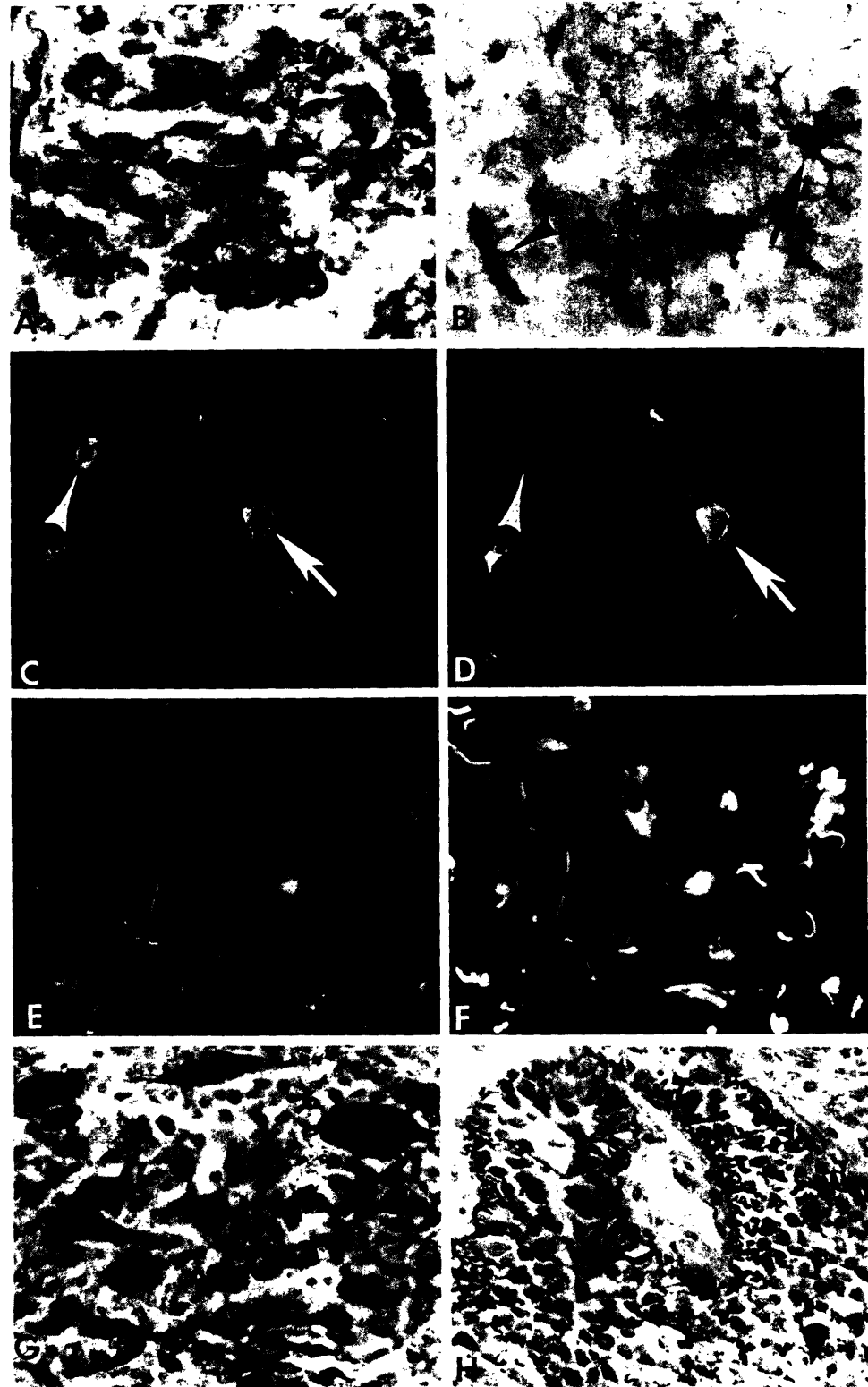
FIG. 7. Representative nestin positive tumor samples are illustrated here. A shows perikaryal nestin immunoreactivity in neoplastic cells of a frozen PNET biopsy sample, while a large nestin positive stellate cell (arrow) and a blood vessel (arrowhead) in this PNET are seen in B. C and D demonstrate a double immunofluorescence experiment on a frozen PNET section using anti-nestin 129 (C) and an anti-NF-M MAb (RMdO20) (D). Note that the cell indicated by an arrow is positive for both nestin and NF-M, but the cell indicated by an arrowhead shows only nestin immunoreactivity. E and F, are also double immunofluorescence experiments conducted on frozen PNET sections labeled with anti-nestin 129 (E) and an anti-GFAP MAb (2.2B10) (F). Many cells coexpress nestin and GFAP. G, Cytoplasmic immunostaining for nestin is seen in large multinucleated cells as well as in small tumor cells of this glioblastoma multiforme (ethanol-fixed paraffin section). H, The perivascular arrangement of nestin positive tumor cells is illustrated in this anaplastic ependymoma (ethanol-fixed paraffin section). Figure 7A and C to F, ×375; B, G, and H, ×250.

antiserum 129 was produced by injecting the fusion protein subcutaneously into a female NZW rabbit. The characterization of anti-nestin 129 and its specificity for human nestin is described here.

TISSUES AND CELL LINES

Six samples of normal human fetal brain and spinal cord at estimated gestational ages of 6, 11, 17, 20, 27 and 40 weeks were collected from spontaneous or therapeutic abortions and

cases of ectopic pregnancy. As described elsewhere (39), these samples exhibited no developmental or pathologic abnormalities. The protocol for these studies was approved by the Committee on Studies Involving Human Beings of the University of Pennsylvania. The CNS tissues from these cases were fixed with 70% ethanol and 150 mM NaCl for 24 to 36 hours and embedded in paraffin. Then, 6-μm thick tissue sections were cut and mounted onto poly-L-lysine coated slides and dried overnight in an oven at 40° C as previously described (42, 43).

Normal human adult CNS tissues, as well as adult and P6 rat CNS tissues, were prepared in the same manner.

Thirty-four human CNS tumors including 15 PNETs (33–35), 7 astrocytomas, 6 ependymomas and 6 other neuroepithelial tumors were obtained from surgical or autopsy cases. Samples were placed in OCT compound and snap-frozen at −20° C and stored at −70° C until used. For the immunoperoxidase studies, 6- to 8-μm thick frozen sections were prepared. After air drying, they were fixed in cold acetone at −20 ° C for 10 minutes. The endogenous peroxidase was quenched by 0.1% hydrogen peroxide in methanol for 30 minutes and the permeability was improved by 0.1% SDS in 0.1 M Tris HCl and heating with microwave energy for 3 minutes. The nonspecific binding of antibodies was blocked by 0.25% cold water fish gelatin with 2% newborn calf serum in 0.1 M Tris HCl for 30 minutes. Ethanol-fixed paraffin-embedded sections were also prepared in 10 cases in the same manner as described above.

Six human PNET cell lines (*i.e.,* D283 Med, D384 Med, D341 Med, D425 Med, D458 Med and Daoy) were established from posterior fossa medulloblastomas or disseminated metastases from these tumors (11, 12, 18, 19, 22). CHP707m is a PNET cell line derived from a cerebral neuroblastoma (1), and it also was studied here. U251 MG and U373 MG, well characterized malignant glioma cell lines, were also studied (2). The cell lines were cultured in RPMI 1640 medium with 10% fetal calf serum at 37° C in 5% CO_2.

IMMUNOPEROXIDASE STAINING

Sections of paraffin-embedded or frozen tissue were probed with the rabbit anti-nestin antiserum and bound primary antibody was visualized with an avidin-biotin complex peroxidase kit according to the manufacture's (Vectastain) instructions (4, 24). Except as noted, all sections were lightly counterstained with hematoxylin following the immunohistochemical procedures. Several other well described antibodies were used in these studies in addition to anti-nestin 129. These antibodies included: anti-nestin MAb Rat-401 (20), 2 different anti-NF-L MAbs (NR-4, Boehringer Mannheim and RMS12), 3 different anti-NF-M MAbs (RMdO20, RMO254 and HO14), 3 different anti-NF-H MAbs (DP1, TA51 and RMO24) (24, 25), anti-GFAP MAb (2.2B10) (23), anti-vimentin MAb (V9, DAKO) (29) and anti-synaptophysin MAb (SY38, Boehringer-Manheim) (15, 47). TA51 and HO14 are rat MAbs while the others are mouse MAbs. Preimmune serum from the rabbit and spent hybridoma supernatant from unfused mouse myeloma cells (sp2) were applied as the negative controls, but multiple different antibodies with different specificities were run in parallel (so that these antibodies would serve as controls for each other).

INDIRECT IMMUNOFLUORESCENCE

Indirect immunofluorescence studies of cultured cells were performed on poly-L-lysine coated glass coverslips as previously reported (30). The cells were fixed with cold acetone at −20° C for 10 minutes or with 70% ethanol and 150 mM NaCl at room temperature and these preparations were incubated with the primary antibodies for 1 hour at room temperature. After washing with phosphate-buffered saline, the coverslips were incubated with the fluorescein isothiocynate, tetramethyl rhodamine isothiocynate or amino methyl coumarin acetate coupled secondary antibodies (Jackson ImmunoResearch, West Grove, Pennsylvania).

GEL ELECTROPHORESIS AND IMMUNOBLOT ANALYSIS

Samples of each cell line and fresh P6 rat cerebellum were homogenized in cold cytoskeletal extraction buffer (0.1 M MES, 1% Triton X-100, 170 mM NaCl, 0.5 mM ethyleneglycol tetraacetic acid, 1 mM guaniosine triphosphate, 20 μM Taxol, 1 mM

dithiothreitol, and a protease inhibitor cocktail containing 0.5 mM phenylmethylsulfonate, N-tosyl-L-phenylalanine chloromethyl ketone, N-tosyl-L-lysine chloromethyl ketone, soybean trypsin inhibitor, Pepstatin A and Leupeptin) and incubated on ice for 15 minutes. The insoluble cytoskeleton was pelleted at 100,000×g and the pellet was solubilized in a hot Laemmli sample buffer. Cytoskeletal extracts were electrophoresed on 6% polyacrylamide gels. The proteins subsequently were transferred to a nitrocellulose membrane and probed with the primary antibody and bound antibody was visualized using an avidin biotin complex peroxidase kit according to the manufacturer's instructions.

REFERENCES

1. Baker DL, Ready UR, Pleasure S, Hardy M, Williams M, Tartaglione M, Biegel JA, Emanuel BS, Lo Presti P, Kreider B, Trojanowski JQ, Evans A, Roy A, Venakatkrishnan G, Chen J, Ross AH, Pleasure D: Human central nervous system primitive neuroectodermal tumor expressing NGF receptors: CHP707m. Ann Neurol 28:136, 1990
2. Bigner DD, Bigner SH, Ponten J, Westermark B, Mahaley MS Jr, Ruoslahti E, Herschman H, Eng LF, Wikstrand CJ: Heterogeneity of genotypic and phenotypic characteristics of fifteen permanent cell lines derived from human gliomas. J Neuropathol Exp Neurol 40:201, 1981
3. Cameron RS, Rakic P: Glial cell lineage in the cerebral cortex: a review and synthesis. Glia 4:124, 1991
4. Carden MJ, Trojanowski JQ, Schlaepher WW, Lee VM-Y: Two-stage expression of neurofilament polypeptides during rat neurogenesis with early establishment of adult phosphorylation patterns. J Neurosci 7:3489, 1987
5. Cattaneo E, McKay R: Proliferation and differentiation of neuronal stem cells regulated by nerve growth factor. Nature (London) 347:762, 1990
6. Cruz-Sanchez FF, Rossi ML, Hughes JT, Moss TH: Differentiation in embryonal neuroepithelial tumors of the central nervous system. Cancer 67:965, 1991
7. Deimling A, Kleihues P, Saremaslani P, Yasargil MG, Spoerri O, Sudhof TC, Wiestler OD: Histogenesis and differentiation potential of central neurocytomas. Lab Invest 64:585, 1991
8. Frederiksen K, Jat PS, Levy D, Valtz N, McKay RDG: Immortalization of precursor cells from the mammalian central nervous system. Neuron 1:439, 1988
9. Frederiksen K, McKay RDG: Proliferation and differentiation of rat neuroepithelial precursor cells *in vivo.* J Neurosci 8:1144, 1988
10. Friedman B, Zaremba S, Hockfield S: Monoclonal antibody rat 401 recognizes Schwann cells in mature and developing peripheral nerve. J Comp Neurol 295:43, 1990
11. Friedman HS, Burger PC, Bigner SH, Trojanowski JQ, Wikstrand CJ, Halperin EC, Bigner DD: Establishment and Characterization of the human medulloblastoma cell line and transplantable xenograft D283 Med. J Neuropathol Exp Neurol 44:592, 1985
12. Friedman HS, Burger PC, Bigner SH, Trojanowski JQ, Brodeur GM, He X, Wikstrand CJ, Kurtzberg J, Berens ME, Halperin EC, Bigner DD: Phenotypic and genotypic analysis of a human medul-

loblastoma cell line and transplantable xenograft (D341 Med) demonstrating amplification of c-myc. Am J Pathol 130:472, 1988

13. Fulop Z, Lakos I, Basco E, Hajos F: Identification of early glial elements as the precursors of Bergmann-glia: a Golgi-analysis of the developing rat cerebellar cortex. Acta Morphol Acad Sci Hung 27:273, 1979

14. Geschwind DH, Hockfield S: Identification of proteins that are developmentally regulated during early cerebral corticogenesis in the rat. J Neurosci 9:4303, 1989

15. Gould VE: Synaptophysin: A new and promising pan-neuroendocrine marker. Arch Pathol Lab Med 111:791, 1987

16. Gould VE, Rorke LB, Jansson DS, Molenaar WM, Trojanowski JQ, Lee VM-Y, Packer RJ, Franke WW: Primitive neuroectodermal tumors of the central nervous system express neuroendocrine markers and may express all classes of intermediate filaments. Human Pathol 21:245, 1990

17. Gould VE, Jansson DS, Molenaar WM, Rorke LB, Trojanowski JQ, Lee VM-Y, Packer RJ, Franke WW: Primitive neuroectodermal tumors of the central nervous system: patterns of expression of neuroendocrine markers, and all classes of intermediate filament proteins. Lab Invest 62:498, 1990

18. He X, Skapek S, Wikstrand CJ, Friedman HS, Trojanowski JQ, Kemashead JT, Coakham HB, Bigner SH, Bigner DD: Phenotypic analysis of four human medulloblastoma cell lines and transplantable xenografts. J Neuropathol Exp Neurol 48:48, 1989

19. He X, Wikstrand CJ, Friedman HS, Bigner SH, Pleasure S, Trojanowski JQ, Bigner DD: Antigenic profiles of newly established medulloblastoma cell lines (D384 Med, D425 Med and D458 Med) and their transplantable xenografts. Lab Invest 64:833, 1991

20. Hockfield S, McKay RDG: Identification of major cell classes in the developing mammalian nervous system. J Neurosci 5:3310, 1985

21. Ibayashi N, Herman MM, Boyd JC, Bigner DD, Friedman HS, Collins VP, Donoso LA, Rubinstein LJ: Relationship of the demonstration of intermediate filament protein to kinetics of three human neuroepithelial cell lines. Lab Invest 61:310, 1989

22. Jacobsen PF, Jenkyn DJ, Papadimitriou JM: Establishment of a human medulloblastoma cell line and its hetrotransplantation into nude mice. J Neuropathol Exp Neurol 44:472, 1985

23. Lee VM-Y, Page CD, Wu HL, Schlaepfer WW: Monoclonal antibodies to gel-excised glial filament protein and their reactivities with other intermediate filament proteins. J Neurochem 42:25, 1984

24. Lee VM-Y, Carden MJ, Schlaepfer WW, Trojanowski JQ: Monoclonal antibodies distinguish several differentially phosphorylated states of the two largest rat neurofilament subunits (NF-H and NF-M) and demonstrate their existence in the normal nervous system of adult rats. J Neurosci 7:3474, 1987

25. Lee VM-Y, Otvos L, Carden MJ, Hollosi M, Dietzschold B, Lazzarini RA: Identification of the major multi-phosphorylation site in mammalian neurofilaments. Proc Natl Acad Sci USA 85:1998, 1988

26. Lendahl U, Zimmerman LB, McKay RDG: CNS stem cells express a new class of intermediate filament protein. Cell 60:585, 1990

27. McKay RDG: The origins of cellular diversity in the mammalian central nervous system. Cell 58:815, 1989

28. Molenaar WM, Jansson DS, Gould VE, Rorke LB, Franke WW, Lee VM-Y, Packer RJ, Trojanowski JQ: Molecular markers of primitive neuroectodermal tumors and other pediatric central nervous system tumors. Monoclonal antibodies to neuronal and glial antigens distinguish subsets of primitive neuroectodermal tumors. Lab Invest 61:635, 1989

29. Osborn MJ, Debus E, Weber K: Monoclonal antibodies specific for vimentin. Eur J Cell Biol 34:137, 1984

30. Pleasure SJ, Lee VM-Y, Nelson DL: Site-specific phosphorylation

of the middle molecular weight human neurofilament protein in transfected non-neuronal cells. J Neurosci 10:2428, 1990

31. Pleasure SJ, Lee VM-Y: In vitro cytoskeletal differentiation of neuronal cells induced by retinoic acid in NTere 2 cells (abstr). Soc Neurosci 17:38, 1991

32. Roessmann U, Velasco ME, Gambetti P, Autlio-Gambetti L: Neuronal and astrocytic differentiation in human neuroepithelial neoplasms: an immunohistochemical study. J Neuropathol Exp Neurol 42:113, 1983

33. Rorke LB: The cerebellar medulloblastoma and its relationship to primitive neuroectodermal tumors. J Neuropathol Exp Neurol 42:1, 1983

34. Rorke LB, Gilles FH, Davis RL, Becker LH: Revision of the World Health Organization classification of brain tumors for childhood brain tumors. Cancer 56 (Suppl):1869, 1985

35. Rorke LB, Molenaar WM, Trojanowski JQ: The impact of monoclonal antibody studies on changing nosology and biological concepts of brain tumors, In New Trends in Pediatric Neuro-Oncology, edited by Bleyer A, Packer R, Pochedly C, p 8. New York, Harwood Academic Publishers, 1991

36. Schwechheimer K, Wiedenmann B, Franke KK: Synaptophysin: A reliable marker for medulloblastomas. Virchows Arch [A] 411:53, 1987

37. Tapscott S, Davis R, Thayer MJ, Cheng P-F, Weintraub H, Lassar AB: Myo D1: A nuclear phosphoprotein requiring a myc homology region to convert fibroblasts to myoblasts. Science (Washington) 242:405, 1988

38. Temple S: Characteristics of cell that give rise to the central nervous system. J Cell Sci 97:213, 1990

39. Tohyama T, Lee VM-Y, Rorke LB, Trojanowski JQ: Molecular molestones that signal axonal maturation and the commitment of human spinal cord precursor cells to the neuronal or glial phenotype in development. J Comp Neurol 310:285, 1991

40. Trojanowski JQ, Friedman HS, Burger PC, Bigner DD: A rapidly dividing human medulloblastoma cell line (D283 Med) expresses all three neurofilament subunits. Am J Pathol 126:358, 1987

41. Trojanowski JQ, Kelsten ML, Lee VM-Y: Phosphate-dependent and independent neurofilament protein epitopes are expressed throughout the cell cycle in human medulloblastoma (D283) cells. Am J Pathol 135:747, 1989

42. Trojanowski JQ, Schuck T, Schmidt ML, Lee VM-Y: Distribution of phosphate-independent MAP2 epitopes revealed with monoclonal antibodies in microwave-denatured human nervous system tissues. J Neurosci Method 29:171, 1989

43. Trojanowski JQ, Schuck T, Schmidt ML, Lee VM-Y: Distribution of tau proteins in the normal human central and peripheral nervous system. J Histochem Cytochem 37:209, 1989

44. Trojanowski JQ, Tohyama T, Lee VM-Y: Medulloblastoma and related primitive neuroectodermal tumors of childhood recapitulate molecular milestones in the maturation of neuroblasts. Mol Chem Neuropathol, in press 1992

45. Tzagaloff A, Wu M, Crivellone M: Assembly of the mitochondrial membrane system. J Biol Chem 261:17163, 1986

46. Valtz N, Norregaard T, Hayes T, Liu S, McKay RDG: An embryonic origin for medulloblastoma. New Biologist 3:364, 1991

47. Wiedenmann B, Franke WW: Identification and localization of Synaptophysin, an integral membrane glycoprotein of Mr 38,000 characteristic of presynaptic vesicles. Cell 41:1017, 1985

48. Wiedenmann B, Franke WW, Kuhn C, Moll R, Gould VE: Synaptophysin: A marker protein for neuroendocrine cells and neoplasms. Proc Natl Acad Sci USA 83:3500, 1986

49. Wiedenmann B, Huttner WB: Synaptophysin and chromogranins/secretogranins-widespread constituents of distinct types of neuroendocrine vesicles and new tools in tumor diagnosis. Virchow Arch [B] 58:95, 1989

Chapter 3: Induction of Nestin in Embryonal Carcinoma Cells

Introduction

One model for the neuronal stem cell is the embryonal carcinoma (EC) cell. EC cells are derived from tumors which have properties of early embryonic cells. Embryonal carcinomas can be derived either from spontaneous germ cell tumors or from fetal cells transplanted to an ectopic site. P19 cells are the latter type, derived from *in vitro* culture of a primary tumor caused by transplanting cells from a 7.5 day mouse embryo into the adult kidney capsule. The cells express stage-specific embryonic antigen 1, a marker for early embryos and ES cells. *In vitro*, P19 can be induced to differentiate to cell types representing all three germ layers and some extraembryonic tissues under various conditions. If treated with 0.1 to 1 μM retinoic acid, the cells form neurons and glia (Jones-Villenueve, et al., 1982; Rudniki and McBurney, 1987). They rapidly enter the neuronal differentiation program after induction with retinoic acid. Within four hours, the cells switch from a proliferating, undifferentiated early embryonic state to neuroepithelial stem cells, as judged by Oct-3 expression. Expression of Oct-3, a POU domain transcription factor, is repressed rapidly after differentiation (Okamoto, et al., 1990). This protein is very similar to another POU-domain protein, Oct-4, cloned from F9 embryonal carcinoma cells, which is expressed in the inner cell mass of the 3.5 day embryo (Scholler, 1990). The two predicted proteins differ at the N and C termini and may be formed by alternative splicing.

Nestin was expected to be induced in these cells the initiation of the differentiation program because it is expressed in a cell type which is intermediate between the 7.5 day embryo and adult neurons. The results presented here show that nestin protein is induced within 24 hours of retinoic acid treatment. The transition out of the nestin positive state is accompanied by rapid changes in the other IF subunits present in the cell. One possible function of nestin and vimentin is to set up a scaffold of intermediate filaments which is taken over by the type IV IFs in neurons and the Type III IF GFAP in glia. To determine whether nestin colocalizes with neurofilaments in differentiating neurons, P19 cells were differentiated and examined by immunofluorescence.

Materials and Methods

Cell Culture

P19 embryonal carcinoma cells were obtained from Michael Rudniki and from John Dinsmore. Cells were grown in α-MEM (Gibco) supplemented with 0.1 mg/L biotin, 1.36 mg/L vitamin B12, 50 mg/L ascorbic acid, penicillin and streptomycin (Gibco), 7.5% newborn calf serum and 2.5% fetal calf serum (Sigma). They were subcultured by incubating in 0.05% trypsin in 10mM EDTA for 10 minutes, vigorously pipetted with a Gilson pipetman to obtain a single cell suspension, and plated at a density of 10^5 cells/ml. Differentiation was carried out either on suspended cells which formed aggregates, or on cells plated on glass coverslips. Aggregates were formed by treating 10^5 cells/ml with 300 nM RA in petri dishes for 4 days with one change of medium (Rudniki and McBurney, 1987). On day 4, cells were plated onto glass coverslips or onto tissue culture plastic. For adherent cultures, 12 mm diameter glass coverslips were treated with 0.015 mg/ml poly-ornithine in 24 well plates. Cells were plated at 10^5/ml in 0.5 ml medium per well, after the coverslips were washed twice with PBS. In both cases, α-MEM was supplemented with 300 nM retinoic acid (RA) from a 1 mM ethanol stock stored in the dark at -20°C.

Immunofluorescence

Cells were fixed for 15 minutes in 4% paraformaldehyde in 0.1M borate buffer, pH 9.5, for nestin and neurofilaments. Anti-neurofilament -light and -medium, anti-MAP2, and anti-tubulin III were all obtained from Sigma. The antinestin sera are described in Chaper 2. Secondary antibodies were: affinity purified goat anti mouse conjugated to Lissamine rhodamine and affinity purified goat anti rabbit conjugated to fluorescein (Cappel).
Coverslips were washed in five changes of PBS between antibody applications. For double labelling, antibodies were applied sequentially without postfixing.

Western Blots

Western blotting was performed as in Chapter 2.

RNA was prepared by GTC extraction and CsCl centifugation by standard methods (Sambrook, et al., 1989) 1.5% formaldehyde agarose gels were run and transferred to Gene-Screen Plus (duPont) or nitrocellulose (Schliecher and Schuell) in 10x SSC. ^{32}P-CTP (New England Nuclear) labelled probes were prepared by random priming reactions using a reagents from Boehringer Mannheim.

Results

The time course of nestin expression in the mouse embryo shown in Figure 7 is similar to that in the rat (Lendahl, et al., 1990). Nestin mRNA is high at embryonic day 13 and drops quickly in the cortex. In the cerebellum, which develops later, the message remains present until after birth. Nestin is not detectable in the adult.

P19 cells differentiate to neurons and glia in high concentrations of retinoic acid (RA; 1 mM). When differentiated in aggregate suspension, neuron-specific anitigenic markers can first be seen at day 2. The expression of nestin should precede neurofilament expression if the cells are going through the normal stages of embryonic development from undifferentiated inner cell mass through neuroepithelium to terminally differentiated neurons, glia and oligodendrocytes. A Western blot showing the induction of nestin expression in aggregated differentiating P19 cells shows that expression is elevated on day 1 and rises steadily to a peak at day 7 (Figure 8). There is a low basal level of nestin expression in these cells, which rises when they are grown at low density. When cells are aggregated without retinoic acid, this basal level drops below detection by day 2.

In order to examine the onset of nestin and neurofilament expression in individual cells by immunofluorescence, cells were differentiated without aggregation. Long, strongly staining neurofilament positive processes were still formed under these conditions, although the number of neuronal processes was reduced (Berg and McBurney, 1990). Nestin staining is elevated within 24 hours of RA addition in nearly every cell. Neurofilament -light and -medium staining is first seen on day 2 and becomes abundant by day 3.

By day 2, some cells co-express NFM and nestin in the same process (Figure 9), This co-expression is transient. On day 4, P19 cultures

80

contain thick clumps of neurons which grow on top of nestin positive and nestin negative flat cells. Doubly stained processes in these cultures are rare (Figure 10). NF-L has a similar pattern of expression at four days (Figure 11). At four days and later, neurons are abundant and processes profuse. Neurofilament staining is confined to processes while nestin stains cytoplasm of underlying cells. The co-expression of nestin and neurofilament is transient. Nestin is not found in mature neurons expressing tubulin III (Figure 12), nor does it colocalize with MAP2 (Figure 13).

Discussion

The expression of nestin mRNA in the mouse correlated well with that in the rat. Nestin message remained present longer in the late-developing cerebellum than it did in the cortex. The weak signal on the Northern blot is due to the low homology of the rat probe to this region of the mouse gene, in the distal end of the tail (see Figure 3). This region of the tail is not well conserved between rat and human.

P19 cells are an inducible system in which the factors repressing or activating nestin transcription during development can be studied. In the characterization of the nestin promoter, this could prove to be a tractable model system as P19 cells form neurons and glia upon treatment with retinoic acid. Neurons continue to mature in culture, eventually forming synapses and expressing a variety of neurotransmitters (McBurney, et al., 1988). Undifferentiated P19 cells express SSEA-1, a marker for early embryos, embryonic stem cells and embryonal carcinomas. During retinoic acid-induced differentiation, various cell type-specific markers appear. In neurons, HNK-1 is expressed shortly before neurofilaments. A2B5 staining, which is present in 15-30% of the undifferentiated cells, becomes expressed in a large fraction of neurons and some non-neuronal cells. Neurons express the three neurofilament subunits, synaptophysin, have high affinty GABA uptake sites and choline acetyl transferase activity.

Since P19 was derived from a stage prior to the onset of nestin expression, we wanted to determine whether nestin was expressed before the cells differentiate into neurons. Such a system would be a model for the early stages of neurulation. The onset of nestin expression is difficult to study in primary cultures because of the lack of material. This work makes use of the high avidity antisera against nestin to show that nestin is induced within one day of

retinoic acid treatment. The transient coexpression of nestin and neuronal antigens suggests that nestin is downregulated when neurons differentiate. These experiments suggest that P19 cells would be a good model system to study the regulation of nestin expression.

The abrupt changes in the intermediate filament patterns in developing neurons suggested the hypothesis that earlier types of IFs set up a scaffolding which is filled out by later IF types. The P19 line may be a good system in which to study the changes in IF pattern. However, the system has some disadvantages as well. Although the line takes up DNA in most transfection protocols, expression of foreign DNAs in selected clones always takes place in a mosaic pattern. The effects of the transient expression of foreign gene constructs are therefore difficult to assess unless the frequency of expression was very high. If these difficulties can be overcome, P19 would be an excellent system to study the effect of nestin mutations on the proliferation and differentiation of CNS precursors and their differentiated products.

References

Berg, R. and McBurney, M. (1990). Cell density and cell cycle effects on retinoic acid-induced embryonal carcinoma cell differentiation. Devel 138, 123-135.

Jones-Villenueve, E., McBurney, M., Rogers, K. and Kalnins, V. (1982). Retinoic acid induces embryonal carcinoma cells to differentiate into neurons. J Cell Biol 94, 253-262.

Lendahl, U., Zimmerman, L. and McKay, R. (1990). CNS stem cells express a new class of intermediate filament protein. Cell 60, 585-595.

McBurney, M., Reuhl, K., Ally, A., Nasipuri, S., Bell, J. and Craig, J. (1988). Differentiation of embryonal carcinoma-derived neurons in culture. J Neurosci 8, 1063-1073.

Okamoto, K., Okazawa, H., Okuda, A., Sakai, M., Muramatsu, M. and Hamada, H. (1990). A novel octamer binding transcription factor is differentially expressed in mouse embryonic cells. Cell 60, 461-472.

Rudniki, M. and McBurney, M. (1987). Cell culture methods and induction of differentiation of embryonal carcinoma lines. In Teratocarcinomas and embryonic stem cells: A practical approach (Oxford: IRL Press), pp. 19-49

Sambrook, J., Fritsch, E. and Maniatis, T. (1989). Molecular Cloning: A Laboratory Manual (Cold Spring Harbor: Cold Spring Harbor Press)

Figure 7. Nestin expression by Northern blot on RNA from developing and adult mouse brain. ST15A is a nestin positive rat cell line isolated from cerebellum. ACtx: adult cortex; ACb, adult cerebellum; P5Ctx, postnatal day 5 cortex; P5Cb, P5 cerebellum; P1 Ctx; postnatal day 1 cortex, P1Cb, P1 cerebellum; E16Ctx, embryonic day 16 cortex; E16Cb, cerebellum; E13Cb, Embryonic day 13 total brain. Nestin is detected with a rat probe to the less conserved 3' end of the rat message, so bands are weak. Nestin is expressed prenatally, declines more quickly in cortex than in cerebellum, and is extinguished in adult.

A.

ST15A ACtx ACb P5Ctx P5Cb P1Ctx P1Cb E16Ctx E13Cb

NESTIN-

28 S -

18S-

B.

Band Intensity

10

5

E13 E16 P1
ctx P5
ctx Adult
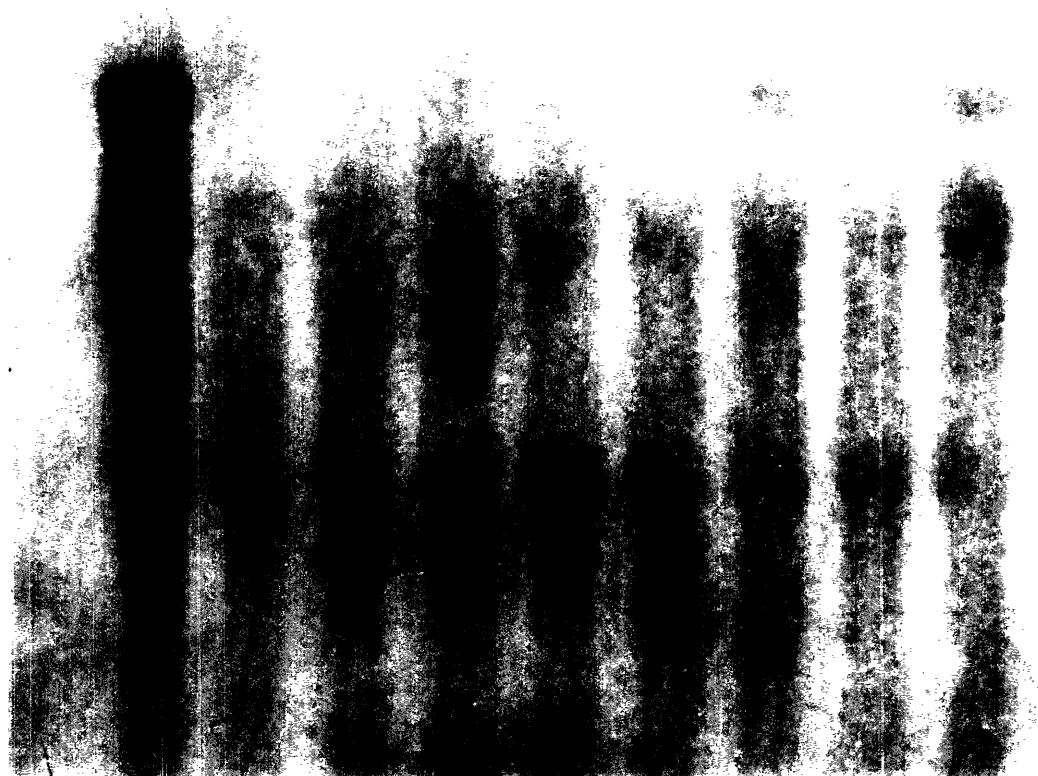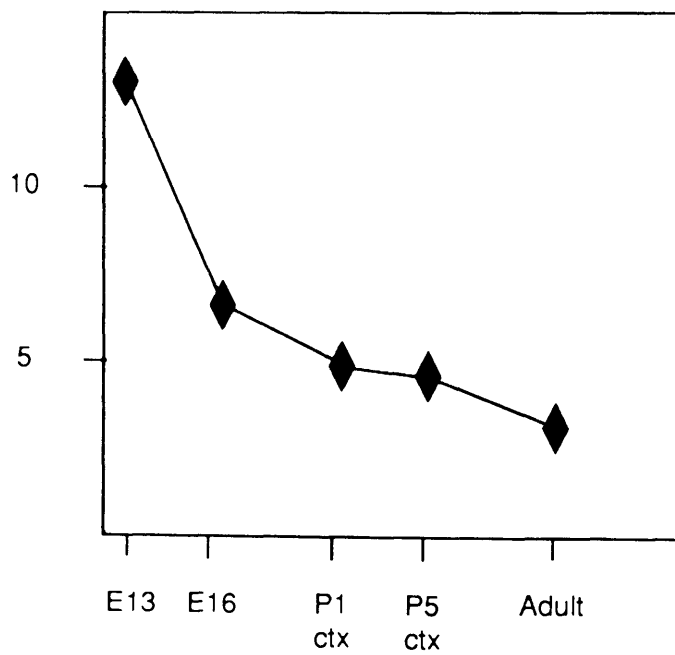
Figure 8. Western blot demonstrating nestin expression following induction of differentiation by retinoic acid and aggregation in P19 cells. Nestin reactivity is low in passaging P19 cells. It is induced within one day of exposure to retinoic acid. Nestin expression peaks at three days following exposure to RA. Expression declines slightly after day 3, but rises again as nestin positive cells proliferate and overgrow the plate.

Days after
retinoic acid

Band
intensity

Neuronal differentiation

Replated
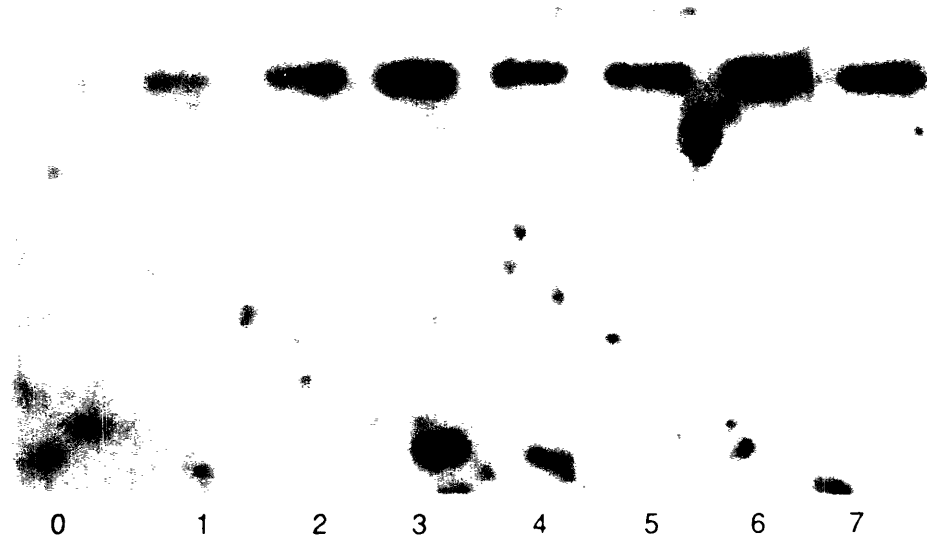
Days after
retinoic acid
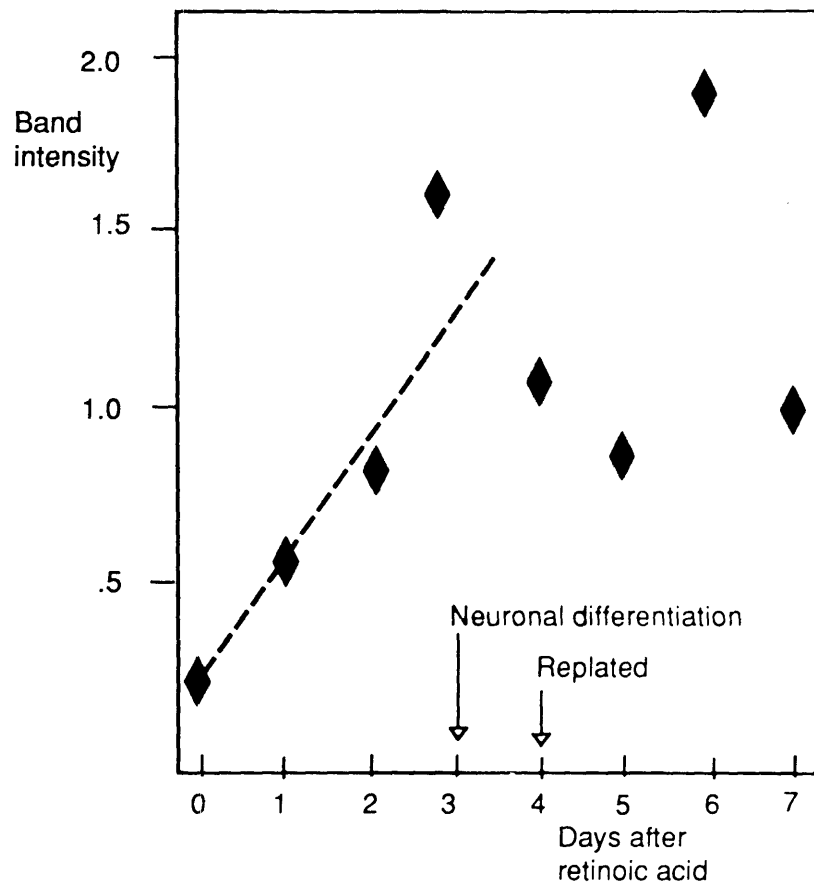
Figure 9. P19 cells differentiated for two days and stained for NFM and nestin. *(Top panel)* NFM stain. *(Bottom)* Nestin expression is seen in processes, but is weak compared to NFM stain. The underlying cells are nestin positive *(arrowhead)*. In the processes marked with the *arrow*, nestin expression coincides with NFM expression.

Figure 10. *Top:* NFM stain in P19 cells at 4 days after induction with retinoic acid. *Bottom:* Nestin stain in the same field of cells. NFM positive neurons are profuse, but nestin immunoreactivity is low in most *(arrowheads)*. A nestin positive process is marked with the *arrow*.
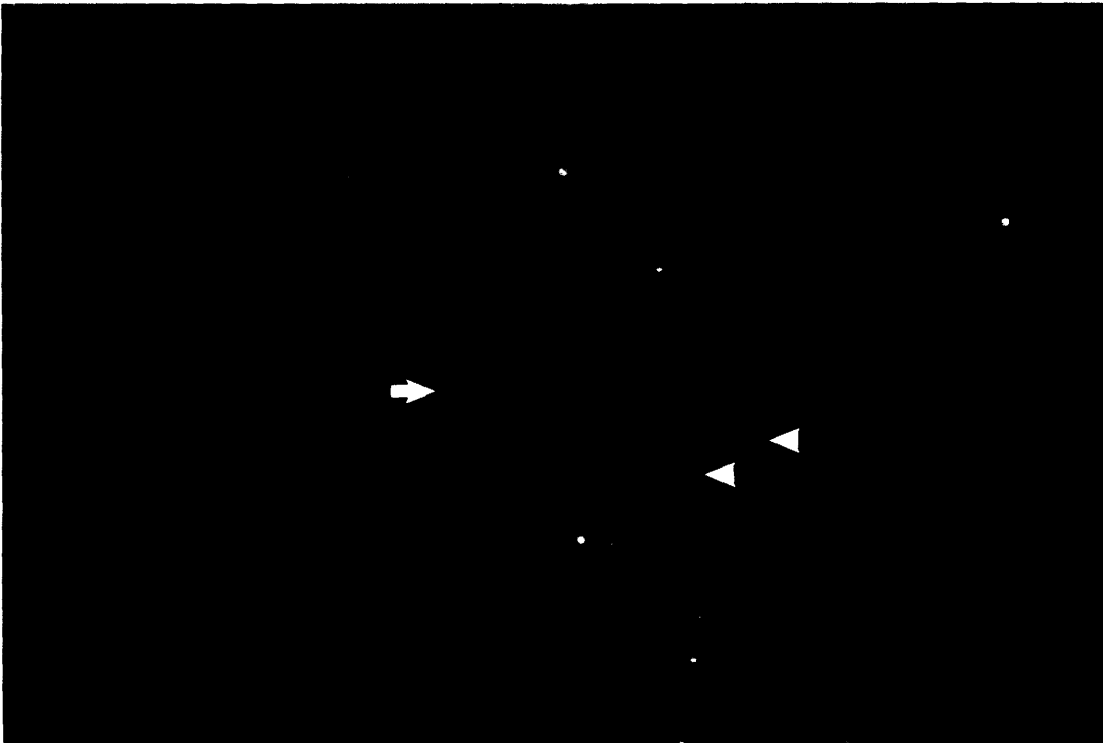
Figure 11. *Top:* NFL stains neurons in P19 cells four days after differentiation begins. *Bottom:* Nestin is co-expressed with NFL in some neuronal processes *(large arrow). Arrowhead* marks nestin negative process. Small arrows mark nestin positive, NFL negative processes.
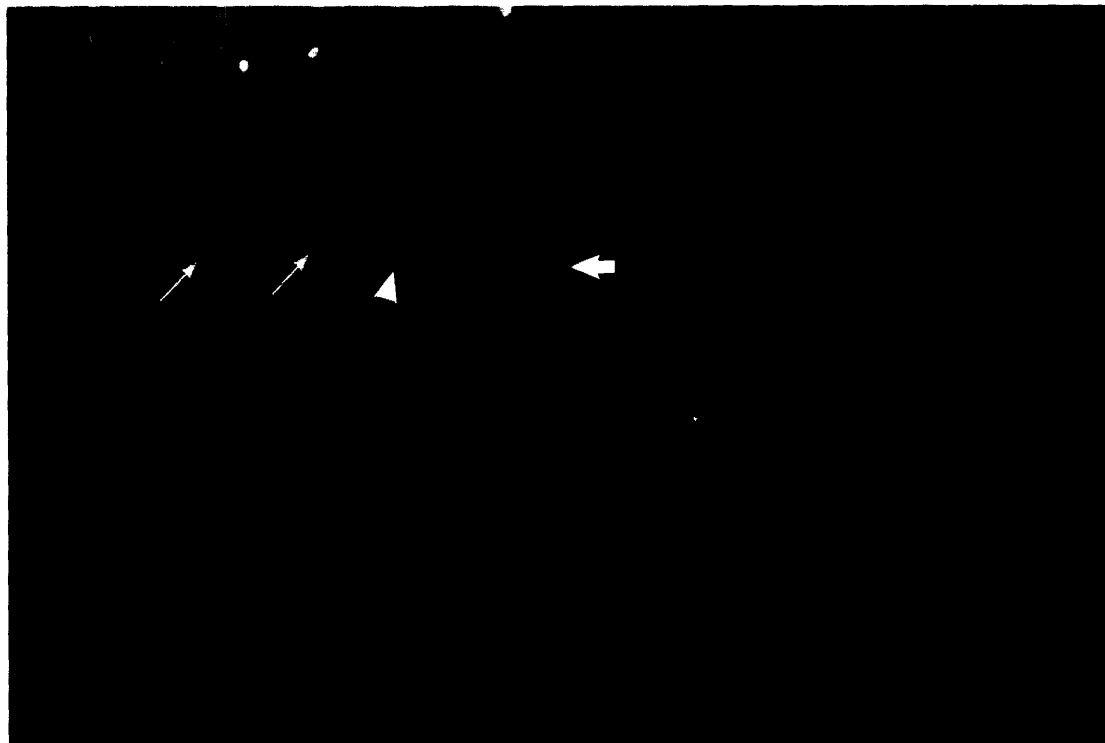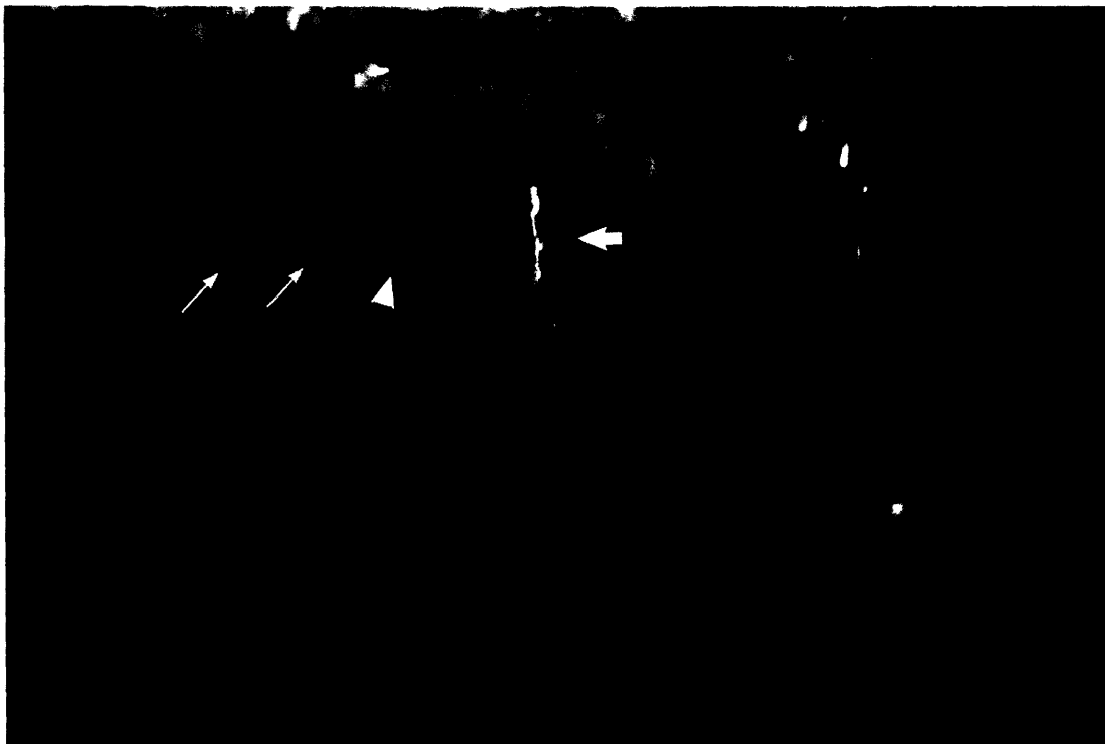
Figure 12. P19 cells differentiated for four days. *Top:* Cells stained for the neuronal marker tubulin III. *Bottom:* Nestin stain. Most tubulin III positive neurons are nestin negative. Nestin stains some processes that tubulin does not. Some of the underlying cells are nestin positive.

95
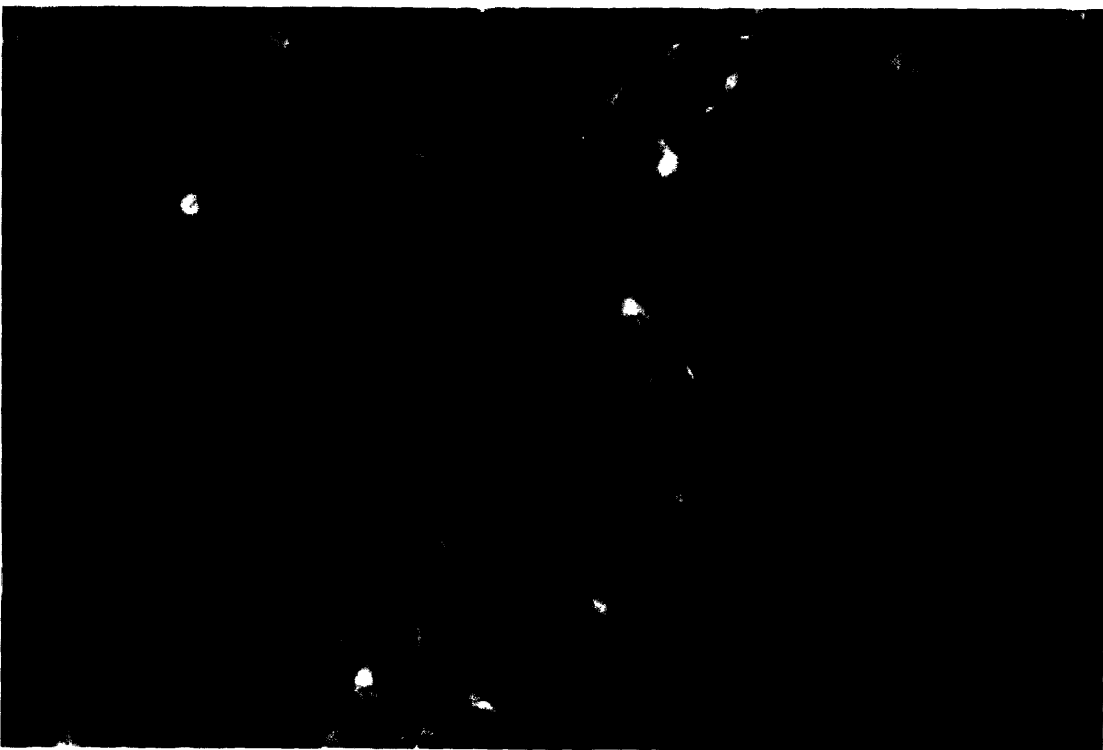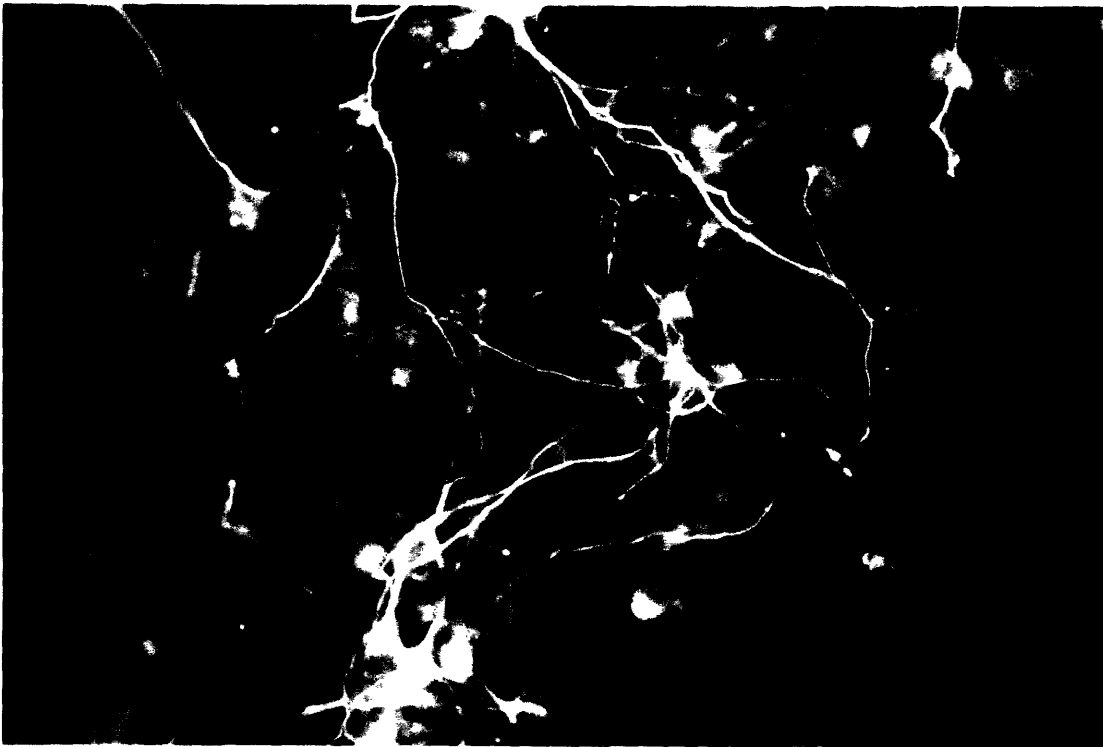
Figure 13. P19 cells differentiated for four days. *Top:* MAP-2 staining is found in cell bodies and processes, while nestin *(bottom)* is expressed in the underlying cells.
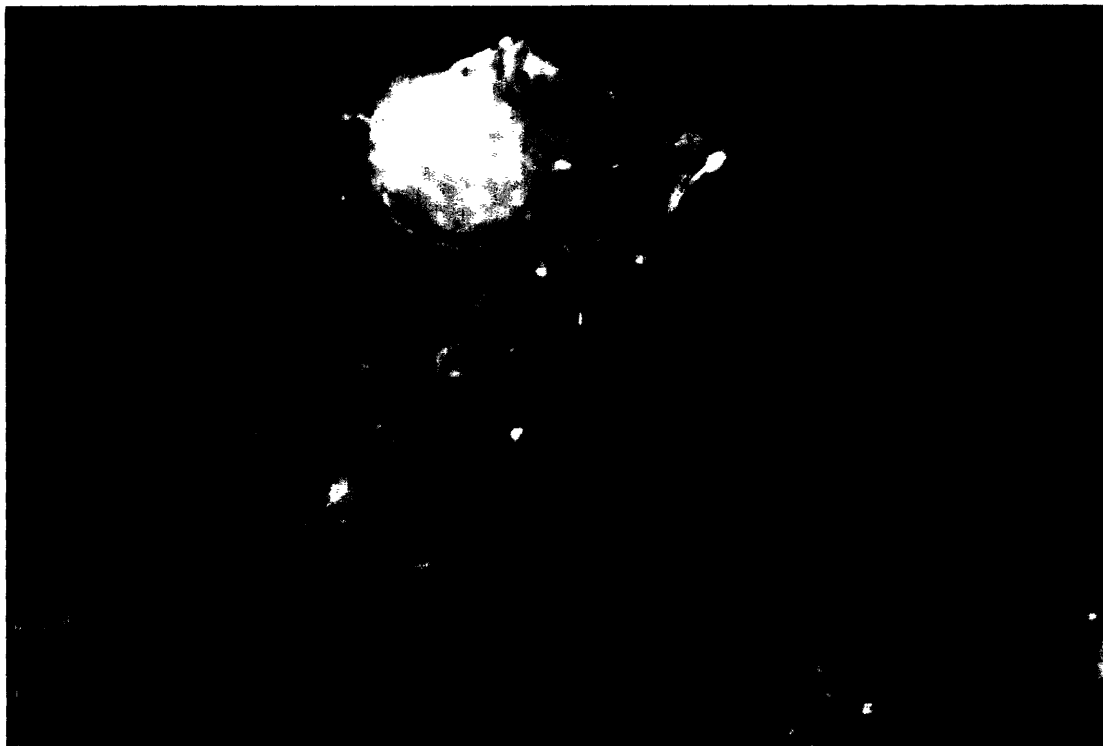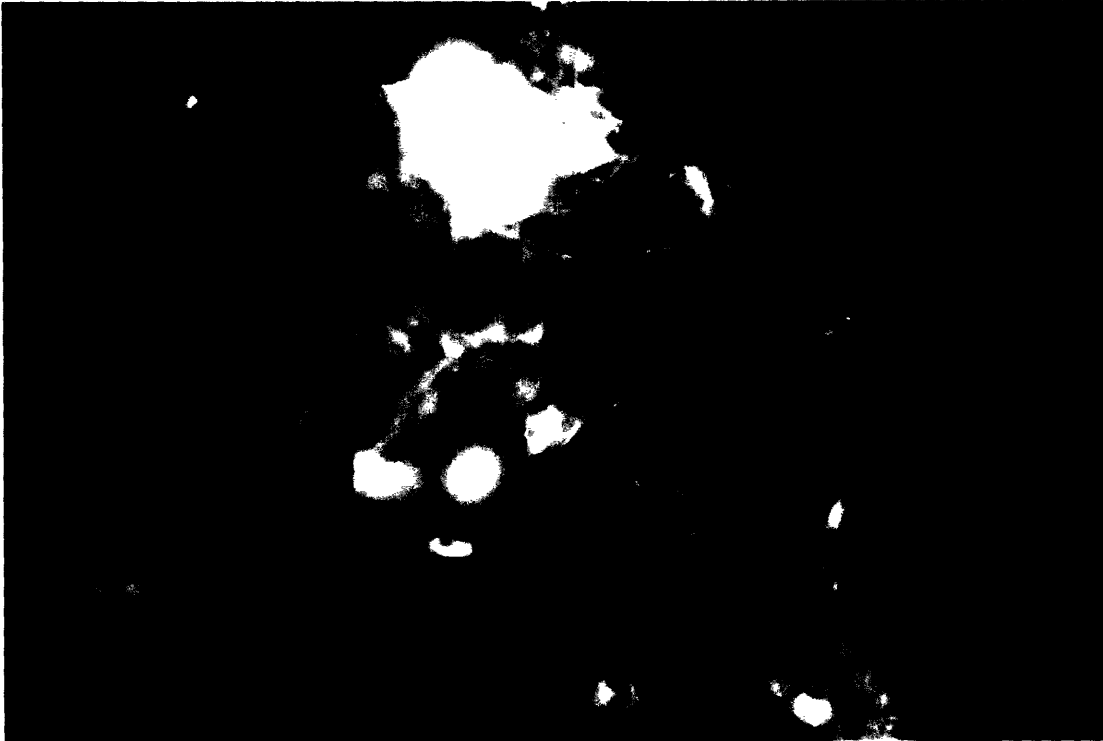
Chapter 4: Nestin deletions

Introduction

Nestin assembly

Individual intermediate filament subunits have different requirements for assembly that are not entirely dependent on the class into which the protein falls. Only keratins have an absolute requirement for a 1:1 ratio of a Type I and Type II subunit for assembly into filaments. The Type III subunits vimentin, desmin, peripherin and GFAP are capable of self-assembly, whereas some of the neuronal, Type IV filaments are competent for assembly individually and some require a partner. Since nestin is most related to the neurofilaments, its self-assembly capacity was open to question.

Since nestin is nearly always expressed with vimentin, it was necessary to use a vimentin-free cell to assess filament assembly competence. The experience of some authors with desmin in keratin positive cells suggested that a keratin-free line might yield a clearer result. For both desmin and vimentin, it has been noted that although the keratin and vimentin filament networks are independent, de novo vimentin and desmin filament assembly associates with the keratin network (Raats, et al., 1990; Sarria, et al., 1990). SW13, a human adenocarcinoma line derived from adrenal medulla, lacks all intermediate filaments and has a flattened shape suitable for study of the cytoskeleton by conventional indirect immunofluorescence (Hedberg and Chen, 1986; Sarria, et al., 1990). It has been used in numerous studies on the assembly of IFs (Andreoli and Trevor, 1994; Ching and Liem, 1993; Lee, et al., 1993; Meng, et al., 1994). About 1% of the cells in any culture of SW13 vim⁻ are revertants that express vimentin. A vimentin positive subclone was used for nestin assembly studies in the presence of an existing vimentin network (Sarria, et al., 1990).

Sequences in the head domain play an important role in the regulation of filament assembly (Beuttenmuller, et al., 1994; Herrmann, et al., 1992; Hoffmann and Herrmann, 1992). The head domain of vimentin is essential for normal assembly and without it, vimentin is rendered soluble, and can assemble with wild type subunits only if it comprises one fourth or less of the tetramer

components (Andreoli and Trevor, 1994). A deletion in the head domain of desmin also renders it incapable of self assembly, but not of assembly with existing vimentin filaments (Raats, et al., 1990; van den Heuvel, et al., 1987). However, desmin and vimentin contain a peptide sequence in the head domain that regulates filament assembly, which GFAP lacks (Hatzfeld and Weber, 1992; Herrmann, et al., 1992; Hoffmann and Herrmann, 1992; Nicholl and Quinlan, 1994). GFAP is capable of assembly in the absence of other IFs in astrocytes in vivo (Yang, et al., 1993), although it is often expressed with vimentin in cultured cells (Weinstein, et al., 1991). Type I and II keratins generally require head domains for assembly in at least some of the subunits, but requirements vary for individual proteins.

From the behavior of headless type III filament subunits, it was predicted that nestin, which is almost entirely headless, would lack the ability to self assemble. The unusual structure of nestin is intriguing. There are no other IFs which have such a short head domain (7 amino acids), with the exception of the recently cloned Xenopus IF, tanabin (Hemmati-Brivanlou, et al., 1992). Keratin 19 is a naturally tailless Type I subunit which can assemble with keratin partners if they are normal, but not if the tail has been removed (Bader, et al., 1991). Keratins generally require at least one intact head and tail unit per pair, so in a sense, the shortened subunit "borrows" the missing structure from its polymerization partner. Nestin is most closely related to the three Type IV neurofilament triplet proteins, which are all incapable of self assembly, but co-assemble with vimentin, α-internexin, or each other (Gill, et al., 1990; Wong and Cleveland, 1990). Furthermore, NFM and NFL require a large part of their head domains for assembly. Wild type α-internexin is self-assembly competent (Ching and Liem, 1993). Nestin is most closely related to NFH, and shares its general structure of a short head domain and long tail, as well as two of the three intron positions (Dahlstrand, et al., 1992).

To investigate the role of functional domains in the assembly of nestin, I used site-directed mutagenesis to delete regions important to assembly in other IF proteins. The conserved intermediate filament consensus sequence at the end of coil 2B (Figure 2) is an obvious point of interest. The consensus sequence is conserved from the yeast IF to man across all classes of IFs including the nuclear lamins (Fuchs, 1994 for review). Deletions in the consensus sequence result in dominant mutants of variable intensity, as discussed in Chapter 1. Previous studies with other IFs suggested that a second

site essential for assembly lies at the amino end of coil 1A (Fuchs, 1994; Chapter 1). Mutations in this domain result in either dominant or recessive phenotypes depending on the size of the deletion. The effects of site-directed mutagenesis on both the conserved domains on the assembly, subcellular localization and solubility of nestin are reported here.

To determine the extent of nestin incorporation into filaments in the vimentin positive and negative lines, I used a differential extraction procedure (Ching and Liem, 1993). The relatively high solubility of nestin was previously established (Almazan, et al., 1993). The changes in nestin solubility resulting from mutation of the protein were investigated here.

Materials and Methods

Plasmids

Nestin promoter

A fragment of the rat nestin genomic sequence was reconstructed from Charon4A and λgt10 clones isolated in the cloning and sequencing of nestin (Lendahl, et al., 1990). The design of the constructs is shown in Figure 14. NgHA was generated by deletion between two Nco sites at 2013 and 4953 bases upstream of the nestin cap site in a plasmid similar to pNcoNesPlacZ/3introns described by Zimmerman, et al. (1994). Results from expression in transgenic mice indicated that this region was not required for tissue specific expression. In the constructs NgHA and NM5HA, 470 bases from -4953 to -5423 were also present upstream of the promoter.

Primer-mediated mutagenesis was used to generate a five amino acid deletion in the genomic nestin sequence. pNM5HA lacks 5 amino acids from the rod 2B C-terminus. Protocols and reagents from the BioRad Mutagene kit were used throughout. Single-stranded DNA was rescued from bluescript KS(+) containing a 5.3 kb genomic nestin BamH1 insert (BtNesA), out of the *dut ung* E. coli strain CJ236. It was hybridized to the primer CTC CCC ACC AGG ACT AAC TCT CGG TTG CAG, copied with T7 DNA polymerase, and transformed into MV1190 E. coli. The mutagenized sequence was confirmed by sequencing and cloned back into full length genomic nestin between the NsiI site in the second intron and the HindIII site at +3106 in the cDNA. The entire segment of the coding region which underwent the

mutagenesis has not been resequenced as this represents more than 2000 base pairs.

For the amino-terminal deletion construct, ΔNIAHA, the natural ATG of nestin was replaced with the synthetic Shine-Delgarno-Kozak sequence from pSDKlacZpA and ATG from NesP/3introns (Zimmerman, et al., 1994). A deletion of 345 bases from the coding sequence (115 amino acids) was made by fusing the Xho1 site at +427 bp from the message initiation site in frame to an Xho linker placed immediately downstream of the artificial ATG. The first three codons of the deleted protein are therefore ATG GCT CGC. The polyadenylation signal was removed from the λgt10:401:16 cDNA fragment encoding the 3' end of the nestin gene by cleavage at the NheI site. The poly A signal was replaced with the SV40 poly A signal from CMV-β-gal (Clontech).

Epitope flag

All the nestin promoter constructs were flagged with a peptide tag recognized by an antibody to influenza virus hemagglutinin (HA) (Kolodziej and Young, 1991) in order to distinguish between endogenous and wild-type nestin. A pair of synthetic oligonucleotides encoding the epitope was ligated into to the Sma1 site at nucleotide 5276 (aa 1717) near the carboxyl terminus of nestin (aa 1805). The sequence of the coding oligo was G GGG TAC CCC TAC GAC GTC CCC GAC TAC GCC CC. This introduces to the nestin sequence the amino acids (P)G YPYDVPDYA P(G). The amino acids in the center are the HA epitope and those in parentheses represent the natural nestin sequence at the SmaI site.

CMV promoter

A non-neuronal promoter was used for expression of nestin in cells which do not normally express it. The coding sequence for CMV-Ng and CMV-NgM5 was the same as that in NgHA and NM5HA, respectively, except that the CMV constructs lack the HA flag. the CMV promoter was derived from CMV-β-gal (Clontech) by deletion of β-galactosidase between the NotI sites.

Cell culture

SW13 cells were the gift of Dr Peter Pentchev, NIH, with the kind permission of Dr R. Evans. SW13 cells were grown in DMEM/F12

with 10% FCS. NSELacZHipP2-21 cells were the gift of Dr Timothy Hayes, and were grown in DMEM with 10% FCS. Cells were transfected by the calcium phosphate method of Chen and Okayama (1987). For stable lines, selection vectors were cotransfected at one tenth the concentration of the primary plasmid. pSV2neo was used for G418 resistance and pY3 was used for hygromycin resistance. Stable lines were maintained under selection at all times. Failure to maintain selection resulted in rapid loss of expression of the plasmid. NSElacZHipP2-21 was selected at a concentration of 0.3 mg/mL of hygromycin (Boehringer Mannheim) and SW13 was selected in 0.05 mg/ml G418 (Gibco/BRL).

Immunofluorescence

Cells were fixed in 4% paraformaldehyde in PBS, pH7.2 for 15 minutes, washed 4x in PBS and blocked in 2% goat serum. For tubulin staining, 0.2% glutaraldehyde was added. Primary antibody for nestin was AS 130 (Chapter 2). Monoclonal antibody MAb V9 (Boehringer Mannheim) was used against vimentin. Actin was stained with rhodamine-conjugated phalloidin (Molecular Probes). Tubulin was visualized with MAb DM1A (Sigma).

Protein fractionation

Cytoskeletal preparations were made by the method of (Ching and Liem, 1993). Briefly, cells were incubated in TritonX-100 in 150mM NaCl, 10mM Tris pH 7.5, 1mM EDTA, with 0.5 mM freshly added PMSF, 10μg/ml aprotinin, 2μg/ml pepstatin, 2μg/ml leupeptin, 20μg/ml bestatin, and 20μg/ml 3,4 dichloroisocoumarin and centrifuged at 100,000 x g for 1 hour, then treated with DNAse and washed again in Triton-free buffer at high speed. Proportional amounts of protein were added to each lane in the gel.

Western Blotting

Laemmli gels (6%) were run and transfered to nitrocellulose (Hybond-ECL, Amersham) membranes using Towbin buffer without methanol, blocked in 5% nonfat dried milk and washed in Tris buffered saline (Harlow and Lane, 1988). AS130 was used at dilutions of 1:5000 and higher. Rat 401 tissue culture supernatant was used without dilution. Vimentin antibody V9 was used at 1:100 and rabbit antivimentin was used at 1:1000. Appropriate HRP-conjugated secondary antibodies (Amersham) were used at

recommended dilutions ranging from 1: 2000 to 1:10000. Detection was carried out using a chemiluminescent detection system (Amersham or DuPont/NEN).

Photography

Black and white photographs were taken on Kodak Tri-X 400 film on a Zeiss Axioplan microscope, developed in T-Max developer according to the manufacturer's instructions. For figures, negatives were scanned into Adobe Photoshop (Adobe Systems, Inc; Mountain View, CA) on a Nikon LS-3510AF slide scanner. Contrast and brightness were adjusted to give clear prints to illustrate findings, but no major change from the appearance of the negatives was made.

Results

Nestin genomic constructs

Mutant and wild type nestin constructs were assembled for expression in transfection assays. The features of the wild type and deletion constructs are diagrammed in Figure 14. Two promoters were used in these experiments. The properties of the rat nestin promoter have been investigated (Zimmerman, et al., 1994). Tissue specific sequences reside in the introns, while the upstream promoter can be replaced with another basal promoter without changing tissue specific expression. For expression in nestin-positive cells, the construct NgHA driven by the endogenous promoter was used. To obtain high expression in non-neural cells, the CMV promoter was fused to a site below the cap of the nestin mRNA (construct CMV-Ng). In CMV-NgM5 and NM5HA, the coil 2B conserved sequence was mutated. The complete conserved sequence is EIVTYRTLLEAE (consensus: EIATYRKLLEGE), but there is an intron in the middle of the arginine codon, so to avoid the risk of altering splicing in the genomic constructs, a five amino acid sequence was deleted (LLEAE). Point mutations in the last five amino acids affect assembly capacity and inter-filament interactions (Hatzfeld and Weber, 1991; Letai, et al., 1992; Letai, et al., 1993). The entirety of coil 1A and 61 bases of coil 1B were deleted in the construct ΔN1AHA. This large deletion was analogous to deletions made in NFL and NFM constructs (Gill, et al., 1990; Wong and Cleveland, 1990).

103

The Rat 401 antibody recognizes the rat nestin protein with high avidity, but the mouse protein with low avidity. With careful fixation times and dilution of the antibody, it fails to recognize the endogenous mouse protein in cultured cells. However, in sections of paraformaldehyde fixed mouse tissue, the background of endogenous nestin is high enough to make observations using Rat 401 equivocal. Therefore, all the nestin promoter constructs were flagged with a peptide tag recognized by an antibody to influenza virus hemagglutinin (HA) (Kolodziej and Young, 1991). Since the last seven amino acids at the C terminus of nestin are perfectly conserved between the rat and human genes, while the rest of the tail shows lower homology, a convenient site in a non-conserved stretch was chosen to insert the tag. The region around the Sma1 site is G/P-rich, and therefore unlikely to have helical structure. The location of the flag in a less conserved region was designed to avoid any regulatory or functional sites in the tail.

Expression in SW13 cells

Vimentin Negative Cells

Vimentin negative SW13 cells were transfected with CMV-Ng, encoding wild-type nestin driven by the CMV promoter. In most nestin-expressing cells, a bright haze of soluble protein was evenly distributed across the cytoplasm (Figure 15). In some cells staining was distributed in a grainy pattern throughout the cells (Figure 15, arrows). In a few cells intense spots of stain were collected on the edges and apical surfaces of cells. In focusing through the cells it was clear that the spots were associated with the plasma membrane, and may even have protruded from it (Figure 16). Filamentous structures were never seen. The cells were double labeled to demonstrate the lack of vimentin staining. Occasional transfected vimentin-positive revertants in the same preparation showed the pattern of nestin stain found in vimentin positive cells, demonstrating that this pattern was not due to a general inability to assemble intermediate filament proteins (not shown).

Stably Transfected Vimentin Negative Cells

The stable line SWv⁻CNg21 showed a change in the distribution of nestin over time. At early times following the selection of the cells, nestin was distributed in a pattern of small aggregated spots somewhat concentrated in the more peripheral parts of the cell, but

covering whole cytoplasm (Figure 17). After six weeks of passage, the cells showed plasma-membrane associated spots at a much higher frequency than in transiently transfected cells or in the earlier passages. It is not known whether these nestin-positive blobs are associated with membrane structures (Figure 18).

Vimentin Positive Cells

A vimentin positive subclone of SW13 was used to assess the ability of wild type nestin to assemble with human vimentin. Transient transfections were highly efficient and 5 to 10% of the cells expressed rat nestin. Nestin was found incorporated into filaments four days after transfection. Nestin incorporation was extensive, and double labeling showed that the nestin network entirely overlapped the vimentin filaments (Figure 19). In a minority of the cells, the network was apparently overwhelmed with nestin subunits, and there was very strong diffuse stain whose intensity varied at points across the cytoplasm (Figure 20). In these cells, the intensity of the vimentin stain was reduced, but this may be due to quenching across the fluorescence channels. There were intact vimentin positive filaments in these cells and vimentin stain did not show a diffuse background.

Stably Transfected Vimentin Positive Cells

Two stable clones of SW13 expressing CMV-Ng were selected. The clone SWv+CNg2 looked similar to the majority of the cells transiently expressing CMV-Ng, and 70% of the cells were nestin positive. Nestin and vimentin filaments overlapped completely, although some vimentin filaments had very little nestin (Figure 21). It was noted that the filament network in some nestin expressing cells was slightly more finely divided than that in neighboring nestin negative cells (Figure 22). The phenotype of the nestin positive cells was remarkably even and did not change over time in culture.

The appearance of the second line, SWv+CNg1, was surprising in light of the appearance of the transient transfectants. The intermediate filament network containing both vimentin and nestin was collapsed into a dense ball in a perinuclear position. A few thick, unbranched filaments containing both nestin and vimentin extended to the periphery of the cells (Figure 23). This phenotype was not detected in any of the transient transfectants with the CMV-Ng construct, but was seen in a single cell transfected with the genomic wild-type

nestin, flagged with HA (NgHA). Surrounding cells expressing vimentin alone had a normal filament appearance (Figure 24). The aggregation showed 100% correlation to nestin expression. Since this phenotype was so rare, we have entertained the notion that a mutation may have taken place in a copy of the gene that integrated into this line. The size of the nestin band on Western blots is normal (Figure 37), so no large deletion or degradation has occurred in this line.

Nestin Coil 2B deletion

The five amino acid deletion in nestin showed subtle differences from wild type nestin in its distribution in transiently transfected SW13 cells. While the vimentin network for the most part was unaltered, the mutant nestin was distributed in a spotted pattern along the length of the vimentin filaments. The spotting was not apparent at low power (Figure 25). In a fraction of the cells it appeared that the vimentin network was somewhat retracted from the periphery Figure 26). Overexpressing cells looked similar to those in which wild type nestin was overexpressed: a haze of nestin stain overlapped intact vimentin filaments (Figure 27). In the vimentin channel, there was a slight redistribution of vimentin away from the leading edge on one side of the cell. There was no evidence of major pertubation of the existing vimentin network, and the spotted pattern was visible only at the highest magnification, as in Figure 32.

Stably Transfected Nestin Coil 2B deletion

Two selected lines of cells transfected with CNgM5 were examined. SWv+CNgM5.12 expressed nestin in 22% of cells and SWv+CNgM5.13 expressed in 71%. The mild phenotype of the transiently transfected cells intensified in the line SWv+CNgM5.12 so that it became apparent that nestin was causing a retraction of vimentin from the periphery of the cells in many of the cells in which it was expressed (Figure 28, arrows). Non-expressing cells in the same clone maintained dense vimentin filaments out to the edge of the cells (Figure 29). Nestin remained in short filamentous structures that contained variable amounts of vimentin. Nestin-positive short filaments were visible in the outer quarter of the cell (arrows). The ratio of vimentin to nestin in these short filaments varied, but was higher than in the rest of the cytoplasm.

The second line, SWv+CNgM5.13, appeared to have a wild-type like distribution of nestin (Figure 30). Cells expressing the mutant apppeared to have slightly lower levels of vimentin. At high magnification, vimentin retraction was not apparent, but nestin was distributed in spots in the periphery of cells (Figure 31). After three weeks longer in culture, the abnormal appearance of the vimentin network in SWv+CNgM5.13 became more pronounced (Figure 32). Nestin was distributed in a spotty pattern that followed vimentin filaments. Vimentin was radically withdrawn from the plasma membrane only in cells expressing nestin. Not all nestin-expressing cells developed this phenotype, however.

Other cytoskeletal components

Perturbation of the microtubule network with the microtubule destabilizing drug colchicine leads to the collapse of intermediate filaments, including vimentin and nestin, into perinuclear aggregates (Hynes and Destree, 1978; Lendahl, et al., 1990). The appearance of the IFs in SWv+CNg1 was similar to that of colchicine-treated cells. However, when the line was stained with antitubulin antibody, no gross alteration of the microtubule distribution was seen (Figure 33a-b). The same was true of transiently transfected cells expressing CMV-NgM5 (Figure 33c-d).

No alterations of the microfilaments were seen in any of the cell lines, although stress fibers were not seen in all cells and seen more rarely in confluent cultures. Nestin showed no signs of association with microfilaments in nestin positive cells expressing either the wild type (Figure 33e-f) or mutant (Figure 33g-h).

Expression of flagged construct in SW13

In order to determine whether the hemagglutinin flag had an influence on nestin distribution, SW13 cells were transiently transfected with the nestin promoter constructs NgHA, NM5HA and ΔNIAHA. It was not clear beforehand that the nestin promoter would be effective in these cells, but since the genomic constructs under the control of the CMV promoter were quite successful, and since the nestin tissue specific elements in the introns (Zimmerman, et al., 1994) were included in the CMV promoter constructs, it was attempted. In fact, the nestin promoter constructs were as powerful as the CMV constructs in these cells. The lack of endogenous human

nestin expression in SW13 is clearly not due to a dearth of the required transcription factors.

The appearance of the transiently transfected cells 96 hours after transfection was very similar to that of the corresponding CMV promoter driven, unflagged proteins. Wild type nestin integrates along vimentin filaments and the two proteins colocalize completely (Figure 34a-b). At shorter times the wild type protein also showed punctate staining along vimentin filaments. The mutant protein expressed from NM5HA had a lower level of expression, but followed the same pattern as protein from CMV-NgM5 (Figure 34c-d).

Examination of ΔN1AHA-transfected cells demonstrated that this protein was rendered soluble by the deletion of coil 1A (Figure 35). The distribution of nestin in these cells was quite similar to that of wild type nestin in vimentin negative cells. The large deletion mutant lacks the capacity to interact with vimentin. Vimentin filaments did not appear to be perturbed, although the level appeared lower than in untransfected cells. Lower levels of staining may be an artifact of quenching due to the proximity of the chromophores in the doubly stained cells.

Expression of wild type and mutant nestin in nestin-positive cells

The aggregation of nestin protein in SW13 cells over time raises the question of whether mutant nestin can disrupt distribution of endogenous nestin protein. In order to address this problem, NSElacZHipP2-21 (Hip21 hereafter) cells were transfected with the nestin promoter constructs. This cell line is derived from postnatal day 2 (P2) hippocampus of mice transgenic for the neuron-specific enolase promoter driving the bacterial gene for β-galactosidase (Dr. Timothy Hayes, unpublished results).

Cells transfected with the wild type construct NgHA showed overlapping distribution of mouse and flagged rat nestin. Expressing cells were intensely stained in the AS 130 channel because of the higher affinity of the antibody for the rat than the mouse protein (Figure 36a-b). The five amino acid deletion construct NM5HA is distributed in a more markedly perinuclear fashion than the wild type construct. It does incorporate into filaments, but tapers off toward the periphery more quickly than the wild type protein (Figure 36c-d). The disparity in localization of endogenous and transfected nestin may indicate a reduction in translocation of the

mutant protein. It has been noted that vimentin is added to intermediate filaments at the nuclear membrane under some conditions, although in others the assembly takes place throughout the cytoplasm (Ngai, et al., 1990; Vikstrom, et al., 1989). Unlike the result in SW13 cells, the distribution of the endogenous nestin filament network was unaltered after many passages of a stable line.

Nestin solubility

Urea extractions on transient transfectants (SW13v⁻CNg) and on stable lines containing wildtype and mutant nestin demonstrated that the nestin protein is of normal length and shows very little degradation, in contrast to the three bands seen in extractions of the brain cells. This suggests that processing of the proteins differs in various cell types (Figure 37). As discussed in chapter 2, the number of bands seen may correlate with the cell type as well as the method of handling the extracts.

Nestin is unusually soluble for an intermediate filament. A previous study on nestin solubility demonstrated that under normal conditions half of the nestin is found in the soluble fraction in primary O2A cells. Since short filaments were seen in SWv+CNgM5 cells, I used a stringent extraction protocol to avoid loss of aggregated, non-filamentous material to the supernatant. The high speed centrifugation steps ensure that subunits larger than tetramers will partition to the Triton-insoluble fraction (Ching and Liem, 1993).

In the first experiment, the distribution of nestin to soluble and insoluble fractions was investigated. In ST15A cells (Frederiksen and McKay, 1988), approximately 50% of the total nestin protein was found in the Triton X-100 soluble fraction (Figure 38A, lanes 3-4). In these cells, the proportion of nestin to vimentin is high. There is also a relatively high level of vimentin in the soluble fraction, roughly 10% of the total (Figure 38B, lanes 7 and 8). Due to the lability of nestin protein, I was concerned that the soluble nestin was the non-helical tail released from filaments by proteolytic cleavage, but at the resolution obtained on a 6% SDS-PAGE gel, the distribution of the staining in the nestin ladder was similar in the upper bands of the soluble and insoluble fractions. However, due to the large size of nestin, I cannot rule out proteolytic cleavage close to or within the 310 amino acid rod domain that due to electrophoresis conditions

would result in a fragment containing primarily the large tail domain that would migrate very close to the parent protein.

Extracts taken from NSElacZHipP2-21 cells showed a different distribution.. In these cells, the proportion of soluble nestin and vimentin was much smaller. Approximately 1% of total vimentin was soluble (Figure 38A, lanes 5 and 6), whereas 20% of nestin was soluble (Figure 38A, lanes 1 and 2). This may reflect total levels of nestin found in these cells. The amounts of nestin in the two lines cannot be compared directly because AS 130 stains rat nestin more intensely than mouse. Since nestin has not been purified and quantified, only relative levels of protein can be discussed here.

Triton X-100 extractions confirmed the visual impression from immunofluorescence data that nestin was rendered soluble in the absence of vimentin in SW13 cells transiently transfected with the wild-type, unflagged nestin (CMV-Ng). All the detectable nestin in the extracts was found in the soluble fraction (Figure 38B, Lanes 9-10). The results of extractions on the stable line SWv⁻CNg21 which developed aggregated particles at the periphery of the cytoplasm over time are not yet known.

As discussed above, there are a range of phenotypes in the transiently transfected SW13 vim⁺ cells. In order to eliminate the soluble nestin released from highly overloaded cells, extractions were carried out on only the stably transfected lines to assess the incorporation of nestin into filaments in vimentin positive cells. SWv⁺CNg1, which showed collapse of filaments around the nucleus, had nestin distributed evenly between the soluble and insoluble fractions. There were substantial amounts of faster-migrating bands that were the result of proteolytic cleavage. No such short bands were seen in Figure 37, so these must have arisen during the extractions. Included in the extraction were six protease inhibitors covering a wide spectrum of proteases, but they were insufficient to prevent this extensive degradation. In the wild type line with normal IF appearance, SWv⁺CNg2, nestin was highly soluble (Figure ab, lanes 3-4). However, the degradation was extensive and the lower molecular weight bands in the soluble lane may have resulted from cleavage of the fragments containing the AS 130 epitopes from the insoluble protein. The lines expressing the deletion mutant SWv⁺CNgM5.12 and 13 differed in their nestin distributions. Whereas in SWv⁺CNgM5.12 nestin was primarily soluble (Figure 38B

lanes 5-6), in SWv$^+$CNgM5.13 it was evenly distributed (Figure 38B lanes 7-8). These results indicate that the five amino acid deletion mutant has the same range of distribution as the wild type protein. As indicated by immunocytochemistry, the mutant protein does associate to some degree with the vimentin filaments, although its fine distribution along vimentin filaments is altered.

In order to compare these results with the distribution in the animal, Triton X-100 extraction were performed on freshly isolated tissue from E16.5 mouse cerebral cortex. In cortical cells, nestin is primarily insoluble (Figure 38B lanes 11-12). It is primarily a proteolytic cleavage product that is found in the soluble fraction.

Discussion

The predictions about nestin's assembly competence were borne out when nestin was transfected transiently into vimentin and keratin-free SW13 cells. Nestin appears to be soluble by immuno-fluorescence at early times after transfection. Its solubility is confirmed in staining of transiently transfected cells.

Wild type nestin can fully integrate into the endogenous vimentin filament network. SW13 expresses human vimentin, but the minor differences in sequence between the rat and human genes do not affect their ability to coassemble with nestin. The short deletion from coil 2B has a subtle effect on the vimentin filament network. Since the entire consensus region was not deleted, this is consistent with results found for other filament systems (Albers and Fuchs, 1989; Coulombe, et al., 1990; Gill, et al., 1990; Wong and Cleveland, 1990).

The failure of nestin lacking the coil 1A sequence to interact with vimentin is consistent with the result of numerous studies with desmin, neurofilaments and keratins (Chin, et al., 1991; Gill, et al., 1990; Raats, et al., 1990; Wong and Cleveland, 1990). For other IFs, the coil 1A sequence is essential for interaction with other subunits, and without it, IF proteins fail to associate with intact subunits. For most IFs, the head structure is essential for assembly at the earliest stages. The near complete absence of this domain in nestin raised the question of whether the rules differ for a headless IF. These results demonstrate that for nestin as well, the helix initiation sequence is essential for interaction with other IF subunits.

111

It is surprising that in three of the five stably transfected SW13 lines expressing three different forms of nestin, there is a change in the distribution of nestin over time. It is possible that the aggregation is a consequence of prolonged overexpression of nestin. In the vimentin-negative line SWv-CNg21 the aggregation of the protein increases with time, while in the two mutant nestin lines SWv+CNgM5.12 and -13 the severity of vimentin perturbation increases over time. It is highly unusual to see such a slow change. Kinetic studies on incorporation of newly synthesized keratin and vimentin subunits into existing filaments indicate that it is a rapid process (Albers and Fuchs, 1989; Ngai, et al., 1990; Vikstrom, et al., 1989). This was originally surprising in the case of keratins, which due to their great insolubility, were imagined to be rather static components of the cytoskeleton. The slow rate at which the effects of the wild type and mutant proteins took place could be due to accumulation of a modified nestin form. Western blots of the cell lines done early in their development show a single band for nestin (Figure 37). The stable lines of Hip 21 cells transfected with NgHA or NM5HA never showed such changes in distribution over time, suggesting that these modifications in distribution are cell-type specific. The endogenous nestin in Hip 21 cells may alleviate the consequences of the nestin mutant by more successfully competing for binding to vimentin subunits.

In the line SWv+CNg1, the aggregation of nestin perturbs the existing vimentin network. The difference in the appearance of this line and SWv+CNg2 may be due to levels of expression, or to a mutation that has taken place in a copy of the nestin gene in SWv+CNg1. The collapsed IF network in SWv+CNg1 might instead be the fate of one of the cells overexpressing nestin shown in Figure 20. If wild type nestin aggregates in vimentin-positive cells as well as in the vimentin negative line SWv-CNg21, it may be tightly enough bound to vimentin to bring it into the aggregates as well. Clarification of this point will have to wait for more detailed observations on transfected cell lines. It is clear that both the coil 2B deletion and the form present in SWv+CNg1 are capable of disrupting vimentin intermediate filaments. This was not obvious from the transient transfection data, which seemed to indicate that even an enormous excess of nestin had relatively little or no effect on the vimentin network.

112

Nestin is unusually soluble

The relatively high solubility of nestin was previously established in oligodendrocyte precursors. Increased nestin solubility correlates with increased phosphorylation of nestin and vimentin (Almazan, et al., 1993). Since vimentin phosphorylation by cdc2 kinase results in rendering it more soluble (Chou, et al., 1990), it is likely that nestin is phosphorylated correspondingly during mitosis. During differentiation of embryonic neurons, some forms of NFH are transiently soluble. The soluble forms are highly phosphorylated and are identified by reaction with SMI-31, but not SMI-34, which recognizes a different phosphorylated epitope. The results of pulse-chase experiments suggest that soluble NFH comes from a recently synthesized pool (Shea, et al., 1993; Shea, et al., 1990).

The differences in the proportion of soluble nestin in ST15 A and Hip 21 cells may reflect distribution in the cells of origin or the absolute levels of nestin. ST15A was chosen from a screen of immortalized cell lines for the highest nestin expression. Hip21 was selected for this study because of its flat appearance and its glial characteristics on induction of differentiation (Tim Hayes, personal communication). ST15A shows greater differentiation potential than Hip21 has yet demonstrated (Frederiksen and McKay, 1988; Valtz, et al., 1991). ST15A also proliferates more rapidly than Hip21. It may be significant that greater nestin solubilty in ST15A corresponds to greater vimentin solubility. The result of fractionation of E16 cortical cells suggests that the high level of nestin solubility arises in culture, but that in the animal, most of the nestin is bound to IFs. Since vimentin is phosphorylated by p34^{cdc2} during mitosis, the high solubility of both proteins may be a consequence of the rate of proliferation and the proportion of cells in mitosis in cultured cells.

The results of differential fractionations of SW13 lines are complex. Since the AS 130 epitope lies in the tail of the protein, proteolytic cleavage may result in the immunoreactivity shifting to the soluble fraction, even when the rod domain is still involved in binding to vimentin. This makes interpretation of the fractionation results problematic. From the results in Figure 38, it is clear that the rod 2B mutation does not render nestin Triton X-100 soluble. It is notable that nestin from vimentin negative cells suffers from no degradation. While there could be a difference in the protease contents of the vimentin positive and negative cells, it is more plausible that

incorporation into filaments brings nestin into a form which is more accessible to proteases.

References

Albers, K. and Fuchs, E. (1989). Expression of mutant keratin cDNAs in epithelial cells reveals posible mechanisms for initiation and assembly of intermediate filaments. J Cell Biol 108, 1477-1493.

Almazan, G., Afar, D. and Bell, J. (1993). Phosphorylation and disruption of intermediate filament proteins in oligodendrocyte precursor cultures treated with Calyculin A. J Neurosci Res 36, 163-172.

Andreoli, J. and Trevor, K. (1994). Fate of a headless vimentin protein in stable cell cultures: soluble and cytoskeletal forms. Exp Cell Res 214, 177-188.

Bader, B., Magin, T., Freudenmann, M., Stumpp, S. and Franke, W. (1991). Intermediate filaments formed de novo from tail-less cytokeratins in the cytoplasm and in the nucleus. J Cell Biol 115, 1293-1307.

Beuttenmuller, M., Chen, M., Janetzko, A., Kuhn, S. and Traub, P. (1994). Structural elements of the amino-terminal head domain of vimentin essential for intermediate filament formation in vivo and in vitro. Exp Cell Res 213, 128-142.

Chen, C. and Okayama, H. (1987). High-efficiency transformation of mammalian cells by plasmid DNA. Mol Cell Biol 7, 2745-2752.

Chin, S., Macioce, P. and Liem, R. (1991). Effects of truncated neurofilament proteins on the endogenous intermediate filaments in transfected fibroblasts. J Cell Sci 99, 335-350.

Ching, G. and Liem, R. (1993). Assembly of Type IV neuronal intermediate filaments in nonneuronal cells in the absence of preexisting cytoplasmic intermediate filaments. J Cell Biol 122, 1323-1335.

Chou, Y.-H., Bischoff, J., Beach, D. and Goldman, R. (1990). Intermediate filament reorganization during mitosis is mediated by p34^{cdc2} phosphorylation of vimentin. Cell 62, 1063-1071.

Coulombe, P., Chan, Y.-M., Albers, K. and Fuchs, E. (1990). Deletions in epidermal keratins leading to alteration in filament organization in vivo and in intermediate filament assembly in vitro. J Cell Biol 111, 3049-3064.

Dahlstrand, J., Zimmerman, L., McKay, R. and Lendahl, U. (1992). Characterization of the human nestin gene reveals a close evolutionary relationship to neurofilaments. J Cell Sci 103, 589-597.

Frederiksen, K. and McKay, R. (1988). Proliferation and differentiation of rat neuroepithelial precursor cells in vivo. J Neurosci 8, 1144-1151.

Fuchs, E. (1994). Intermediate filaments and disease: mutations that cripple cell strength. J Cell Biol 125, 511-516.

Gill, S., Wong, P., Monteiro, M. and Cleveland, D. (1990). Assembly properties of dominant and recessive mutations in the small mouse nuerofilament (NF-L) subunit. J Cell Biol 111, 2005-2019.

Harlow, E. and Lane, D. (1988). Antibodies: A Laboratory Manual (Cold Spring Harbor: Cold Spring Harbor Press)

Hatzfeld, M. and Weber, K. (1991). Modulation of Keratin Intermediate Filament Assembly by single amino acid exchanges in the consensus sequence at the C-terminal end of the rod domain. J Cell Sci 99, 351-362.

Hatzfeld, M. and Weber, K. (1992). A synthetic peptide representing the consensus sequence motif at the carboxy-terminal end of the rod domain inhibits intermediate filament assembly and disassembles preformed filaments. J Cell Biol 116, 157-166.

Hedberg, K. and Chen, L. (1986). Absence of intermediate filaments in a human adrenal cortex cercinoma-derived cell line. Exp Cell Res163, 509-517.

Hemmati-Brivanlou, A., Mann, R. and Harland, R. (1992). A protein expressed in the growth cones of embryonic vertebrate neurons

defines a new class of intermediate filament protein. Neuron 9, 417-428.

Herrmann, H., Hoffmann, I. and Franke, W. (1992). Identification of a nonapeptide motif in the vimentin head domain involved in intermediate filament assembly. J Mol Biol 223, 637-650.

Hoffmann, I. and Herrmann, H. (1992). Interference in vimentin assembly in vitro by synthetic peptides derived from the vimentin head. J Cell Sci 101, 687-700.

Hynes, R. and Destree, A. (1978). 10 nm filaments in normal and transformed cells. Cell 13, 151-163.

Kolodziej, P. and Young, R. (1991). Epitope tagging and protein surveillance. Methods Enzymol 194, 508-519.

Lee, M., Xu, Z., Wong, P. and Cleveland, D. (1993). Neurofilaments are obligate heteropolymers in vivo. J Cell Biol 122, 1337-1350.

Lendahl, U., Zimmerman, L. and McKay, R. (1990). CNS stem cells express a new class of intermediate filament protein. Cell 60, 585-595.

Letai, A., Coulombe, P. and Fuchs, E. (1992). Do the ends justify the mean? Proline mutations at the ends of the keratin coiled-coil rod segment are more disruptive than internal mutations. J Cell Biol 116, 1181-1195.

Letai, A., Coulombe, P., McCormick, M., Yu, Q.-C., Hutton, E. and Fuchs, E. (1993). Disease severity corrlelates with position of keratin point mutations in patients with epidermolysis bullosa simplex. PNAS 90, 3197-3201.

Meng, J.-J., Khan, S. and Ip, W. (1994). Charge interactions in the rod domain drive formation of tetramers during intermediate filament assembly. J Biol Chem 269, 18679-18685.

Ngai, J., Coleman, T. and Lazarides, E. (1990). Localization of newly synthesized vimentin subunits reveals a novel mechanism of intermediate filament assembly. Cell 60, 415-427.

Nicholl, I. and Quinlan, R. (1994). Chaperone activity of α–crystallins modulates intermediate filament assembly. EMBO 13, 945-953.

Raats, J., Pieper, F., Vree Egberts, W., Verrijp, K., Ramaekers, F. and Bloemendal, H. (1990). Assembly of amino-terminally deleted desmin in vimentin-free cells. J Cell Biol 111, 1971-1975.

Sarria, A., Nordeen, S. and Evans, R. (1990). Regulated expression of vimentin cDNA in cells in the presence adn absence ofa preexisting vimentin filament network. J Cell Biol111, 553-565.

Shea, T., Beermann, M. and Fischer, I. (1993). Transient requirement for vimentin in neuritogenesis: intracellular delivery of anti-vimentin antibodies and antisense oligonucleotieds inhibit neurite initiation but not elongation of existing neurites in neuroblastoma. J Neurosci Res 36, 66-76.

Shea, T., Sihag, R. and Nixon, R. (1990). Dynamics of phosphorylation and assembly of the high molecular weight neurofilament subunit in NB2a/d1 neuroblastoma. J Neurochem 55, 1784-1792.

Valtz, N., Hayes, T., Norregard, T., Liu, S. and McKay, R. (1991). An embryonic origin for medulloblastoma. New Bioologist 3, 364-371.

van den Heuvel, R., van Eys, G., Ramaekers, F., Quax, W., Vree Egberts, W., Schaart, G. and Cuypers, H. (1987). Intermediate filament formation after transfection with modified hamster vimentin and desmin genes. J Cell Sci 88, 475-482.

Vikstrom, K., Borisy, G. and Goldman, R. (1989). Dynamic aspects of intermediate filament networks in BHK-21 cells. PNAS 86, 549-553.

Weinstein, D., Shelanski, M. and Liem, R. (1991). Suppression by antisense mRNA demonstrates a requirement for the glial fibrillary acidic protein in the formation fo stable astrocytic processes in response to neurons. J Cell Biol 112, 1205-1213.

Wong, P. C. and Cleveland, D. W. (1990). Characterization of dominant and recessive assembly-defective mutation in mouse neurofilament NF-M. J Cell Biol 111, 1987-2003.

Yang, H.-Y., Lieska, N., Shao, D., Kriho, V. and Pappas, G. (1993). Immunotyping of radial glia and their glial derivatives during development of the rat spinal cord. J Neurocytol 22, 558-571.

Zimmerman, L., Lendahl, U., Cunningham, M., McKay, R., Parr, B., Gavin, B., Mann, J., Vassileva, G. and McMahon, A. (1994). Independent regulatory elements in the nestin gene directs transgene expression to neural stem cells or muscle precursors. Neuron 12, 11-24.

Figure 14. Diagram of wild type and mutant constructs used for nestin expression in cells. *a:* Nestin genomic construct CNg under the control of the CMV promoter. The location of the 5 amino acid deletion in construct CNgM5 from the 2B consensus sequence is indicated by (Δ) *b:* Genomic construct NgHA under the endogenous nestin promoter. The 5 amino acid deletion in construct NM5HA is marked with a (Δ). *c:* The construct ΔN1AHA has a large deletion from the ATG through coil 1A into coil 1B. (HA) indicates the location of the influenza hemagglutinin epitope flag. *d:* cartoon indicating the location of the structural features of the nestin rod relative to the locations of mutations.

A

B

C

D

NM5HA/CMV-NgM5
EIVTYRT*LLEAE*

ΔNlAHA deletion

N 1A 1B 2A 2B C
   L1 L12 L2
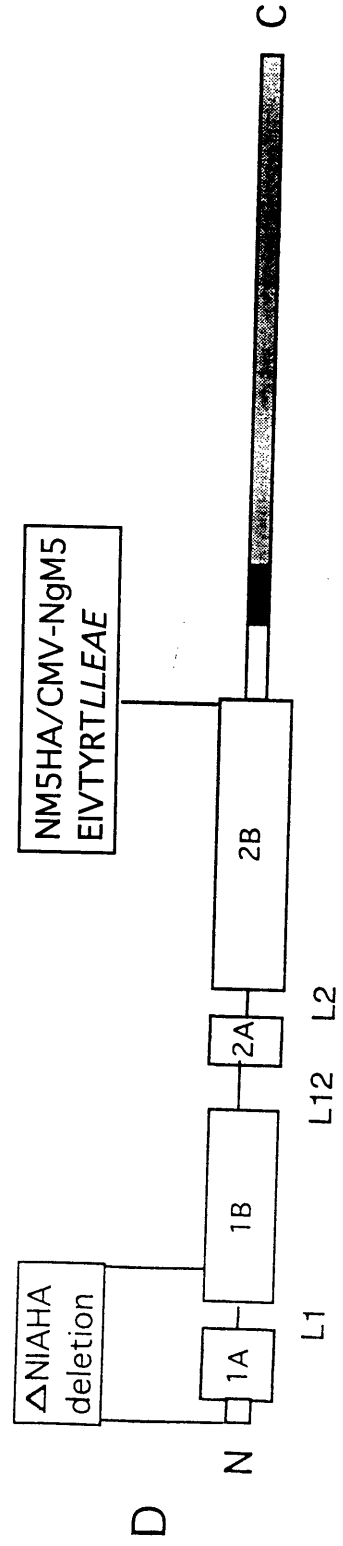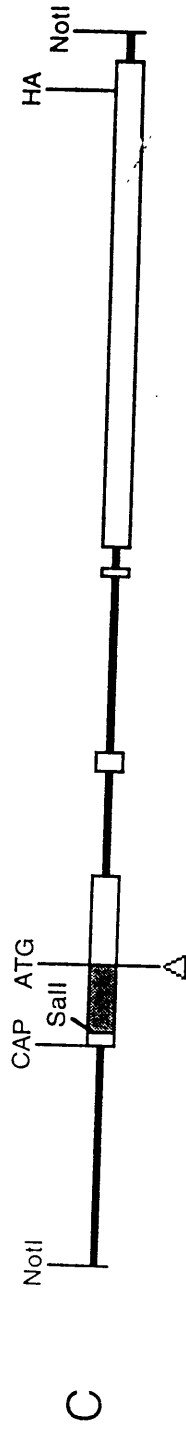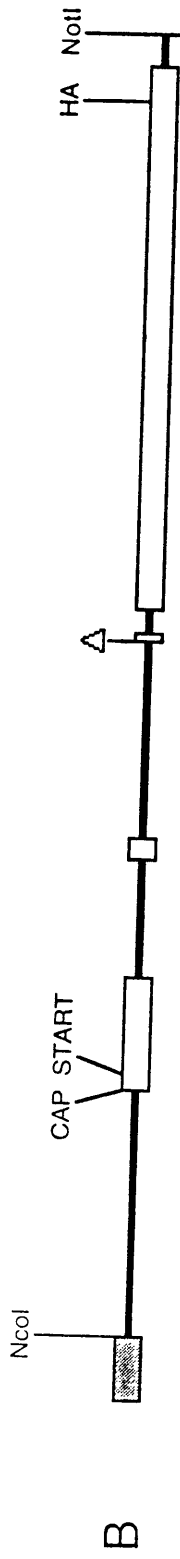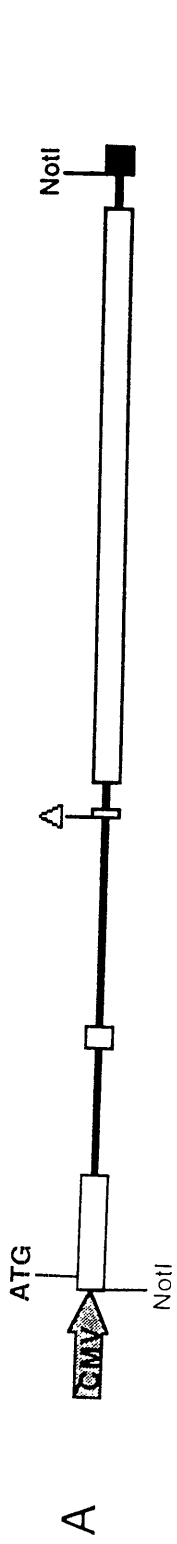
Figure 15. SW13 vimentin negative cells transiently transfected with nestin CMV-Ng and double labeled with AS 130 for nestin and mAb V9 for vimentin. *Top:* Nestin stain with AS 130. Cells expressing three different levels of nestin protein. *Arrow:* Cells with grainy stain in cytoplasm. *Bottom:* Vimentin stain with mouse monoclonal antibody V9. No staining above background is seen. Magnification 630x. Bar 15.9 microns.
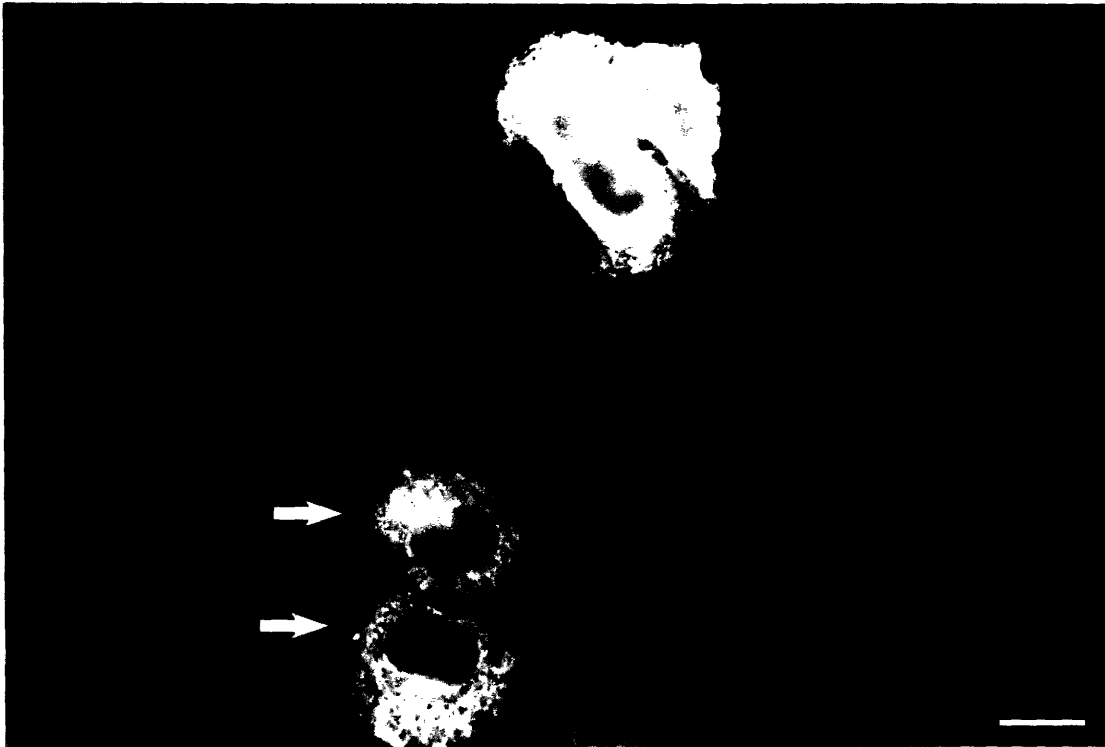
Figure 16   Cells transfected as in Figure 15.   *Top:*   AS 130 antiserum. Note the aggregates of nestin positive material protruding from the plasma membrane in the cells marked by *arrow*. *Bottom:*   Anti-vimentin stain on same field reveals no vimentin positive filaments. Magnification 400x   Bar 25 microns
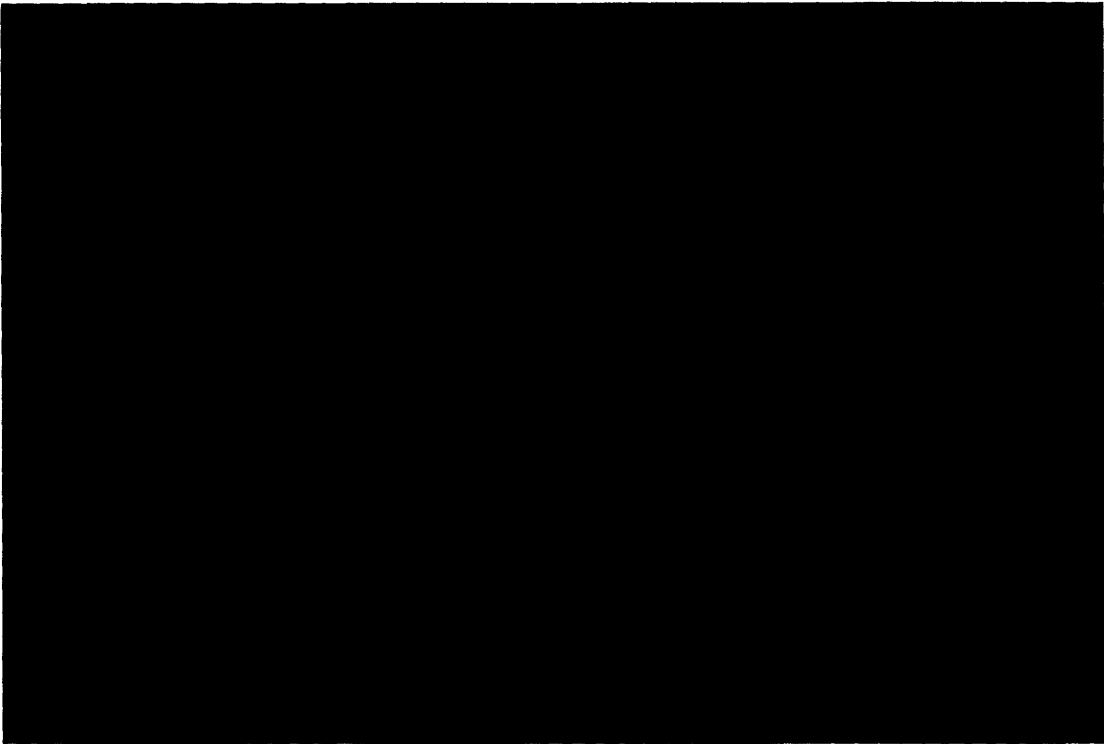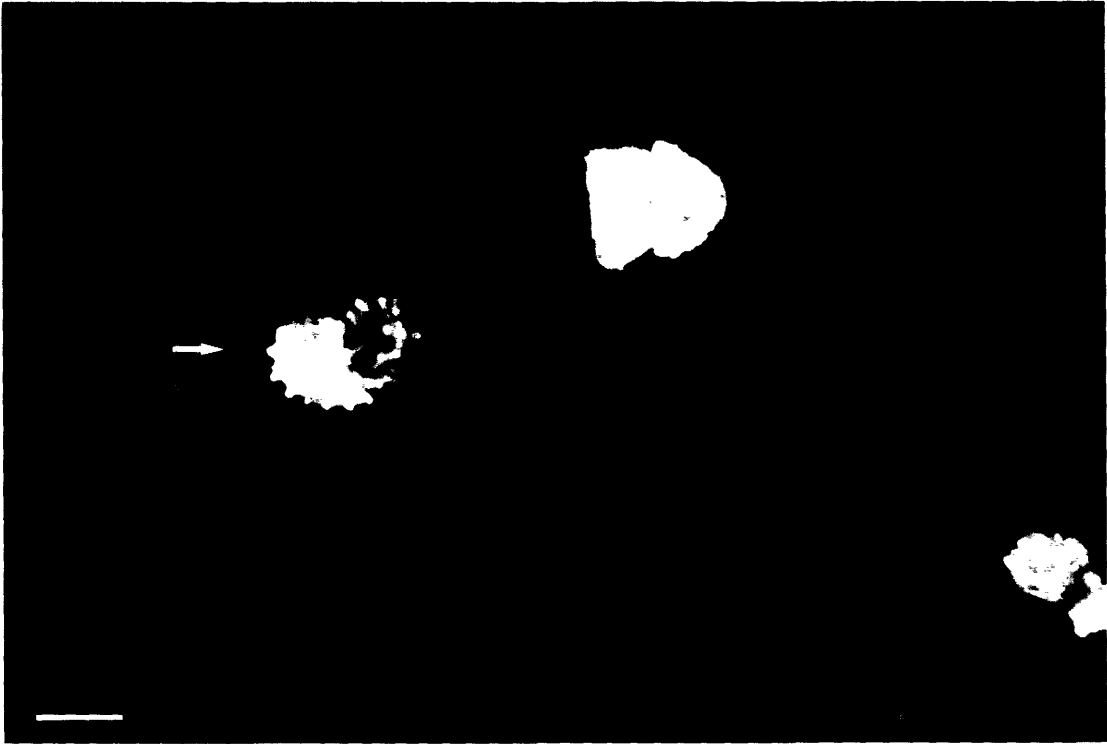
Figure 17   Stable vimentin negative line SWv⁻CNg 21 expressing nestin.   *Top:*   Cells show aggregation of nestin protein, and distribution to the outer third of the cytoplasm. Aggregates also collect near the nuclear membrane.   The distribution in the cytoplasm is similar in all the cells, despite differences in the level of expression.   *Bottom:*   In the same field, cells remain negative with vimentin antibody.   Magnification 1000x   Bar 10 microns.

Figure 18. Stable vimentin-negative line SWv⁻CNg 21 three weeks later in passage than those shown in Figure 17. *Top:* Nestin stain is now concentrated in peripheral aggregates which protrude from the the cell (examples at arrows). At this stage, 70% of the cells have this phenotype. *Bottom:* Tubulin stain is undisturbed. The aggregates, however, do have tubulin positive immunoreactivity. Magnification 1000X.

Figure 19. SW13 vimentin positive cells 96 hours after transfection with CNg. *Top:* AS 130 stains in a filamentous pattern which entirely overlaps with vimentin *Bottom:* The vimentin pattern is unchanged in nestin positive cells. Magnification 630x

Figure 20. Vimentin positive SW13 transient transfectants expressing an excess of nestin. *Top:* Nestin stain is distributed evenly in a granular pattern across the entire cytoplasm, but the nucleus is spared. Note that nestin is seen even in leading edges and cytoplasmic ruffles *(arrow)*. *Bottom:* Vimentin stain does not differ from the surrounding nestin negative cells. The concentration of vimentin in a perinuclear spot is not substantially different from staining seen throughout these cultures. Magnification 630x.
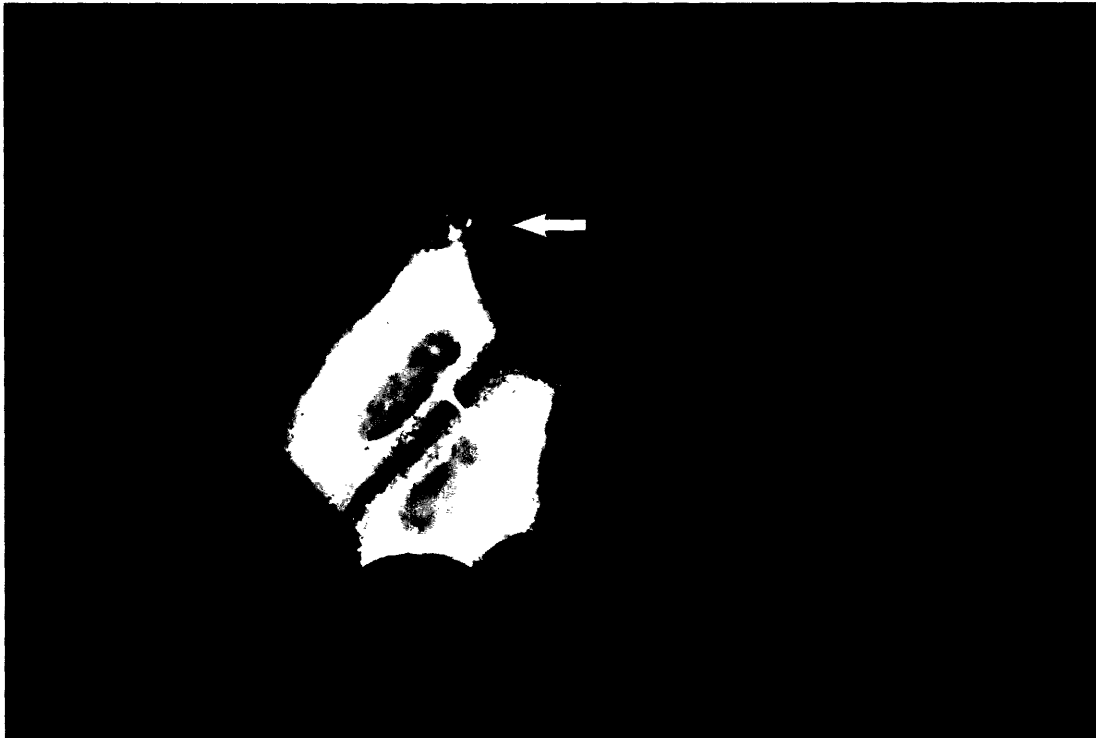
Figure 21. Stably selected nestin positive line SWv$^+$CNg2 double stained for nestin and vimentin. Anti-nestin stain *(top)* overlaps with anti-vimentin *(bottom)* stain in most cells. Magnification 1000x

Figure 22. SWv⁺CNg2 line at low magnification shows that nestin*(top)* colocalizes with vimentin*(bottom)* and that vimentin stain is more finely divided in some cells *(arrows)* that express nestin. Magnification 400x

Figure 23. SWv+CNg1 line shows a marked aggregation of nestin stain*(top)* in the perinuclear region. A few thick filaments which branch less than in untransfected cells extend to the periphery. Vimentin stain *(bottom)* overlaps with that of nestin in both the periphery and the aggregates in cells that express nestin. Magnification 1000x
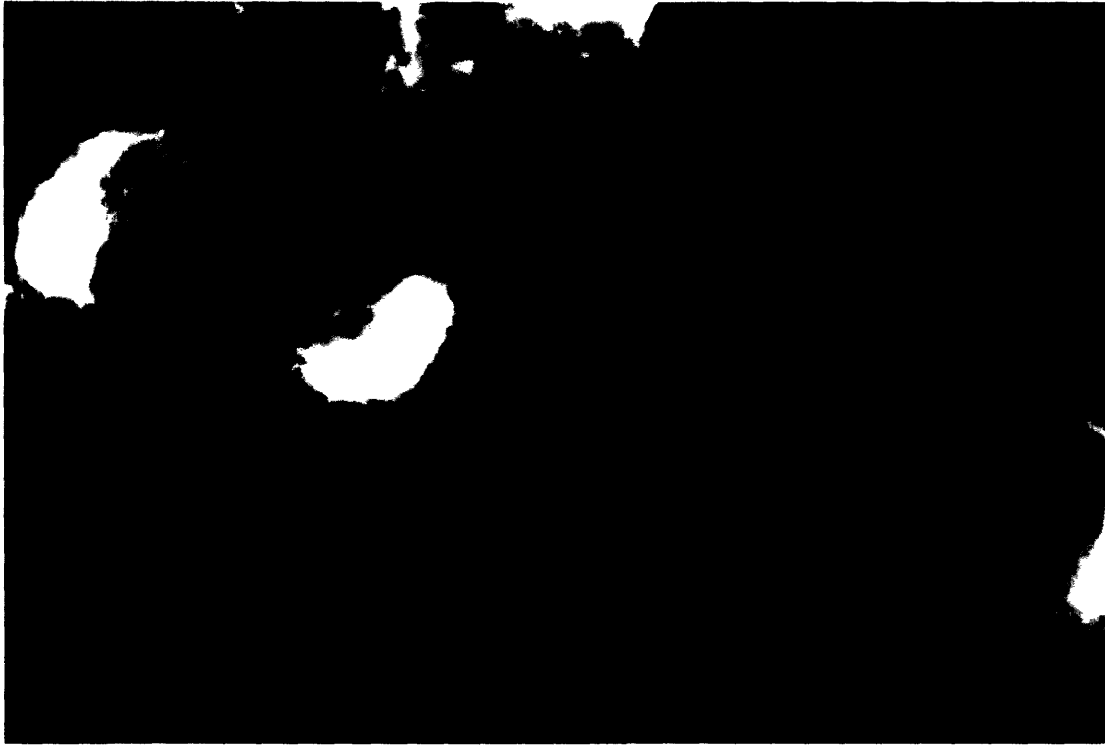
Figure 24. At low magnification, it is obvious that only cells expressing nestin *(top)* have collapsed vimentin filaments *(bottom)*. Sometimes the aggregate completely surrounds the nucleus (arrow in both panels). Magnification 40x
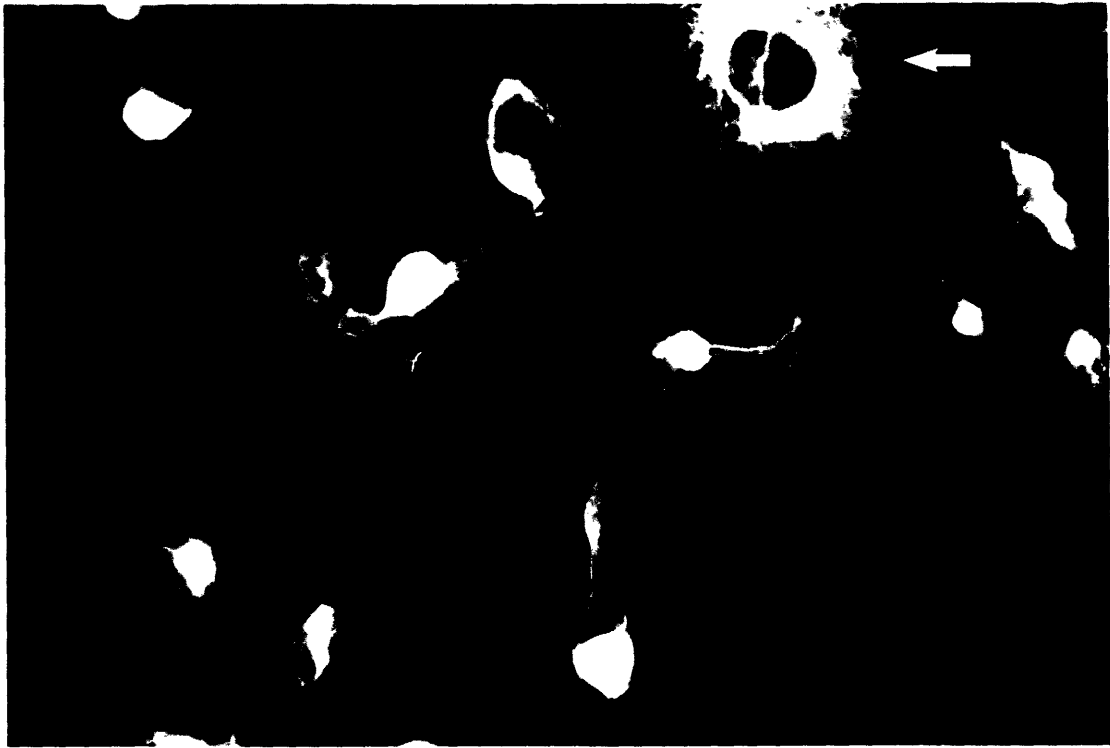
Figure 25. SW13 vimentin-positive cells transiently transfected with the 5 amino acid deletion mutant CNgM5. *(Top)* Nestin distribution follows vimentin filaments *(Bottom)*. Nestin and vimentin stain are indistinguishable at this magnification. Magnification 630x
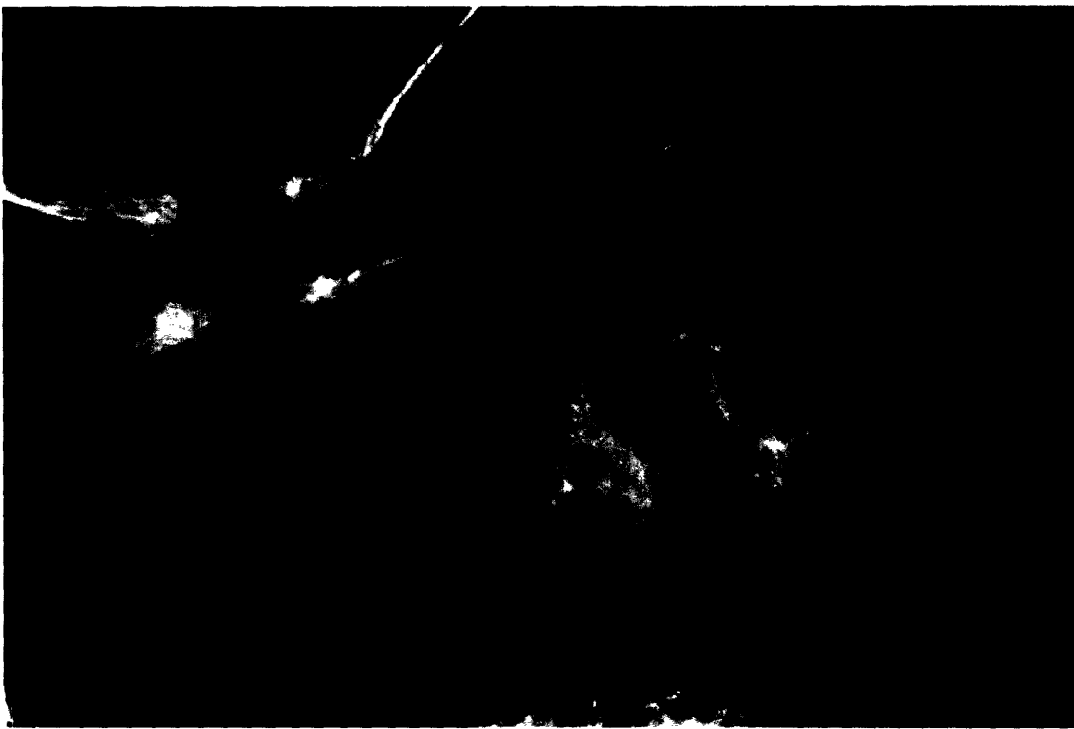
Figure 26. SW13 cells transiently transfected with CNgM5. *(Top)* Nestin is distributed along vimentin filaments but is aggregated in small, discrete particles, identified by arrows. *(Bottom)* Vimentin distribution is altered in zones at the periphery of the cell in which nestin is distributed in small spots *(arrowheads)*. Vimentin extends to periphery of the cell in most places. Magnification 1000x

143

Figure 27. Cell from the same transfection with CNgM5 shown in Figure 26, expressing higher levels of nestin. *(top)* Nestin distribution looks like that in cells overexpressing wild type nestin. *(bottom)* Vimentin expression is still filamentous and largely undisturbed. Magnification 630x

146
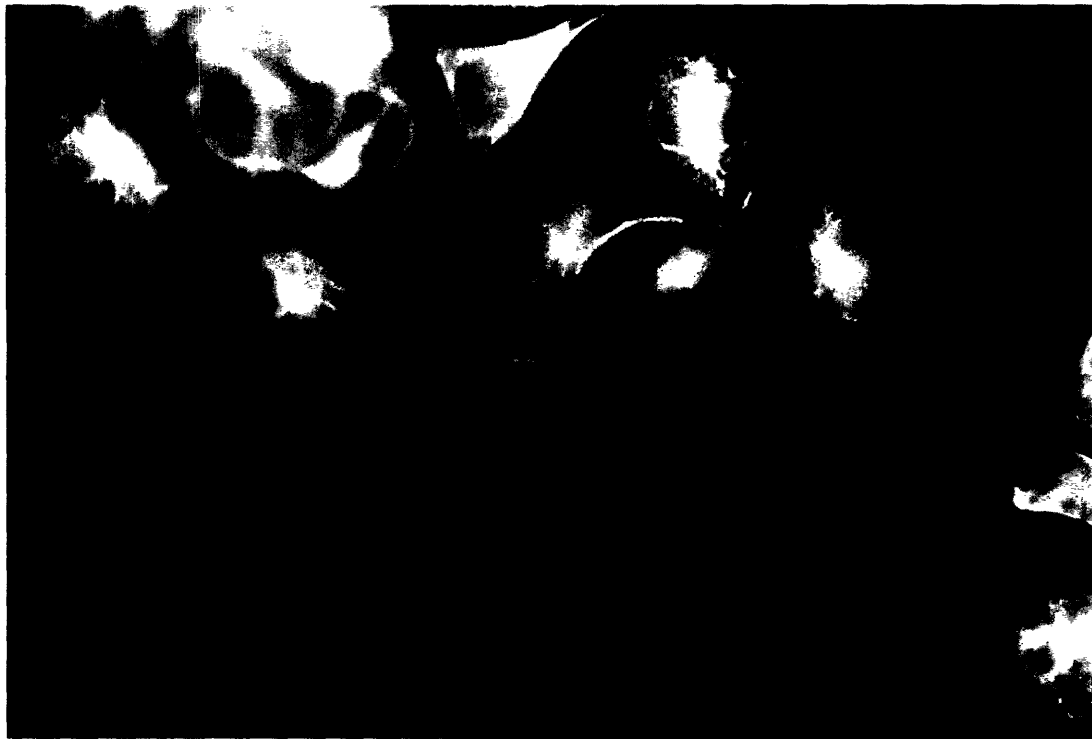
Figure 28. Line SWv+CNgM5.12, selected for stable expression of CNgM5. *Top:* Nestin mutant protein is localized along filaments and in short filament-like structures that lie in the cell periphery. *Bottom:* Vimentin is slightly retracted from the cell periphery in places where the short nestin filaments appear*(arrows)*. Magnification 1000x

Figure 29. Line SWv+CNgM5.12, at lower magnification, shows that cells expressing nestin mutant *(Top)* have retraction of vimentin network *(Bottom)*, whereas cells lacking nestin have normal vimentin distribution. Cells on the left have fragmentation of vimentin network in cell periphery as well. Magnification 400x
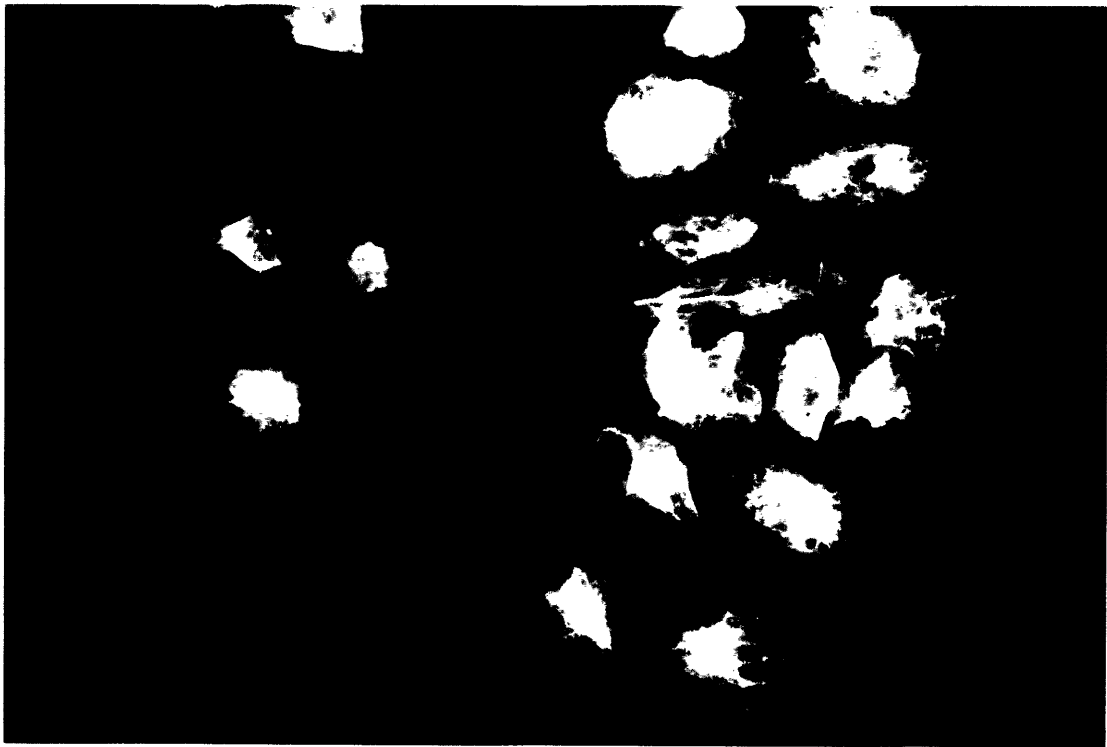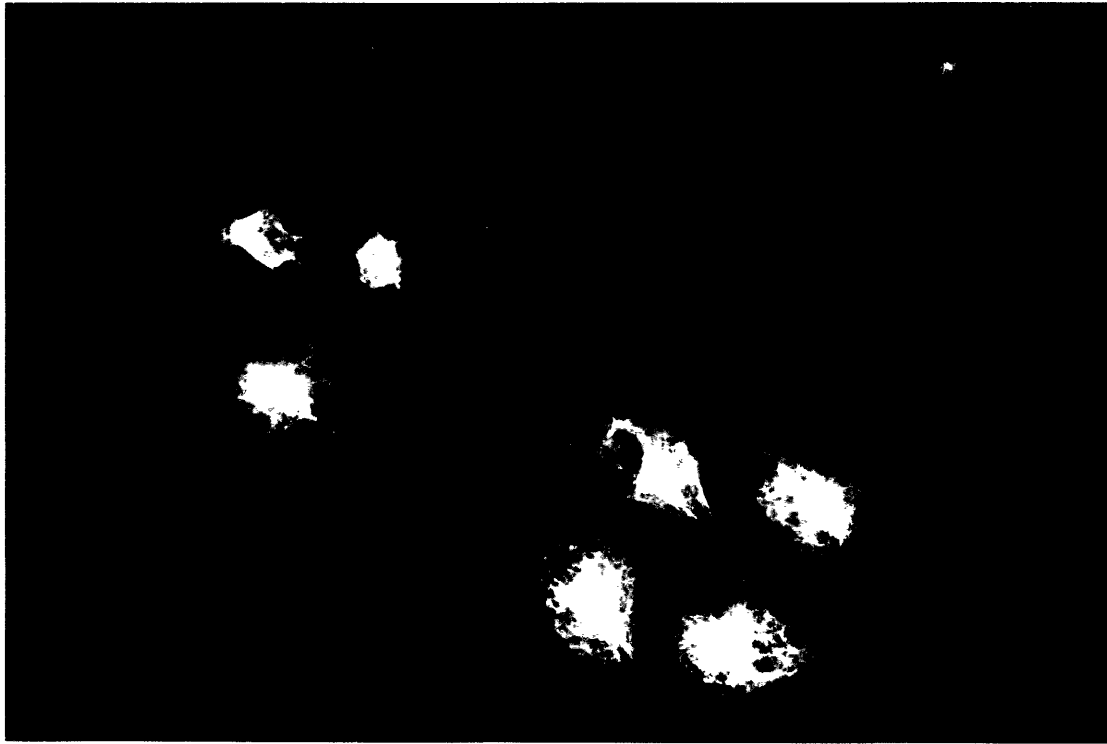
Figure 30. Line SWv+CNgM5.13 does not show fragmentation of nestin stain at early passages. *Top:* Nestin stain and *Bottom:* Vimentin stain overlap as they do in wild type cells. Magnification 400x

Figure 31. Line SWv+CNgM5.13 at high power. *Top:* Nestin shows spotty distribution of stain in the periphery, but is in general filamentous. *Bottom:* No retraction of vimentin is apparent in these cells. Magnification 1000x

Figure 32. At a higher passage (three weeks later), the line SWv+CNgM5.13 shows attenuation of both nestin and vimentin stain in the periphery of cells. *Top:* Nestin. *Bottom:* Vimentin. The outline of the cytoplasm can be seen in the anti-nestin panel. Although retracted, both channels show filaments, not aggregates. One cell not expressing nestin has a normal vimentin distribution. Magnification 1000x
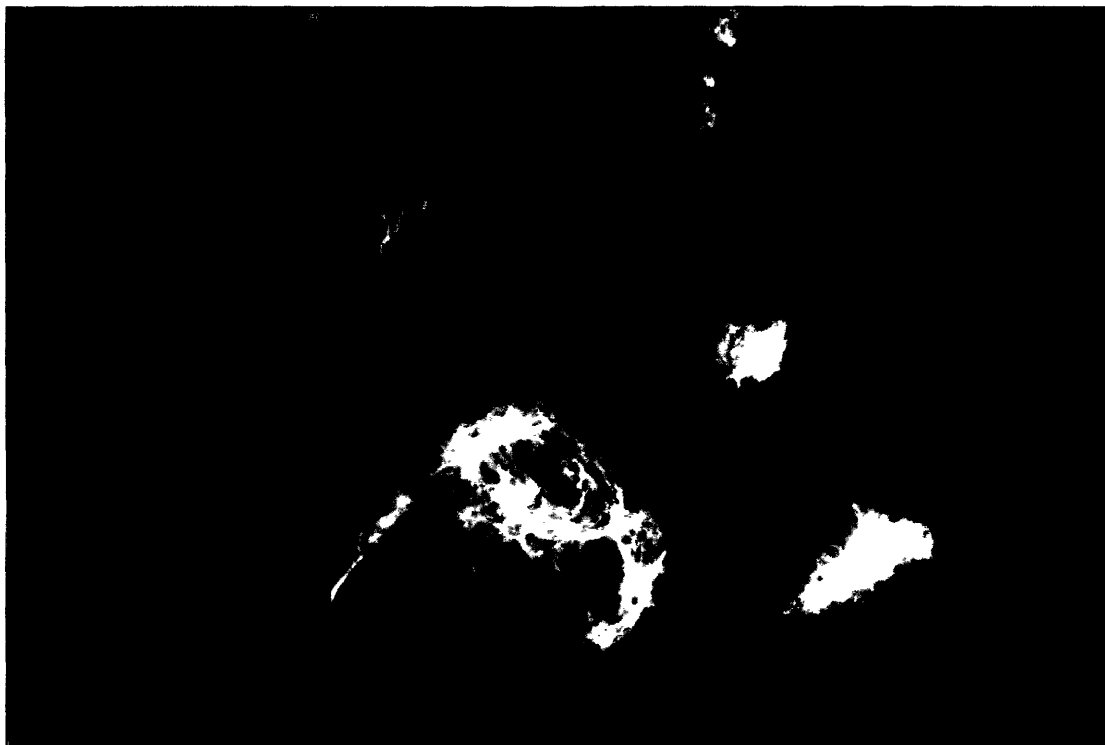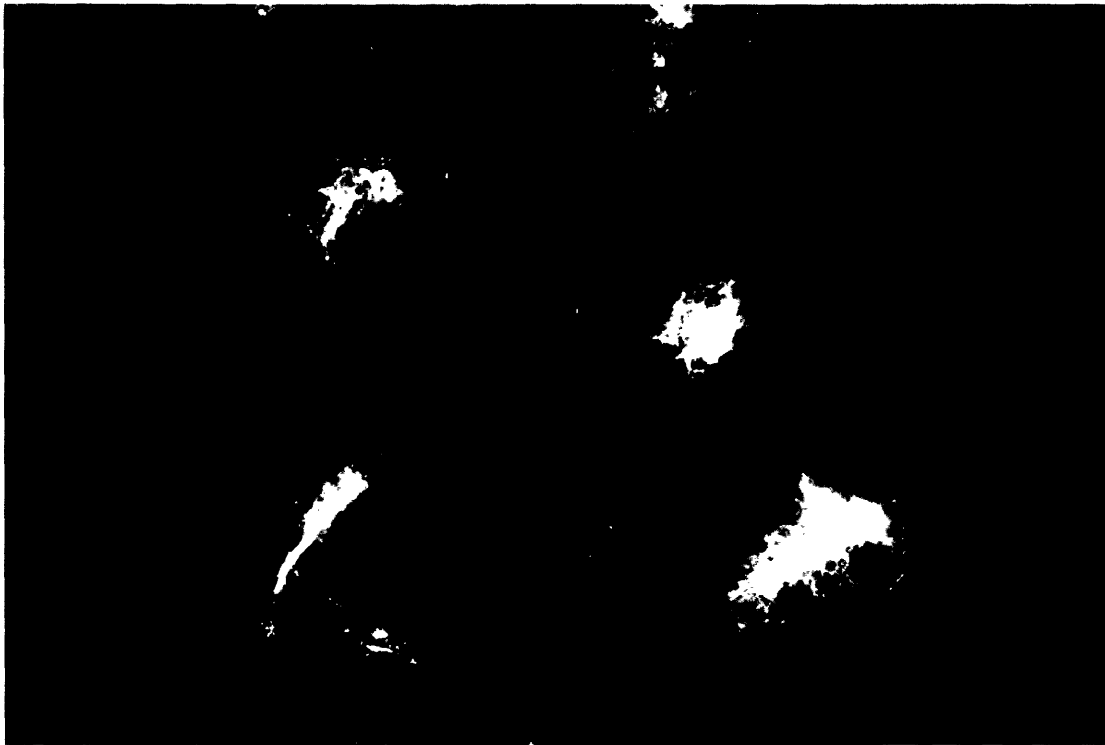
Figure 33. SW13 cells double stained for nestin and other cytoskeletal proteins. a,c,e,g. Nestin stain. b,d. Tubulin stain. f,h. actin stain. In SWv$^+$CNg1 line, (a) nestin is collapsed around the nucleus, while (b) tubulin is undisturbed. Surrounding cells are out of the focal plane. Magnification 630x. In SWv+CNgM5-13 (c) nestin is distributed in small spots except near the nucleus where it is still filamentous. (d) Tubulin is normally distributed. The fixation condition used for optimal tubulin stain is somewhat disruptive to the nestin pattern and causes high background. Magnification, 1000x. Wild type nestin line SWv+CNg-2 (e) does not affect actin distribution (f). Magnification 100x. In cells transiently transfected with CNgM5 nestin mutant, nestin (g) again does not affect actin distribution (h).
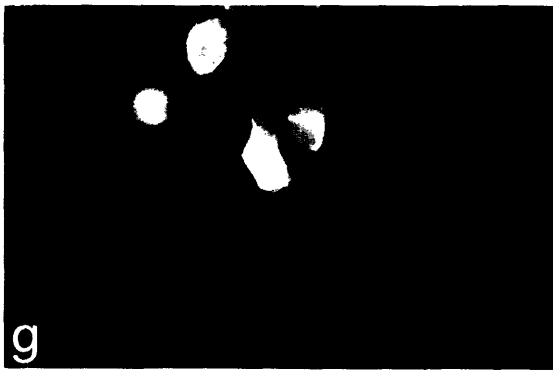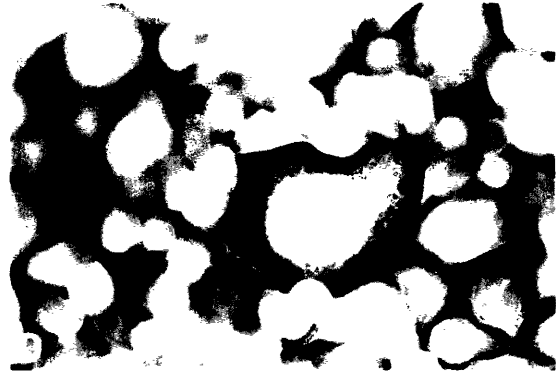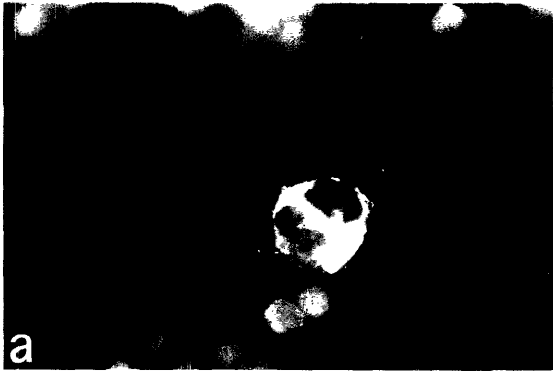
Figure 34.   (a) Nestin expression in SW13 cells transiently transfected with flagged nestin construct NgHA.   These cells express nestin abundantly and its distribution overlaps with vimentin.   (b) Vimentin pattern is identical to nestin in the center cell. (c) Nestin mutant NM5HA transfected SW13 cells.   Nestin colocalizes with vimentin (d) but does not disrupt in this case.   Cells were fixed 96 hours after transfection.   Magnification 1000x

Figure 35. *Top:* SW13 cells transiently transfected with the amino-terminal deletion construct dNIAHA. *Top:* Nestin stain. *Bottom:* Vimentin stain. The mutant nestin is distributed in a slightly grainy pattern across the cell, similar to that seen for wild type nestin in vimentin free cells. Vimentin staining pattern is within the normal range, as seen in the sister cells in the lower half of the frame. Magnification 1000x
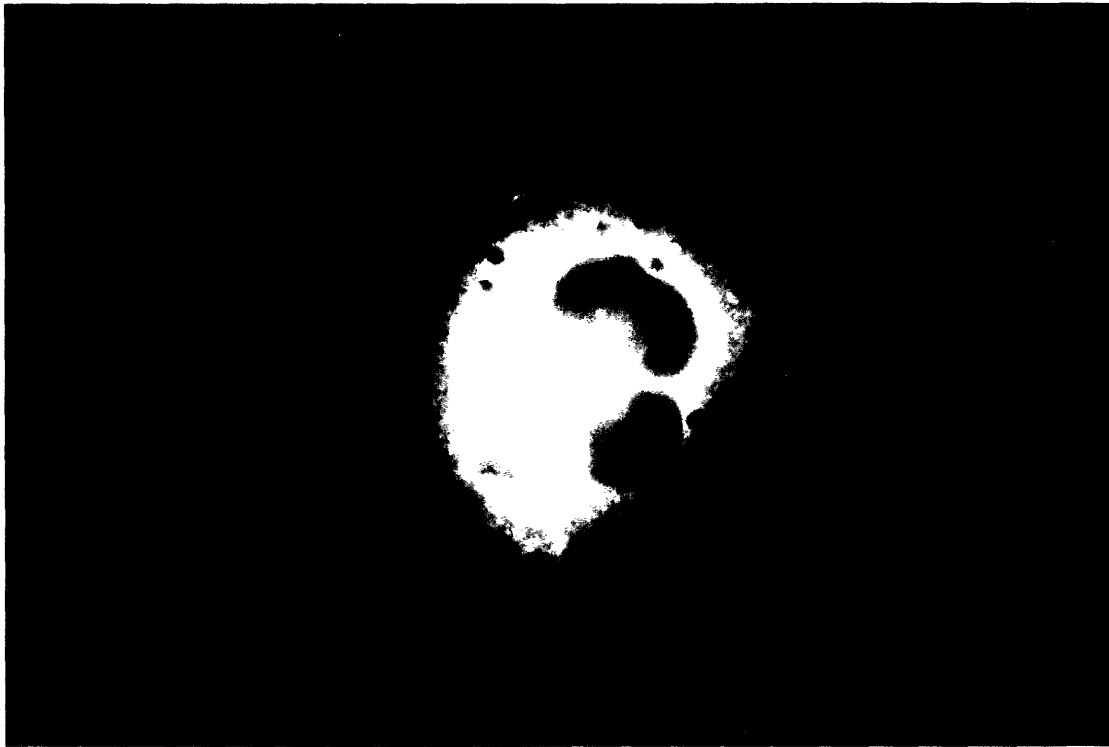
Fig 36. (a,b) NSE-LacZHipP2-21 (Hip21) cells transfected with NgHA wild type nestin. (a) Flagged nestin is stained with anti-HA antibody. (b) Endogenous and flagged nestin are stained with AS130. Both proteins are distributed in the same manner throughout the cells. (c,d) Hip21 cells from stable selected line Hip21-NMHA9, nestin mutant NM5HA. (c) Cells are stained for the HA flag on nestin. (d) Same cells expressing endogenous nestin. The mutant protein does not stain all the way to the periphery of the cells. Magnification 1000x
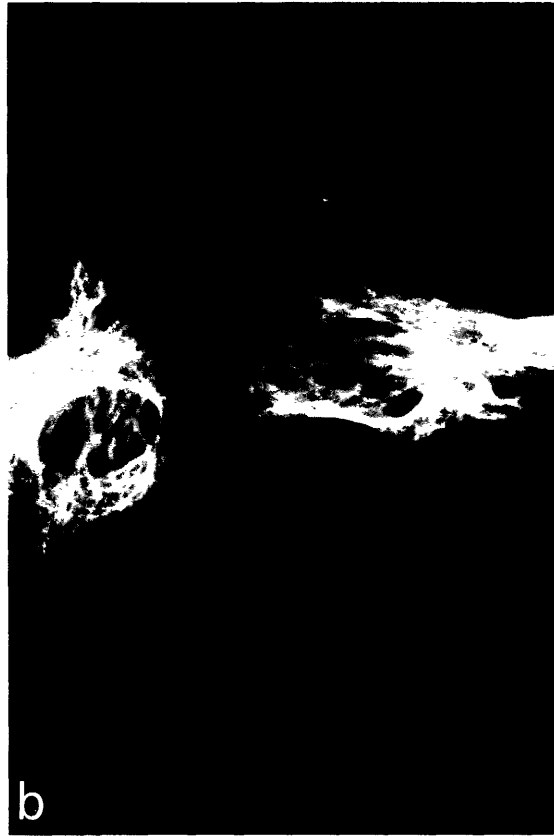
Figure 37. Western blot of Nestin and vimentin in SW13 cells. *Upper panel:* Nestin immunoreactivity on proteins extracted from nestin-transfected SW13 cells. *Lower panel:* Vimentin immunoreactivity on the same extracts. Lane 1, SWv+CNgM5.13. Lane 2, SWv+CNgM5.12. Lane 3, SWv+CNg2. Lane 4, SWv+CNg1. Lane 5, untransfected vimentin positive SW13 cells. Lane 6, untransfected vimentin negative cells.

NESTIN

1   2   3   4   5   6

— 220

— 110

— 75

— 220

— 110

— 75
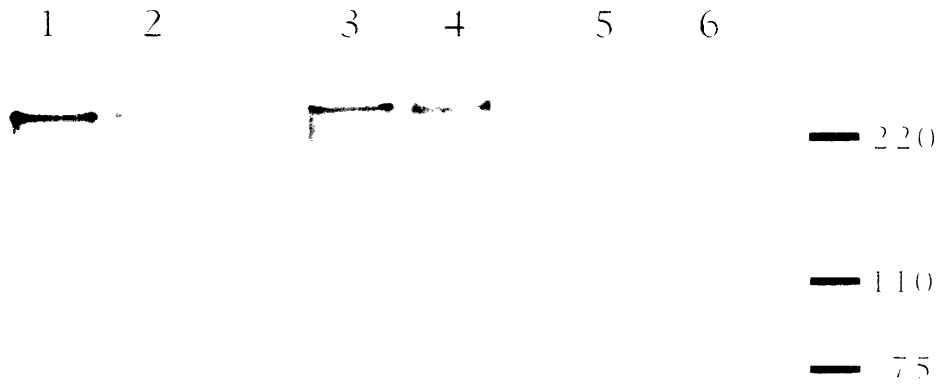
VIMENTIN

Figure 38. TritonX-100 fractionations of cells. Panel A: Lanes 1-4, nestin Lanes 5-8, vimentin. Lanes 1, 2, 5, 6, Hip 21 cells. Lanes 3, 4, 7, 8, ST15A cells. Panel B: Fractionations of nestin-expressing SW13 cells. Lanes 1-2, SWv+CNg1. Lanes 3-4 SWv+CNg2. Lanes 5-6 SWv+CNgM5.13. Lanes 7-8 SWv+CNgM5.12. Lanes 9-10 Transiently transfected SW13 vimentin negative cells expressing CMV-Ng. Lanes 11-12, Extract of E16 cortex.
S is soluble, P is pellet.
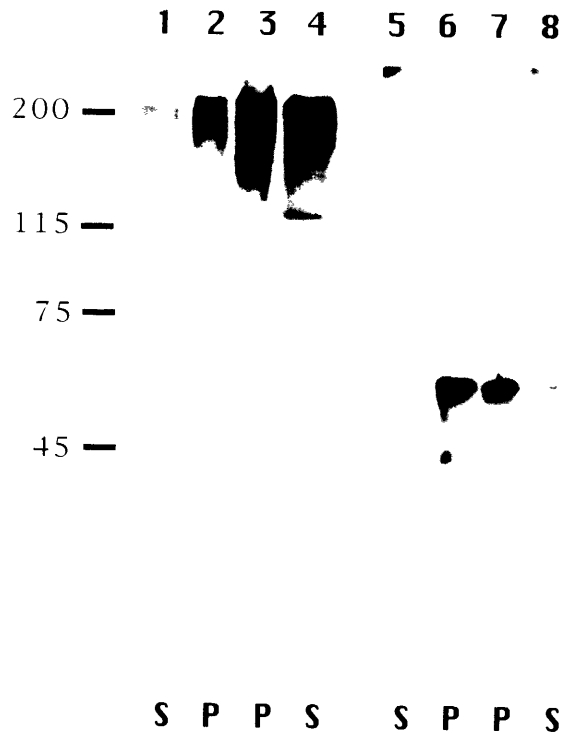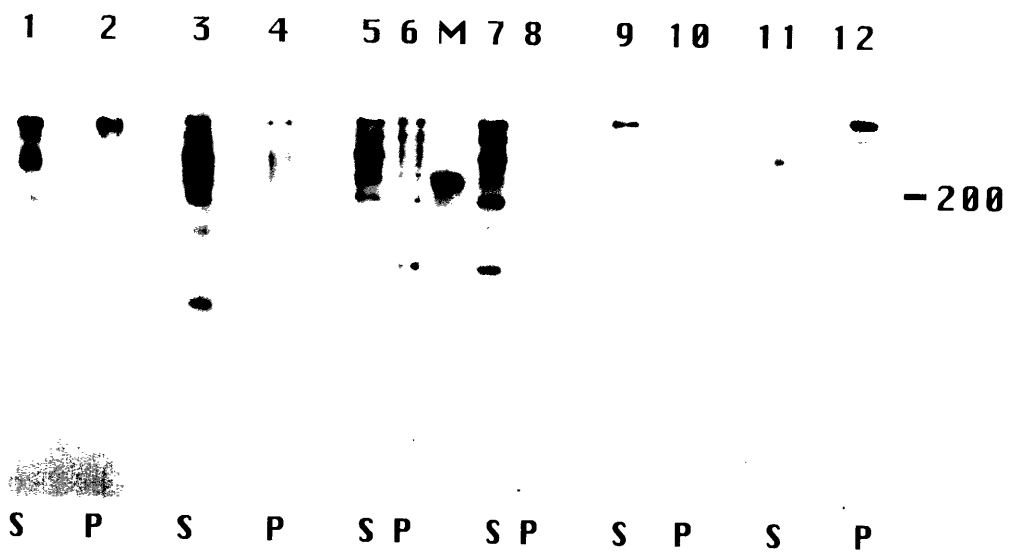
Chapter 5: Transgenic animals

Introduction

While many mutations in intermediate filaments produce visible perturbations in the cytoskeletal structure in cells, they do not affect cell viability. Monolayer culture is a highly artificial situation which cannot be used to test protein functions which are required at the level of organs, tissues and organisms. Transgenic technology offers a way to assess the biological effects of mutant proteins in the whole animal. Until dominant keratin 14 mutant proteins were expressed in transgenic mice, no function for intermediate filaments had been demonstrated unequivocally in any system. As a result of study of the keratin 14 animals, it became clear that keratin intermediate filaments provide mechanical support to epithelial cells. These cytoskeletal elements are essential to the structural integrity of the epidermis. Without a functional intermediate filament system, epithelial cells are unable to resist mechanical trauma, and detach from adjacent layers of the skin, resulting in blistering (Vassar et al., 1991; (Chan, et al., 1994; Rugg, et al., 1994) and others). In vitro, there is a case of cell death caused by IF collapse (Yu, et al., 1994). The cause was apparently the physical interaction between the aggregate and the nucleus, rather than the lack of IFs in the cytoplasm. Cultured cells of many types including myoblasts and epithelial cells are capable of sustained proliferation with collapsed and aggregated IF networks (Albers and Fuchs, 1989; Coulombe, et al., 1990; Schultheiss, et al., 1991). SW13 cells are capable of survival without any IF networks, and are not negatively affected by collapsed networks, as witnessed by the line SWv+CNg1. Therefore, the most informative experiments on IF function have come from in vivo studies.

The nestin-vimentin intermediate filament system is more complex in the developing CNS than in cultured cells; for example, the developing CNS has a polarity that is lost in monolayer culture. The developing neural tube is comprised of columnar epithelial cells which span the radius of the structure. The nuclei of the cells are located in the central third of the neural tube near the ventricle. These nuclei migrate toward the ventricle during mitosis, while releasing the process attached to the pial (outer) surface. Following cell division, it is believed that the pial attachment is regained and that the nuclei move toward the outer side of the ventricular zone.

Later in development, radial glial cells are also polarized, supporting the migration of newly born neurons outward along their pial processes (Jacobson, 1991). The dynamic relationship between the cell body and the pial surface suggests that the pial attachment must serve a function in development.

The polarity of radially arrayed CNS cells is apparent early. There is substantial evidence that the subpial zone in the developing spinal cord, cortex and optic tectum is a molecularly distinct compartment with active mechanisms to preferentially localize proteins and mRNA. Nestin mRNA is detected only in the outer half of the spinal cord. In contrast, endogenous vimentin mRNA and β-galactosidase mRNA expressed from the nestin promoter in transgenic mice are located throughout the cytoplasm of the nestin-positive cells (Zimmerman et al., 1994; Dahlstrand et al., 1994). Due to the greater volume of the ventricular side of the cell, this gives the appearance of ventricular localization for the vimentin and β-galactosidase mRNAs. The differential localization of nestin and β-galactosidase or vimentin mRNAs demonstrates that there is a mechanism for the distribution of particular messages toward the pial surface of the cell.

Rat 401 staining is first detected at the pial surface of the columnar epithelial cells of the spinal cord in rat E11 embryos, then spreads toward the ventricular zone along vimentin-positive filaments. Nestin first appears in a disk-like structure on the pial surface of the neural tube. Later, the nestin positive structure widens and nestin-positive filaments which extend to the ventricular zone originate from it (Hockfield and McKay, 1985). Although this structure has not been identfied as a hemidesmosome, keratin IFs are well known to associate with and be anchored to desmosomes (Skalli, et al., 1994; Stappenbeck, et al., 1993; Troyanovsky, et al., 1993; Wiche, et al., 1993). The nestin positive pial endfoot structure may serve as such an anchorage point.

Several antibodies other than Rat 401 react with radial glial endfeet preferentially. A recently published study of a set of antibodies raised against chick tectum identified changes in the molecular organization of radial glia through development. Two of the antibodies stain the whole length of the glial cell spanning the neuroepithelium at early times, but later become localized to the pial endfeet and superficial processes. The alteration of the distribution over time in vivo is distinct from anti-vimentin immunoreactivity.

Vimentin protein is present in filaments that span the distance from the ventricle to the pial surface throughout development (Herman et al., 1993). As the radial glia begin to differentiate into astrocytes late in development, GFAP immmunoreactivity is first detected at the endfeet in E16 rat spinal cord (Yang et al., 1993). The localization of so many cytoplasmic elements to the pial surface suggests that specialized functions are required at this site.

To study the influence of cell polarity on nestin localization and function in development, we expressed wild type and coil 2B mutant rat nestin in transgenic mice. Both the mutant and possibly the wild type form were able to disrupt the vimentin network in cultured cells (Chapter 4). The animal system differs from SW13 cells in that it expresses endogenous nestin. Competition between the mutant and wild type subunits was expected to moderate the phenotype as it did in Hip 21 cells. Transgenic animals using both constructs were performed to determine the influence of nestin overexpression on the developing CNS and to test the effects of a mutant subunit in a polarized system.

Materials and Methods

Transgenic animals

Egg donors, stud males (C57BL/6 x C3H F1), recipient females and vasectomized males (ICR) were obtained from Bommice, Denmark or from NCI-Frederick. Egg donors were superovulated, mated and eggs were harvested as described (Hogan, 1986). Egg pronuclei were microinjected with linearized DNA constructs at a concentration of 2-5 ng/μl. Eggs were transferred to recipient females by oviduct transfer.

DNA preparation

DNA was cut and linearized by digestion with Cla1 and Nhe1. Restriction enzymes were removed with Gene-Clean (Bio101) Fragments were separated on a 10 to 40% sucrose gradient. Gradient fractions containing the desired fragment were dialysed into injection buffer containing 10 mM Tris pH 7.5, 0.1 mM EDTA (Mann and McMahon, 1993).

Sectioning

E11.5-E12.5 embryos were collected from pregnant recipient mice or from a female naturally mated to a male bearing the transgene. After removal of all extraembryonic tissue, animals were fixed overnight in 4% paraformaldehyde in PBS, pH 7.2. The trunks of the embryos were embedded in OCT and cut on a Microm cryostat at a thickness of 40 microns.

PCR for transgenes

Yolk sacs were digested in Proteinase K overnight (Laird, et al., 1991). DNA was subjected to 25 cycles of one minute each at 94º, 60º, and 72ºC. The primer sequences were: *gNesup* GGAAGGCAATGGGTTGT-GTG; *gNesdn:* ACAAGAGACACAGACAGAGG. Reactions were carried out in Taq polymerase buffer with 2.5 mM MgCl$_2$, 0.8 mM primers with Taq polymerase (Perkin-Elmer). The primers were designed to detect the rat genomic DNA exclusively and are located in the second intron (primers kindly designed by Jonas Dahlstrand).

Antibody Staining

Sections were permeablilzed and blocked in 0.2% TritonX-100 and 2% goat serum and incubated with MAB 12CA5 (Berkeley) and AS130 for 3 hours at room temperature. Secondary antibodies were affinity purified LRSC rhodamine conjugated donkey anti-rabbit and fluorescein goat anti-mouse (Jackson).

Confocal microscopy

Sections were examined using a BioRad confocal microscope at 40x magnification. A series of 4 optical sections at intervals of 1.98 microns were taken and projected onto a single image. Images from double stained embryos were collected simultaneously on separate channels and the filters were adjusted so that not cross-channel exitation was seen.

Results

Transgenic mouse embryos

172

Transgenic mouse embryos developing from DNA injected eggs were collected at E11.5 to E12 from a recipient female. Embryos from a transgenic line were collected at the same gestational age from a female naturally mated to founder male NM5HA-102.

The numbers of transgenic animals obtained from each experiment are given in Table 1. The wild type construct NgHA was expressed on the protein level in 100% of the animals examined, whereas only 50% of the NM5HA animals positive by PCR expressed protein as detected by staining of sections with the anti-HA antibody 12CA5. Since the expression of transgenes often depends on the quality of the DNA used and the integration site, embryos from a transgenic line carrying NM5HA were also examined. As expected for a heterozygous founder, the rat nestin gene was transmitted to approximately 50% (47%) of the offspring. Of the animals which inherited the transgene, only 43% expressed detectable flagged nestin protein. The founder is a F2 C57BL/6 x C3H hybrids and was backcrossed to C57BL/6 females. Variation in the genetic background might accound for the variable penetrance. Since the founders and the line had the same variable expression, it is not likely to be due to integration sites. Currently, several new lines of both wild type and mutant nestin transgenic mice are being established to expand these studies.

Localization of Transgenic Nestin Protein in the Spinal Cord Wild type Construct

At E11.5-12.5, mice bearing the wild type nestin construct NgHA show strong nestin staining in radial processes in the spinal cord. At this stage, motor neurons are beginning to differentiate in the ventral horns. The endfeet of the radial glial cells are particularly prominent in the ventrolateral region of the spinal cord. In more dorsal regions, positive endfeet are smaller and more dispersed (Hockfield and McKay, 1985) In order to follow individual radial processes, confocal microscopy was used to eliminate out of focus fluorescence and to generate optical sections that were projected onto a single plane. Therefore, the density of processes appears greater than would be seen in a single focal plane. A wild type nestin transgenic embryo was reacted with each of the primary antibodies singly to show that there was no cross-channel exitation (Figure 39).

Each of the transgenic embryos carrying the wild type-flagged construct expressed protein as detected by the anti-HA antibody 12CA5. Embryos were doubly labeled with antinestin AS 130 and the anti-HA antibody 12CA5. The antibodies detected radial glial endfeet and radially arrayed processes that spanned the spinal cord from the ventricular zone to the pial surface. Staining was strongest at the pial endfeet and processes proximal to them for both antibodies, as described for Rat 401 (Hockfield and McKay, 1985). The distribution of flagged rat nestin was identical to that of endogenous nestin (Figure 40). These views are of the ventrolateral pial surface. The processes are contiuous to the ventricular zone except where interrupted by cutting of the section. The intensity of the anti-HA staining varied between the embryos, but all animals showed staining throughout the length of the cell. No gross abnormalities of the CNS were noted. Eight founder animals bearing an unflagged nestin construct otherwise identical to NgHA were normal in appearance and behavior, bred well, and lived beyond the age of one year.

NM5HA Mutant Construct

Ten transgenic mouse embryos bearing the construct NM5HA were examined at E11.5 and found to be normal in appearance. The size and structure of the brain was identical to that of non-transgenic littermates. Embryos derived from founder animal NM5HA-102 were also normal in appearance.

All the animals which express the mutant nestin construct show a different subcellular distribution for the transgenic protein than for endogenous nestin. The mutant protein localizes almost exclusively to the pial endfoot and to the filaments adjacent to it in the marginal layer of the spinal cord, as seen in the ventrolateral views presented in Figure 41. In Figure 41a, the endfoot stain was separate from adjacent endfeet and the stained structure was smaller than for the endogenous protein shown in 41b. In Figure 41c, there are distinct processes visible stained for the transgene, but they fail to extend far from the pial surface. This does not apparently affect the distribution of endogenous nestin seen in Figure 41d. Figure 42a-b shows a lateral view of the pial surface. Nestin stain appears to be continuous along the pial surface due to the projection of several optical planes into one figure. Nestin is excluded from filaments, but the arrows indicate light perinuclear staining in a few cells. Anti-HA stain was sometimes restricted to small dots similar to those seen at

the onset of nestin expression, but the endogenous protein was not restricted (Figure 42c-d). The small nestin positive spots were similar to those seen in E11 rat. E11 rats are at a developmental stage equivalent to E9.5-E10 mice.

Discussion

The subcellular distribution of wild type rat nestin followed the endogenous protein closely, but nestin localization was strikingly altered by the deletion of five amino acids from the coil 2B conserved sequence. The results emphasize the polarization of the cells of the early CNS. Nestin was known to be first expressed at the pial surface, but this data shows that the polarity of expression and the specialization of pial structures is maintained through development.

This result was not predicted by experiments with the same constructs in cultured cells. In SW13, a non-neuronal, vimentin positive line, nestin-containing filaments were distributed throughout the cytoplasm in a pattern identical to that of vimentin. The mutant protein showed the ability to disrupt the vimentin filaments near the plasma membrane. Wild type rat nestin co-distributed with endogenous nestin in the hippocampal line Hip 21, while the mutant protein was found concentrated in the perinuclear zone. There are three hypotheses which could account for the behavior of mutant nestin in different cellular environments.

If the mutant protein is unstable it might be degraded too rapidly to participate in the vimentin-nestin network in CNS stem cells. Therefore it would be detected only a short time after synthesis. Considering the localization of nestin mRNA near the pial surface of the spinal cord, it is likely that nestin translation takes place there. Rapid protein turnover would make nestin appear only in the structures at the pial surface, as it does when the protein is first detected. Rapid degradation might also explain the lack of HA-reactive protein in half the transgenic embryos. In the negative embryos, the rate of degradation could be too rapid to allow any accumulation of the mutant nestin protein. The small amount of mutant protein found in the perinuclear zone of the radial cells might then be simply soluble degradation products from proteolytic digestion of nestin.

175

Alternatively, the mutant protein may be restricted to the pial surface via a passive or active mechanism. If mutant nestin protein had a reduced capacity to interact with the endogenous vimentin-nestin filament network well enough to be transported from the site of synthesis, it would remain at the pial surface. To extend this theory to the results in cultured cells, the synthesis of nestin in Hip 21 cells would be presumed to take place near the nucleus. Therefore, the nascent mutant protein would remain localized near site of synthesis. The lack of competing endogenous nestin in SW13 would explain the apparently normal distribution of mutant protein in those cells.

Finally, nestin could instead be restricted to the pial surface by active means. If nestin has two roles, one depending on the coiled-coil region and the second on the tail domain, weakening the coiled-coil interaction with the rod would leave only the domain responsible for interaction with the pial surface intact. The mutant protein might bind preferentially to its peripheral binding site rather than to the vimentin-nestin network. The data in SW13 cells suggests that the nestin mutant protein can affect the interaction of vimentin IFs with the periphery of the cell. The data in Hip 21 cells seems to suggest that the interference of mutant nestin with peripheral interactions does not take place in the presence of endogenous nestin. However, other intermediate filaments with coil 2B mutations show a tendency to cause aggregation of filaments, rather than a decreased affinity for their assembly partners (Albers and Fuchs, 1989; Coulombe et al., 1990; Gill et al., 1990; Raats et al., 1992; Raats et al., 1991; Rorke et al., 1992; Wong and Cleveland, 1990). The five amino acid deletion mutant described here does not promote filament clumping in cultured cells. This construct differs from most other coil 2B deletion construct in that the tail domain is intact. The tail may prevent the aggregation of filaments, as has been suggested for vimentin (Heins, et al., 1993).

Keratin intermediate filaments are known to interact with desmosomes. A class of proteins including plectin and desmoplakin are able to bind keratins, vimentin and desmosomal proteins. Plectin serves an IF cross-linker, while desmoplakin links keratin IFs to desmosomal plaques (Stappenbeck, et al., 1993; Wiche, et al., 1993). Two desmin point mutants of the 2B conserved region were found to block autoassembly of desmin and to redistribute the mutant protein to colocalize with desmoplakin in cultured vimentin-free, keratin positive MCF-7 cells (Raats et al., 1992). The thickened nestin-

positive structure seen by EM may be a candidate for a competing binding site for nestin and may serve as an anchor point for the vimentin-nestin filaments.

Several experiments will be necessary to resolve these possibilities. First, metabolic labeling of proteins would allow comparison of the rates of protein turnover in mutant and wild type animals. Western blotting is required to determine whether the rat proteins are full length in both types of animals. If the mutant nestin protein were held at the pial surface by a passive mechanism, it would be expected that the polarized distribution of the protein would vanish when monolayer cultures were made from spinal cord. To distinguish between the active and passive localization at the cell surface, additional constructs would be helpful. Constructs containing portions of the rod or tail domains only would help to identify what domains are responsible for localization along filaments or at the cell surface. More detailed electron micrographic and immunocytochemical studies of the developing spinal cord are needed to elucidate the nature of the Rat 401 positive structure at the pial surface.

References

Albers, K. and Fuchs, E. (1989). Expression of mutant keratin cDNAs in epithelial cells reveals posible mechanisms for initiation and assembly of intermediate filaments. J Cell Biol 108, 1477-1493.

Chan, Y.-M., I, A.-L., Yu, Q.-C., Jackel, A., Zabel, B., Ernst, J.-P. and Fuchs, E. (1994). A human keratin 14 "knockout": the absence of K14 leads to severe epidermolysis bullosa simplex and a function for an intermediate filament protein. Genes & Dev 8, 2574-2587.

Coulombe, P., Chan, Y.-M., Albers, K. and Fuchs, E. (1990). Deletions in epidermal keratins leading to alteration in filament organization in vivo and in intermediate filament assembly in vitro. Journal of Cell Biology 111, 3049-3064.

Dahlstrand, J., Lardelli, M. and Lendahl, U. (1994). Nestin mRNA expression correlates with the CNS progenitor cell state in many, but not all, regions of the CNS. Dev Brain Res in press

Gill, S., Wong, P., Monteiro, M. and Cleveland, D. (1990). Assembly properties of dominant and recessive mutations in the small mouse nuerofilament (NF-L) subunit. J Cell Biol 111, 2005-2019.

Heins, S., Wong, P., Muller, S., Goldie, K., Cleveland, D. and Aebi, U. (1993). The rod domain of NF-L determines neurofilament architecture, whereas the end domains specify filament assembly and network formation. J Cell Biol 123, 1517-1533.

Herman, J.-P., Victor, J. and Sanes, J. (1993). Developmentally regulated and spatially restricted antigens of radial glial cells. Dev Dynamics 197, 307-318.

Hockfield, S. and McKay, R. (1985). Identification of major cell classes in the developing mammalian nervous system. J Neurosci 5, 3310-3328.

Hogan, B. (1986). Manipulating the mouse embryo (Cold Spring Harbor: Cold Spring Harbor Press)

Jacobson, M. (1991). Developmental Neurobiology (New York: Plenum Press)

Laird, P., Zijderveld, A., Linders, K., Rudniki, M., Jaenisch, R. and Berns, A. (1991). Simplified mammalian DNA isolation procedure. Nucl Acids Res 19, 4293-4294.

Mann, J. and McMahon, A. (1993). Factors Influencing Frequency Production of Transgenic Mice. In Guide to Techniques in Mouse Development (San Diego: Academic Press, Inc), pp. 771-781

Raats, J., Gerards, W., Schreuder, M., Grund, C., Henderik, J., Hendriks, I., Famaekers, F. and Bloemendal, H. (1992). Biochemical and structural aspects of transiently and stably expressed mutant desmin in vimentin-free and vimentin containing cells. Eur J Cell Biol 58, 108-127.

Raats, J., Henderik, J., Verdijk, M., van Oort, F., Gerards, W., Ramaekers, F. and Bloemendal, H. (1991). Assembly of carboxy-terminally deleted desmin in vimentin-free cells. Eur J Cell Biol 56, 84-103.

Rorke, E., Crish, J. and Eckert, R. (1992). Central rod domain insertion and carboxy-terminal fusion mutants of human cytokeratin K19 are incorporated into endogenous keratin filaments. J Invest Dermatol 98, 17-23.

Rugg, E., McLean, W., Lane, E., Pitera, R., McMillan, J., Dopping-Hepenstal, P., Navsaria, H., Leigh, I. and Eady, R. (1994). A functional "knockout" of human keratin 14. Genes & Dev 8, 2563-2573.

Schultheiss, T., Lin, Z., Ishikawa, H., Zamir, I., Stoeckert, C. and Holtzer, H. (1991). Desmin/Vimentin intermediate filaments are dispensible for many aspects of myogenesis. JCB 114, 953-966.

Skalli, O., Jones, J., Gagescu, R. and Goldman, R. (1994). IFAP 300 is common to desmosomes and hemidesmosomes and is a possible linker of intermediate filaments to these junctions. J Cell Biol 125, 159-170.

Stappenbeck, T., Bornslaeger, E., Corcoran, C., Luu, H., Virata, M. and Green, K. (1993). Functional analysis of desmoplakin domains: specification of the interaction with keratin versus vimentin intermediate filament networks. J Cell Biol 123, 691-705.

Troyanovsky, S., Eshkind, L., Troyanovsky, R., Leube, L. and Franke, W. (1993). Contributions of cytoplasmic domains of desmosomal cadherins to desmosome assembly and intermediate filament anchorage. Cell 72, 561-574.

Vassar, R., Coulombe, P. A., Degenstein, L., Albers, K. and Fuchs, E. (1991). Mutant keratin expression in transgenic mice causes marked abnomalities resembling a human genetic skin disease. 64, 365-380.

Wiche, G., Gromov, D., Donovan, A., Castanon, M. and Fuchs, E. (1993). Expression of plectin mutant cDNA in cultured cells indicates a role of COOH-terminal domain in intermediate filament association. J Cell Biol 121, 607-619.

Wong, P. C. and Cleveland, D. W. (1990). Characterization of dominant and recessive assembly-defective mutation in mouse neurofilament NF-M. J Cell Biol 111, 1987-2003.

Yang, H.-Y., Lieska, N., Shao, D., Kriho, V. and Pappas, G. (1993). Immunotyping of radial glia and their glial derivatives during development of the rat spinal cord. J Neurocytol 22, 558-571.

Yu, K., Hijikata, T., Lin, Z., Sweeney, H., Englander, S. and Holtzer, H. (1994). Truncated desmin in PtK2 cells induces desmin-vimentin -cytokeratin coprecipitation, involution of intermediate filament networks, and nuclear fragmentation: A model for many neurodegenerative diseases. PNAS (USA) 91, 2497-2501.

Zimmerman, L., Lendahl, U., Cunningham, M., McKay, R., Parr, B., Gavin, B., Mann, J., Vassileva, G. and McMahon, A. (1994). Independent regulatory elements in the nestin gene directs transgene expression to neural stem cells or muscle precursors. Neuron 12, 11-24.

Nestin Transgenic Animals

| Construct	Total	Positive	Protein
NgHA	3 2	6	6
NM5HA	6 4	1 0	5
Line NM5HA-102	1 5	7	3

Table 1.   Numbers of transgenic embryos examined for the wild type rat nestin construct NgHA and the mutant construct NM5HA.   The embryos in the first two rows developed from the DNA injected eggs. Line NM5HA-102 describes the offspring of a founder animal bearing NM5HA.   Positive column describes animals positive by PCR.   Protein indicates animals which had detectable staining with anti-HA flag antibody 12CA5 by immunofluorescence and confocal microscopy.

Figure 39. Control showing sections of animal NgHA505 with one of the primary antibodies omitted. A, HA antibody recognizes radial glial endfeet and processes in the spinal cord. B, Secondary donkey anti rabbit antibody alone does not react with any structure in the spinal cord. C, Secondary goat anti mouse does not react. D, AS 130 identifies radial glia and processes in the spinal cord.
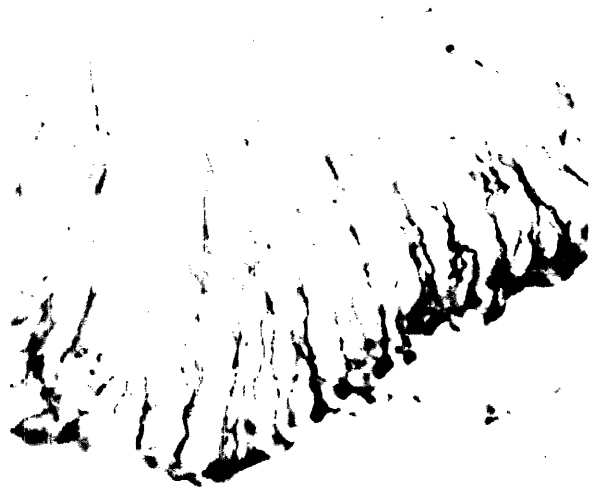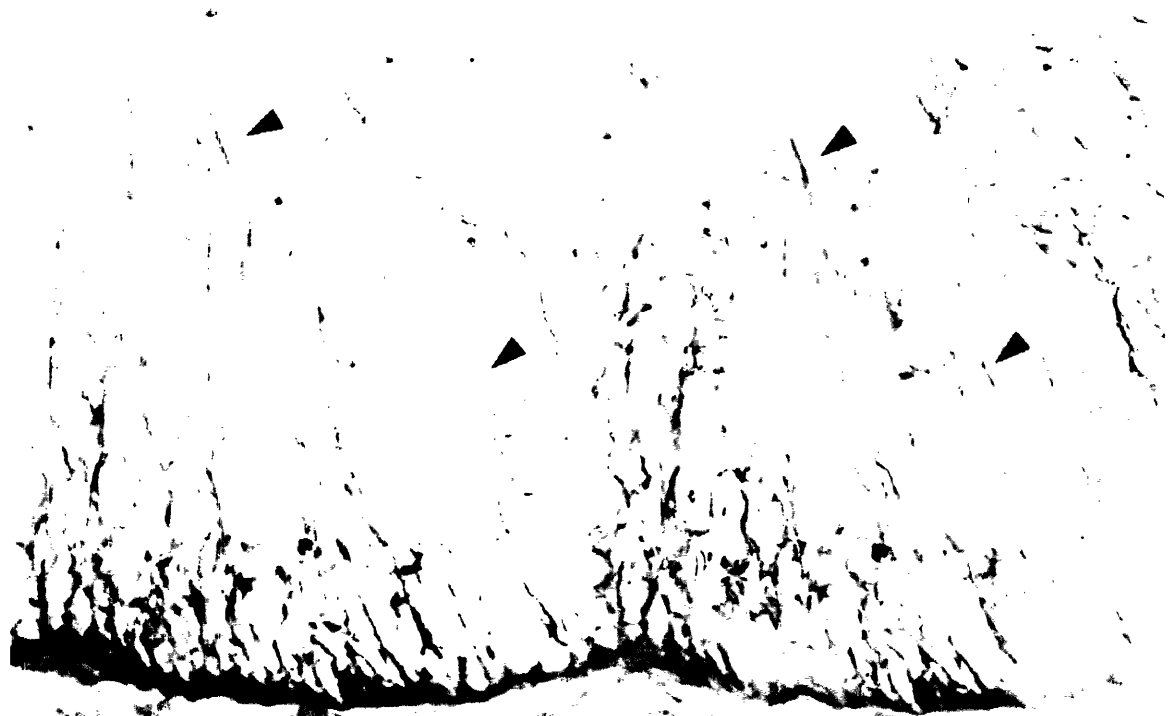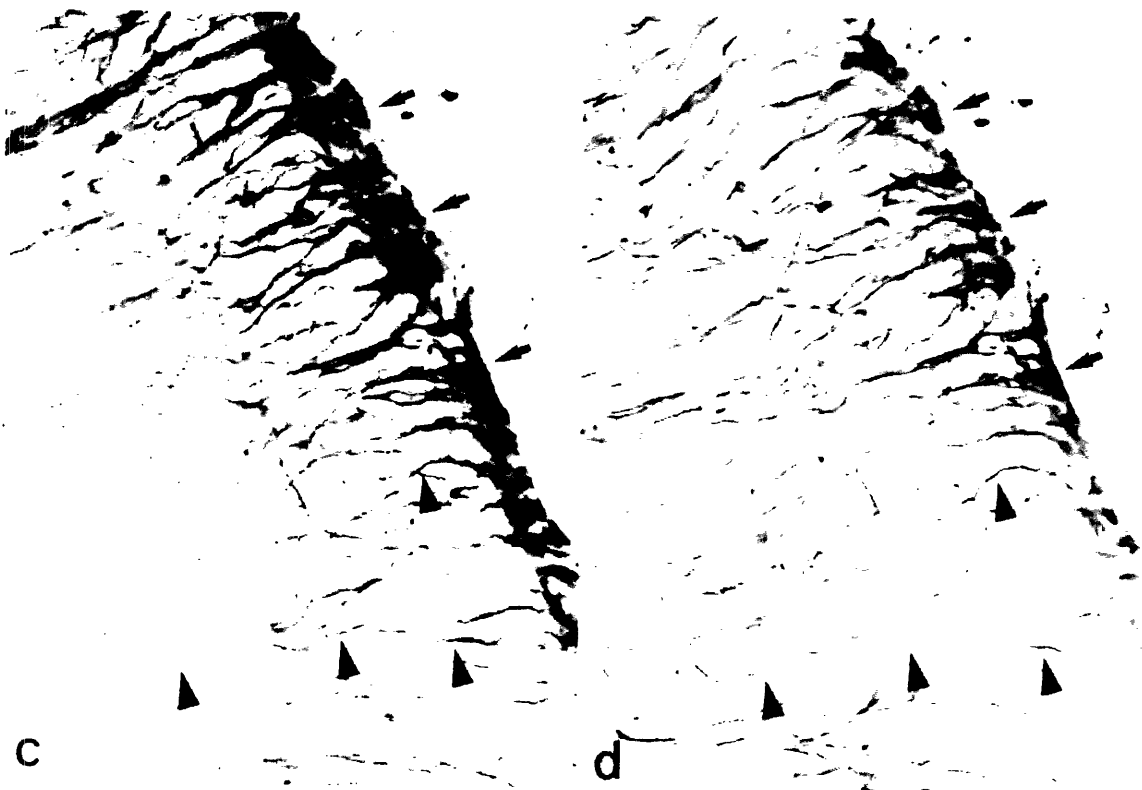
a

b
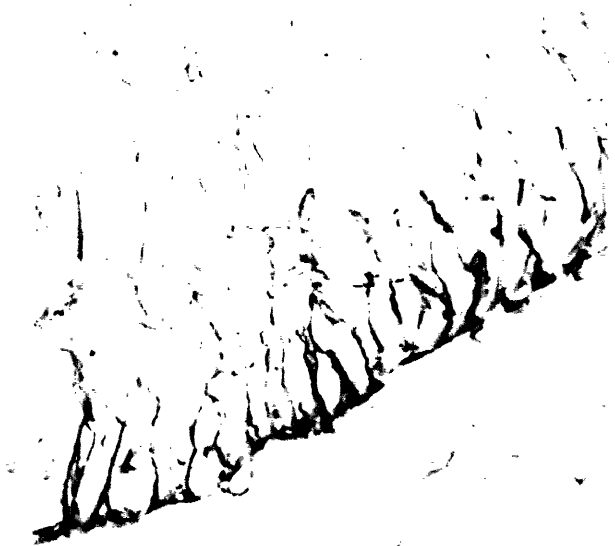
c

d

Figure 40. Wild type transgenic animals doubly stained for HA (a,c) and nestin (b,d). (a, b) NgHA 522. Arrowheads show localization of both endogenous and exogenous nestin in processes radiating from the ventricular zone. The endfeet of the radial cells are strongly stained in both channels (c,d) NgHA 523. arrows indicate endfoot profiles at the pial surface.

Figure 41.   One offspring (F2M11) of founder animal NM5HA-102 doubly stained for HA (a,c) and nestin (b,d).   Nestin staining appears normal in the subpial layer and extends to the ventricular zone.   Anti HA stain is concentrated at the pial surface and in very short processes in the marginal layer.   No staining is seen in perinuclear regions in the ventricular zone.

c   d

Figure 42. Mutant nestin transgenic embryos doubly stained for HA (a,c) and nestin (b,d) (a,b) NM5HA-5: HA stain is localized to the pial surface. *Arrows* indicate perinuclear staining near the ventricular zone. Nestin stain spans the width of the spinal cord. (c,d) Offspring of founder animal NM5HA-102 (F2M2). Endfoot profiles are stained with HA. In this animal the protein is localized to a small structure within the endfoot. Nestin stain is unaltered from controls.
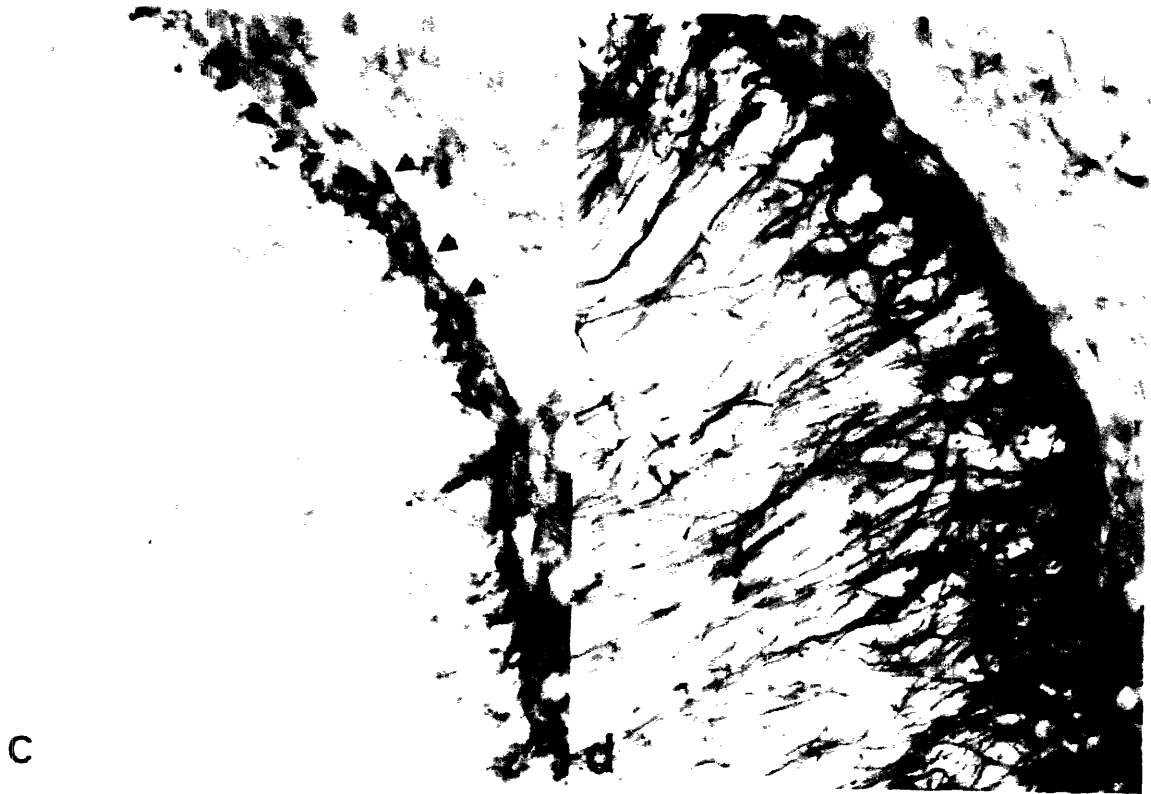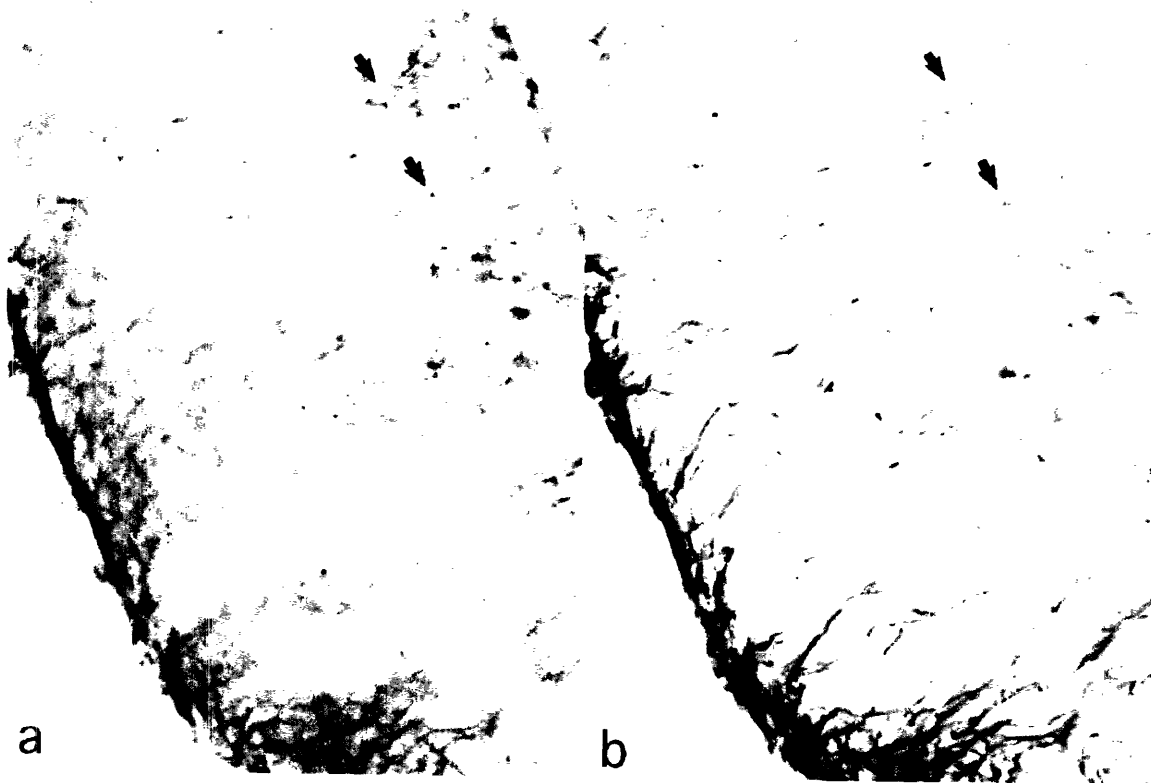
Chapter 6: Conclusions

Nestin expression in neuroepithelial stem cells

Nestin is a novel type of IF expressed in CNS stem cells. It is found transiently during a narrow window of development in the common precursor to neurons and glial cells. The stem cells of the CNS are rapidly dividing, with a striking polarity across the radius of the neural tube. The polarity is most clearly manifested during mitosis when the nucleus migrates toward the ventricular zone and the pial connection is released. CNS stem cells must remodel the intermediate filament system during the frequent cell divisions. The IF expression of stem cells change upon differentiation. The rapid changes during development suggest a role for IFs in differentiation. This work investigated the role and the properties of nestin in CNS stem cells.

Nestin Assembly

While nestin is clearly a member of the intermediate filament family from its sequence, its unusual headless structure and long tail invited speculation on its ability to self-assemble and the role of the tail domain in vivo. This work showed that nestin is assembly incompetent in the absence of other IF proteins and is rendered soluble in Triton X-100. In the presence of vimentin, it is incorporated into filaments. If nestin is highly overexpressed in cells, it partitions to both the filaments and to the soluble phase. This suggests that nestin is capable of saturating the vimentin network and that the excess remains soluble. This was suggested by the solubility of headless vimentin filaments, which can incorporate into a wild type vimentin network, but only at ratios of less than 1:3 (Andreoli and Trevor, 1994). The stoichiometry of nestin-vimentin filaments, and the composition of tetramers assembled in the presence of both proteins will be a topic for future research. In long term culture of cells expressing nestin without vimentin, nestin forms large aggregates in the periphery of SW13 cells. The ultrastructure of these aggregates will also be instructive. Does nestin form oligomeric precursors to IFs, or is it dependent on vimentin for even the earliest stages of assembly? On the level of filament formation, nestin is an obligate partner with vimentin.

Nestin depends on the rod domain for its interaction with vimentin. As with all other intermediate filament proteins examined, the

conserved sequence in coil 1A is required for assembly into filaments. Without coil 1A, nestin is unable to associate with vimentin and remains soluble. The coil 2B domain is also required for the normal assembly of IFs in SW13 cells. In other IFs, the 2B domain operates at a higher level of assembly, in the alignment of oligomers to form 10 nm filaments. Without the complete 12aa conserved coil 2B sequence, IF structure is perturbed by mutant nestin. Overexpression of the coil 2B nestin mutant protein in SW13 cells suggests that the nestin mutant may interfere with the interaction of vimentin with components at or near the plasma membrane.

Intermediate Filament Associated Proteins

There are numerous intermediate filament-associated proteins which have been identified by their colocalization or copurification with IFs. Many IFAPs have been identified on the basis of antigenic properties alone, such as IFAP 70-280 (Yang, et al., 1992) and paranemin, a muscle-associated IFAP, while others are now cloned. One family of IFAPs is represented by plectin, desmoplakin and bullous pemphigoid antigen, which are found joining vimentin and keratin IFs to desmosomal and hemidesmosomal plaques and cross-linking IFs (Stappenbeck, et al., 1993; Wiche, et al., 1993). Under the current criteria for IFAPs established by Goldman and colleagues (Yang, et al., 1992), assembly-incompetent IF proteins such as the neurofilaments and nestin cannot be distinguished from unrelated associated proteins. Their sequences identify them as IF proteins by the length and conservation of the rod domain and by the presence of the two rod end conserved sequences. IFAPs such as the desmoplakin family have longer rod domain sequences which do not show homology to the IF family. At present, the criteria for the distinction between associated and integral IF proteins must rest on the sequence. Intermediate filament proteins all have a rod domain of 310-350 amino acids, the heptad repeat motif, and fit the consensus sequences at the ends of the rod domains. The features common to the six classes diagrammed in Figure 1. The ability to affect IF structure is not limited to integral IF proteins. Overexpression of the non-helical carboxyl tail domain of plectin can bring about the collapse of the IF network in cells (Wiche, et al., 1993).

Nestin and NFH have similar structure

This work and earlier data show that nestin is similar in several respects to its closest IF relative, NFH. First, there is the structural homology of the short head and long C-terminal tail domain, as well as the presumed evolutionary relationship based on rod sequence and intron placement (Dahlstrand, et al., 1992). The actual sequences of the tail domains are highly divergent between nestin and NFH, but both nestin and NFH contain potential phosphorylation sites in the tail domain, although the sequences of these sites differ. Phosphorylation of NFH by $p34^{cdc2}$ kinase on a subset of the NFH tail domain kinase sites has been demonstrated in vitro to bring about the dissociation of NFH from microtubules (Hisanaga, et al., 1991). A more likely candidate for the phosphorylation of NFH in neurons is the recently identified cdk 5 (Lew, et al., 1992; Shetty, et al., 1993). The nestin tail contains multiple repeats of an 11 amino acid motif containing potential phosphorylation sites which could be involved in binding other components of the cytoskeleton and remodeling at mitosis.

Secondly, both nestin and NFH can exist in soluble forms. During both mouse brain development and differentiation of the neuroblastoma line NB2a/d1, a fraction of NFH immunoreactivity can be found in soluble forms (Shea, et al., 1993; Shea, et al., 1990). The high-speed supernatants contain tetramers or smaller subunits, while larger oligomers and filamentous forms are pelleted (Ching and Liem, 1993). NFH becomes incorporated into filaments as neurites extend and neurons mature. The high solubility correlates with high phosphorylation on an antigenically identified site in the tail domain. Nestin too is present in a soluble form in cultured cells, and to a small degree in the developing CNS (Figure 38). Nestin solubility is increased in the presence of a phosphatase inhibitor (Almazan, et al., 1993). The degree of nestin incorporation into filaments is likely to be influenced by phosphorylation, as it is for vimentin (Chou, et al., 1990). The significance of the transient presence of soluble forms of NFH in development is not yet clear. It is likely to comprise a soluble pool of subunits available for polymerization in the presence of NFL. For nestin, rapid remodeling of the intermediate filament system during mitosis is likely to be important in the proliferating CNS. Soluble nestin may be a transient form found during mitosis.

The structural and physical similarities of nestin and NFH suggest future directions for research on the cell biology of nestin. NFH has been shown to form cross-bridges between neurofilaments formed from NFL in vitro (Gotow, et al., 1992). The long tail of nestin may be

192

capable of forming cross-bridges or of regulating the spacing of vimentin IFs in CNS stem cells. It is notable that nestin is capable of aggregation when expressed at high levels (Figure 16) or for long periods (Figure 18) in cells lacking vimentin, in spite of its inability to form filaments. The aggregation is not neccessarily due to the presence of the rod domain, but may be due instead to sequences in the tail.

Nestin-vimentin filaments in development

In light of the present work, it is likely that the targeted deletion of vimentin affects nestin localization in the developing CNS (Colluci-Guyon, et al., 1994). The data from SW13 cells predicts that nestin would be soluble and diffused throughout the cells of the early CNS in the absence of vimentin. However, if there is an active mechanism which binds nestin to the thickened structure in the pial endfoot, nestin might instead be localized at the pial surface, as with the coil 2B deletion mutant. The distribution of nestin in a vimentin negative CNS might resolve the present questions regarding the mechanism of nestin localization to the pial surface. Experiments on nestin localization in these animals could help to distinguish between the possible mechanisms resulting in the concentration of nestin at the pial endfoot.

Since nestin is assembly-incompetent without vimentin, it would not be able to compensate for vimentin filament functions. If there are compensatory changes in the cytoskeleton in the vimentin knockout animals, they are unlikely to involve intermediate filaments in the CNS. With both the quail NFL mutant and the NFH-β-galactosidase mutants, microtubules are upregulated in neuronal processes lacking neurofilaments. This might be the case for the vimentin knockout animals as well.

In addition to the study on nestin assembly, this work has generated a widely used antibody which can identify nestin in mammalian cells. The antisera to nestin have been used to identify CNS stem cells in culture and in the adult brain. Several studies have used the antibody to identify undifferentiated stem cells in populations of cells made to proliferate in vitro. In vitro expansion of CNS stem cells will allow their use in therapeutic and research protocols previously limited by the small quantities of tissues from the early embryo. The antinestin antisera also identify some populations of CNS tumors. Data from two studies so far indicate that nestin

193

expression may correlate with more primitive and aggressive tumor types and this knowledge is potentially useful in the choice of therapy. A model system for the onset and shutdown of nestin expression throughout neural differentiation was explored. The P19 system is being explored as an in vitro system for the study of the nestin promoter. The role of the nestin protein in neurite extension and glial differentiation will also be studied in these cells.

References

Almazan, G., Afar, D. and Bell, J. (1993). Phosphorylation and disruption of intermediate filament proteins in oligodendrocyte precursor cultures treated with Calyculin A. Journal of Neuroscience Research 36, 163-172.

Andreoli, J. and Trevor, K. (1994). Fate of a headless vimentin protein in stable cell cultures: soluble and cytoskeletal forms. Experimental Cell Research 214, 177-188.

Ching, G. and Liem, R. (1993). Assembly of Type IV neuronal intermediate filaments in nonneuronal cells in the absence of preexisting cytoplasmic intermediate filaments. Journal of Cell Biology 122, 1323-1335.

Chou, Y.-H., Bischoff, J., Beach, D. and Goldman, R. (1990). Intermediate filament reorganization during mitosis is mediated by $p34^{cdc2}$ phosphorylation of vimentin. Cell 62, 1063-1071.

Colluci-Guyon, E., Portier, M.-M., Dunia, I., Paulin, D., Pournin, S. and Babinet, C. (1994). Mice lacking vimentin develop and reproduce without an obvious phenotype. Cell 79, 679-694.

Dahlstrand, J., Collins, V. and Lendahl, U. (1992). Expression of the Class VI intermediate filament nestin in human central nervous system tumors. Cancer Research 52, 5334-5341.

Gotow, T., Takeda, M., Tanaka, T. and Hashimoto, P. (1992). Macromolecular structure of reassembled neurofilaments as revealed by the quick-freeze deep-etch mica method: difference between NF-M and NF-H subunits in their ability to form cross bridges. Eur J Cell Biol 58, 331-345.

Hisanaga, S., Kusubata, M., Okumura, E. and Kishimoto, T. (1991). Phosphorylation of neurofilament H subunit at the tail domain by cdc2 kinase dissociates the association to microtubules. J Biol Chem 266, 21798-21803.

Lew, J., Beaudette, K., Litwin, C. and Wang, J. (1992). Purification and Characterization of a novel proline-directed protein kinase from bovine brain. J Biol Chem 267, 13383-13390.

Shea, T., Beermann, M. and Fischer, I. (1993). Transient requirement for vimentin in neuritogenesis: intracellular delivery of anti-vimentin antibodies and antisense oligonucleotieds inhibit neurite initiation but not elongation of existing neurites in neuroblastoma. J Neurosci Res 36, 66-76.

Shea, T., Sihag, R. and Nixon, R. (1990). Dynamics of phosphorylation and assembly of the high molecular weight neurofilament subunit in NB2a/d1 neuroblastoma. J Neurochem 55, 1784-1792.

Shetty, K., Link, W. and Pant, H. (1993). cdc2-like kinase from rat spinal cord specifically phosphorylates KSPXK motifs in neurofilament proteins: isolation and characterization. PNAS (USA) 90, 6844-6848.

Stappenbeck, T., Bornslaeger, E., Corcoran, C., Luu, H., Virata, M. and Green, K. (1993). Functional analysis of desmoplakin domains: specification of the interaction with keratin versus vimentin intermediate filament networks. J Cell Biol 123, 691-705.

Wiche, G., Gromov, D., Donovan, A., Castanon, M. and Fuchs, E. (1993). Expression of plectin mutant cDNA in cultured cells indicates a role of COOH-terminal domain in intermediate filament association. J Cell Biol 121, 607-619.

Yang, H.-Y., Lieska, N., Goldman, R., Johnson-Seaton, D. and Pappas, G. (1992). Distinct developmental subtypes of cultured non-stellate rat astrocytes distinguished by a new glial intermediate filament-associated protein. Brain Res. 573, 161-168.